nature portfolio

https://doi.org/10.1038/s41586-025-09020-z

Supplementary information

Programmable control of spatial transcriptome in live cells and neurons

In the format provided by the authors and unedited

SUPPLEMENTARY INFORMATION

Programmable Control of Spatial Transcriptome in Live Cells and Neurons

Mengting Han, Maylin L. Fu, Yanyu Zhu, Alexander A. Choi, Emmy Li, Jon Bezney, Sa Cai, Leann Miles, Yitong Ma, Lei S. Qi

Table of Contents

SUPPLEMENTARY FIGURES

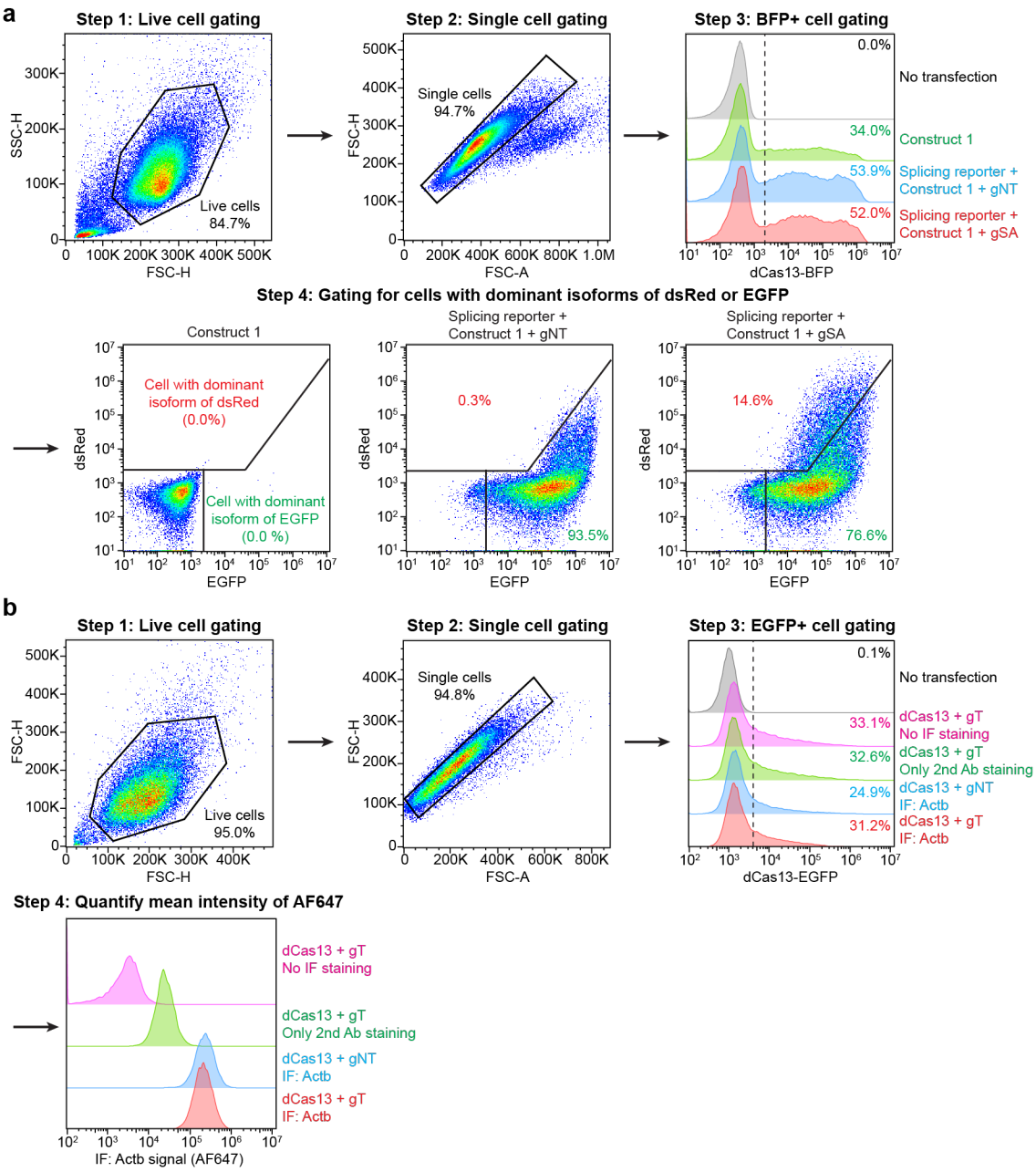

Supplementary Figure 1 | Representative gating strategies for all flow cytometry analyses in this manuscript. a, Representative gating strategies for **Extended Data Fig. 1b-c**. Step 1: live cells were gated from all cell populations. Step 2: single cells were gated from live cells. Step 3: cells expressing BFP (i.e., BFP+ cells) were gated from single cells based on cells without transfection (BFP- cells). Step 4: transfected cells (BFP+) were first gated to select cells expressing splicing reporter based on background EGFP and dsRed signals of cells only transfected with Construct 1. Then cells were further gated to calculate the percentage of cells with dominant isoform of EGFP or dsRed based on the gNT group where cells mainly expressed the EGFP

isoform. Ratio of cells with dominant isoforms of dsRed to EGFP was calculated as % cells with dominant isoform of dsRed divided by % cells with dominant isoform of EGFP to make the column plots in **Extended Data Fig. 1b-c**. **b**, Representative gating strategies for **Extended Data Fig. 4t-u**. Step 1: live cells were gated from all cell populations. Step 2: single cells were gated from live cells. Step 3: cells expressing EGFP (i.e., EGFP+ cells) were gated from single cells based on background EGFP level of cells without transfection. Step 4: the mean fluorescence intensity of Actb protein immunofluorescence (IF) staining signals were quantified for EGFP+ cells to make the column plots in **Extended Data Fig. 4t-u**. Two control groups (no IF staining and only secondary antibody staining) were included here to show the specificity of IF: Actb staining.

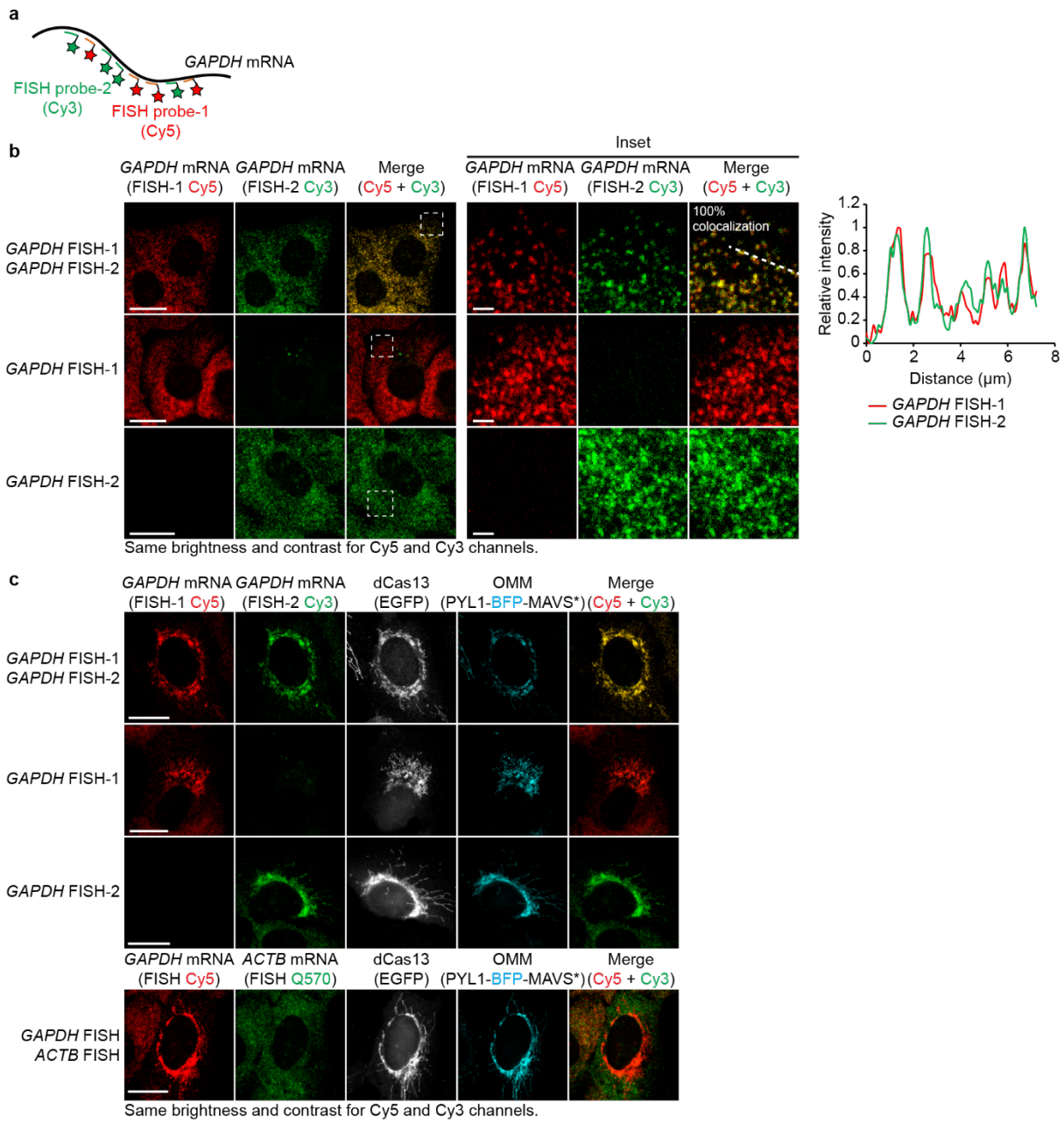

Supplementary Figure 2 | Testing the specificity of designed RNA FISH probes. a, Schematic showing the design of two RNA FISH probe sets targeting *GAPDH* mRNA. **b**, Representative microscopic images showing near-perfect colocalization of staining signals using the two RNA FISH probe sets targeting *GAPDH* mRNA in HeLa cells. Scale bar, 20 μm. Middle: insets of dotted boxes. Scale bar, 2 μm. Right: intensity plots of the dotted line in the left image. See **Supplementary Data**. **c**, Representative microscopic images showing colocalization of the staining signals of the two RNA FISH probe sets targeting *GAPDH* mRNA. In contrast, there is no evident colocalization of staining signals for *GAPDH* mRNA and *ACTB* mRNA in HeLa cells where *GAPDH* mRNA was recruited to the OMM by CRISPR-TO. Scale bar, 20 μm.

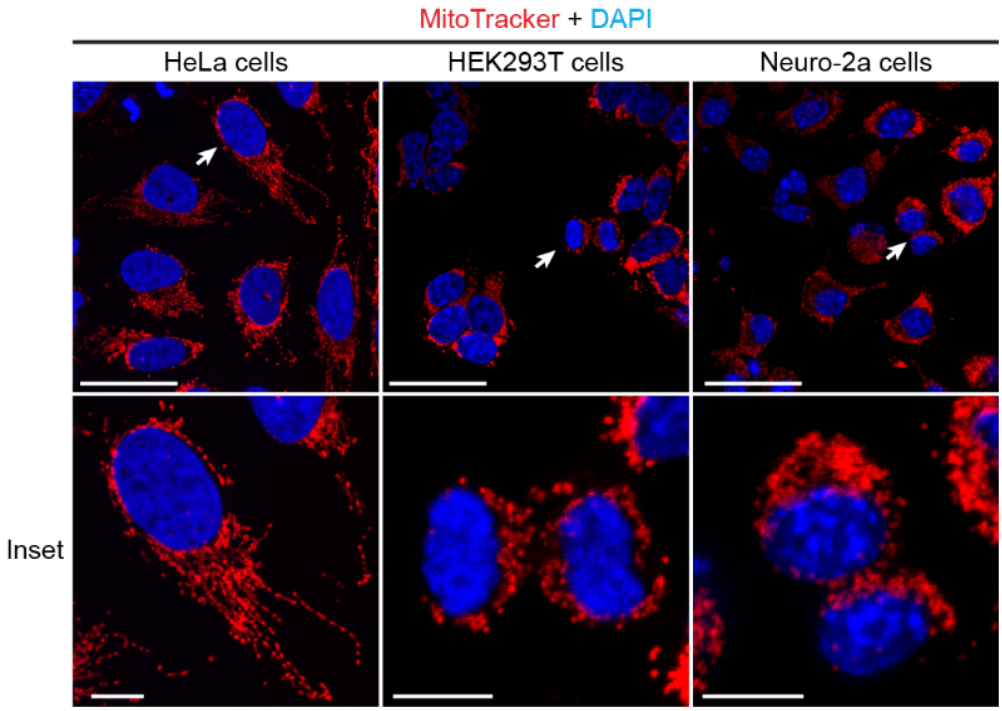

Supplementary Figure 3 | The morphological difference of mitochondria across different cell types. Representative microscopic images showing that mitochondrial morphology is different among HeLa, HEK293T, and Neuro-2a cell lines which were stained with MitoTracker Red CMXRos. Scale bar, 40 μm. Bottom: insets showing cells pointed by the white arrow. Scale bar, 10 μm.

a

Schematics of gRNA design for different CRISPR-Cas systems

GAPDH mRNA	3’-accaactcgtgtcccatgaaataactaccatgtactgttccacgccgagggatc-5’
PspCas13b gRNA	5’-gggtactttattgatggtacatgacaaggtGTTGTGGAAGGTCCAGTTTTGAGGGGCTATTACAAC-3’
RfxCas13d gRNA	5’-gAACCCCTACCAACTGGTCGGGGTTTGAAACgggtactttattgatggtacatgacaaggt-3’
LwaCas13a gRNA	5’-GATTTAGACTACCCCAAAAACGAAGGGGACTAAAACgggtactttattgatggtacatgacaaggt-3’
Cas13bt1 gRNA	3’-gggtactttattgatggtacatgacaaggtGCTGAAGAAGCCTCCGATTTGTGGGGTGATTACAGC-5’
DiCas7-11 gRNA	5’-GTTGATGTCACGGAACgggtactttattgatggtacatgacaaggt-3’

Direct repeat (DR) Spacer Direct repeat (DR)

b

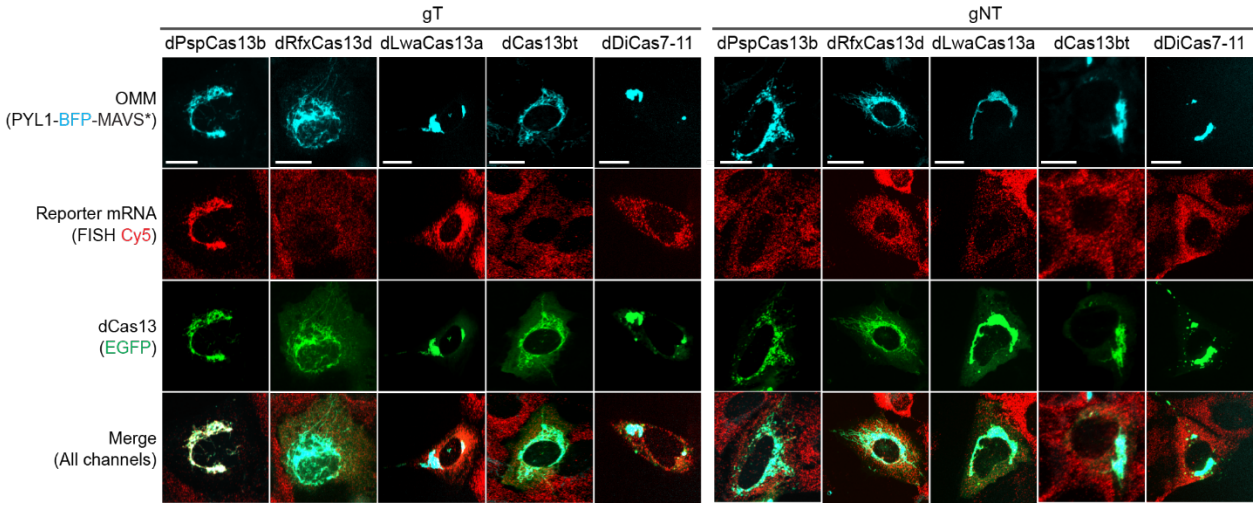

Supplementary Figure 4 | gRNA design and representative microscopic images for different dCas systems for CRISPR-TO application. a, Schematic showing the spacer and direct repeat sequences of different gRNAs used for different CRISPR-Cas systems. These gRNAs use the same spacer sequence of gG1 targeting the same region of endogenous human *GAPDH* mRNA. The target sequence of GAPDH mRNA is in red, the spacer sequence of gRNA is in blue, and the direct repeat sequence is in orange. An extra 5’-g was added to RfxCas13d gRNA considering the U6 promoter requires a "G" nucleotide at the transcription start site for optimal expression. **b**, Representative microscopic images related to **Fig. 1e**. HeLa cells were transfected with CRISPR-TO components containing different dCas systems to recruit endogenous GAPDH mRNA to the OMM. Scale bar, 20 μm.

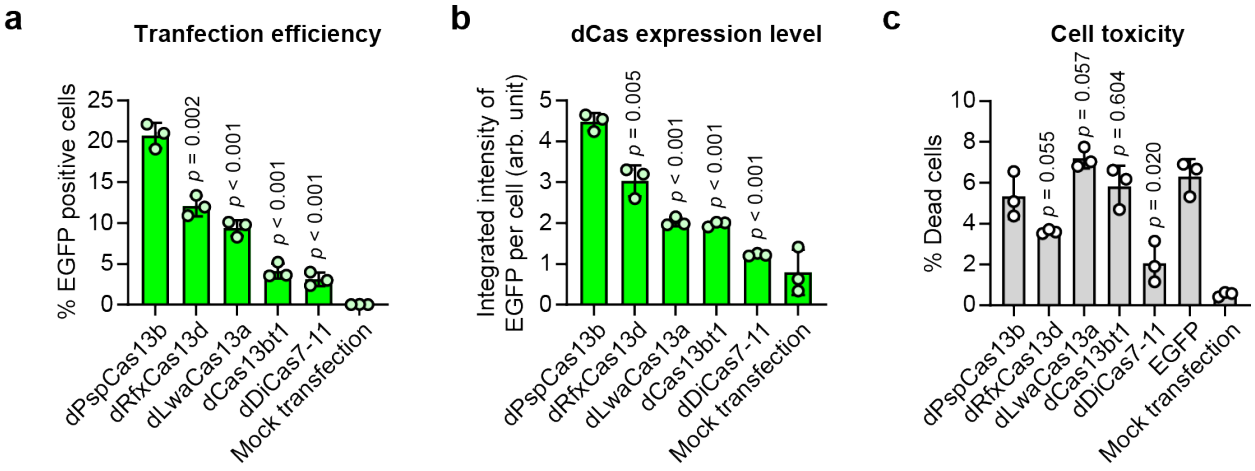

Supplementary Figure 5 | Quantification of transfection efficiency, expression level, and cell toxicity of each dCas effector in HeLa cells. a-b, HeLa cells were transfected with different NES-dCas effector plasmids for two days and imaged under an ImageXpress Micro Confocal system to measure the transfection efficiency (**a**) and dCas expression level (**b**) (**Supplementary Methods**). **c**, HeLa cells were transfected with different NES-dCas effector plasmids for two days and stained with SYTOX Red Dead Cell Stain to measure % dead cells under an ImageXpress Micro Confocal system (**Supplementary Methods**). EGFP is the control group where cells were transfected with the NES-EGFP plasmid. Data is presented as means ± standard deviation. Each dot represents one biological replicate. n = 3 wells per group. Two-sided, unpaired Student's *t*-test.

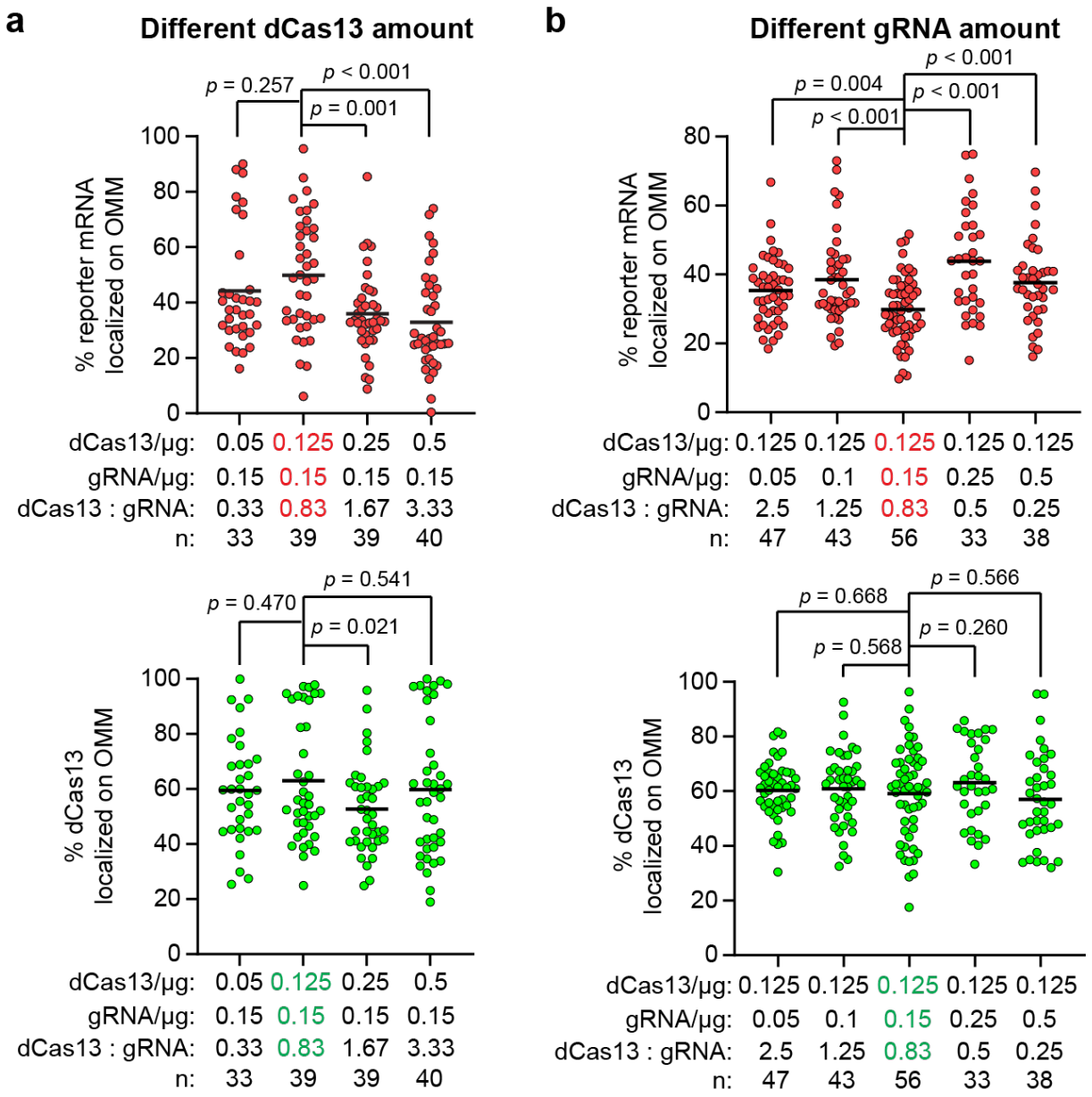

Supplementary Figure 6 | Quantification of the effect of transfection amounts/ratios of dCas13:gRNA plasmids on RNA localization efficiency. a-b, Quantification of % 2×GCN4 reporter mRNA (red bars) and % dCas13 (green bars) localized on the OMM in individual cells with different transfection amounts of dCas13 plasmid (**a**) or gRNA plasmid (**b**) after CRISPR-TO perturbation. Only cells co-expressing dCas13 and MAVS*-PYL1 were analyzed. n indicates the number of quantified cells for each group. Black bar, mean. Two-sided, unpaired Student's *t*-test. The condition indicated in red or green represents the original transfection for CRISPR-TO perturbation.

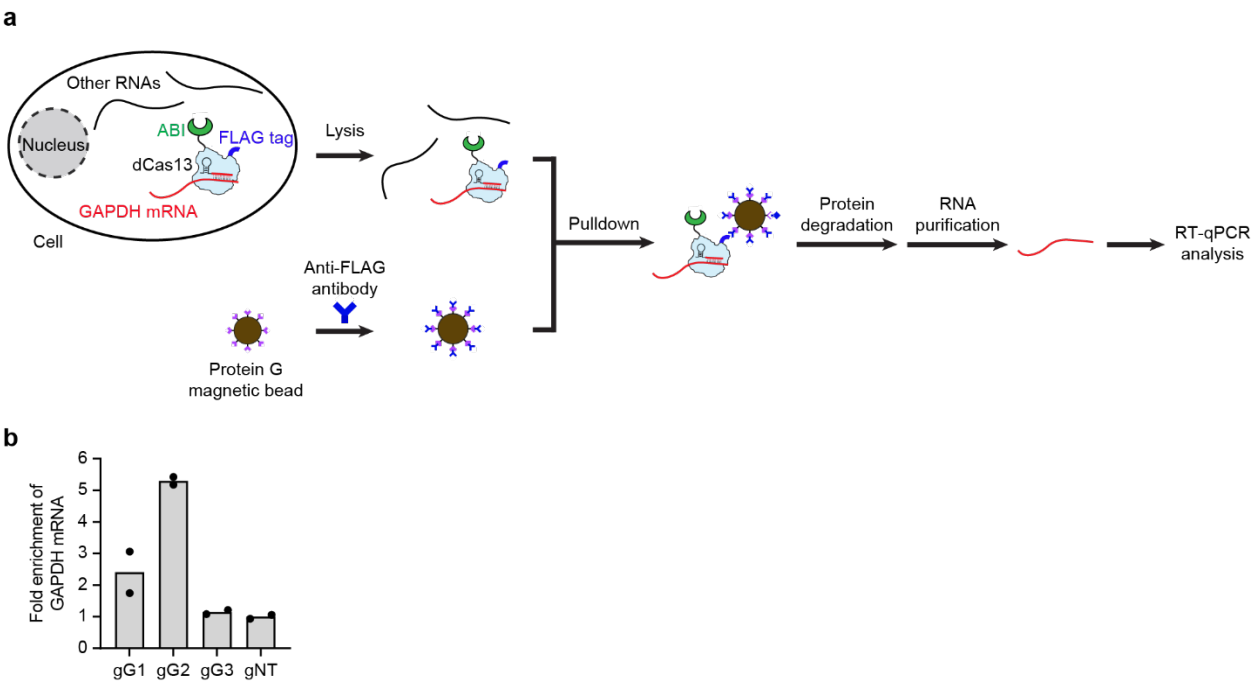

Supplementary Figure 7 | RNA immunoprecipitation for quantifying dCas13 binding affinity on *GAPDH* mRNA with different gRNAs. a, Schematic of the procedures of RNA immunoprecipitation for quantifying dCas13 binding affinity on *GAPDH* mRNA. **b**, Fold enrichment of the purified *GAPDH* mRNA after immunoprecipitation based on the qRT-PCR analysis. Each dot represents one biological replicate.

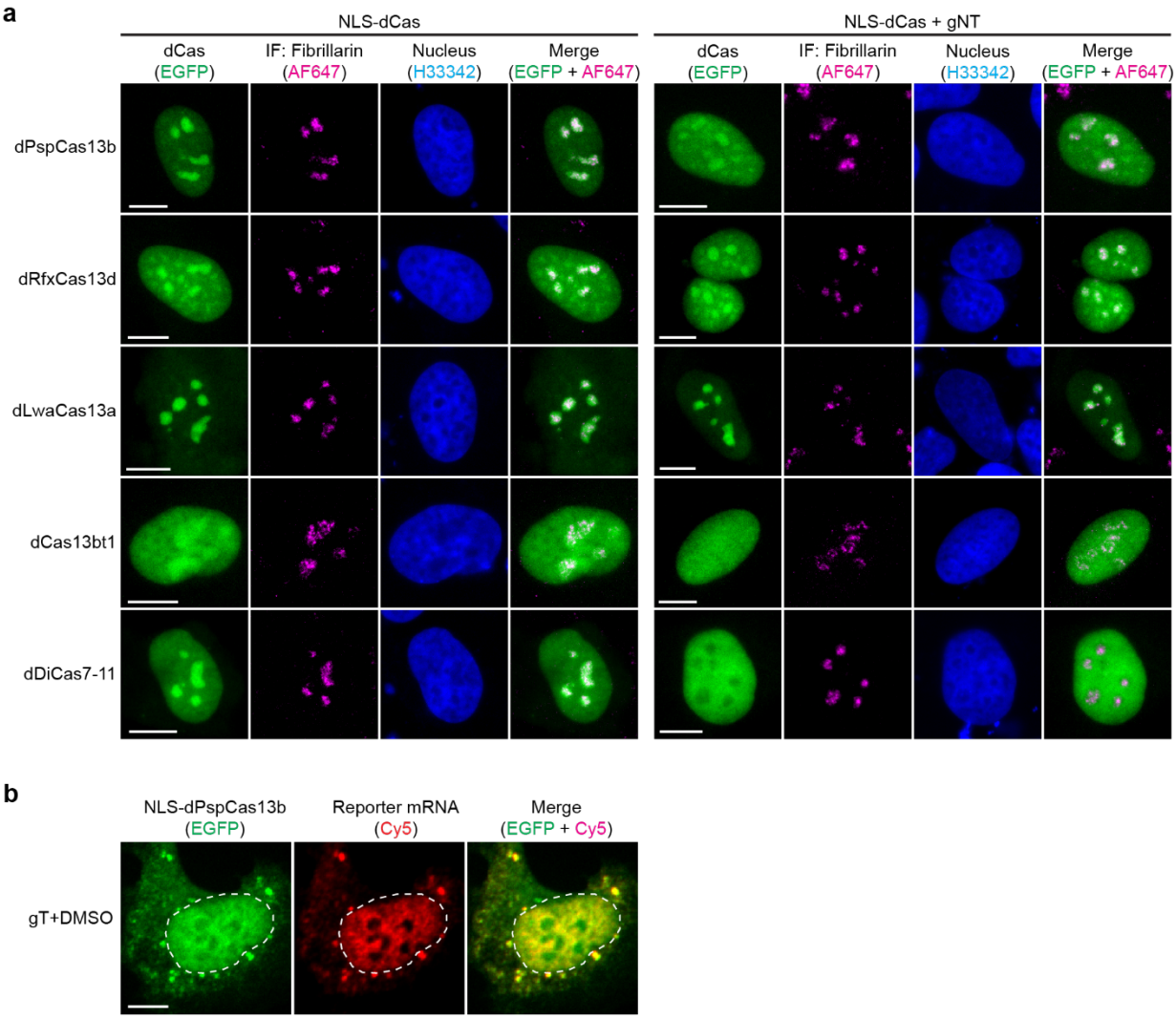

Supplementary Figure 8 | Representative microscopic images showing NLS-dCas protein aggregates in nucleoli. a, HeLa cells expressing different NLS-dCas proteins with gNT or without gRNA were stained with the antibody of Fibrillarin to image the nucleolus. Scale bar, 10 μm. **b**, HeLa cells expressing NLS-dPspCas13b, 24×GCN4 reporter mRNA, and gRNA targeting the reporter mRNA did not have aggregation of NLS-dPspCas13b in nucleoli. Some NLS-dPspCas13b signals are outside of the nucleus because they bind to the target reporter mRNAs that exist in the cytoplasm.

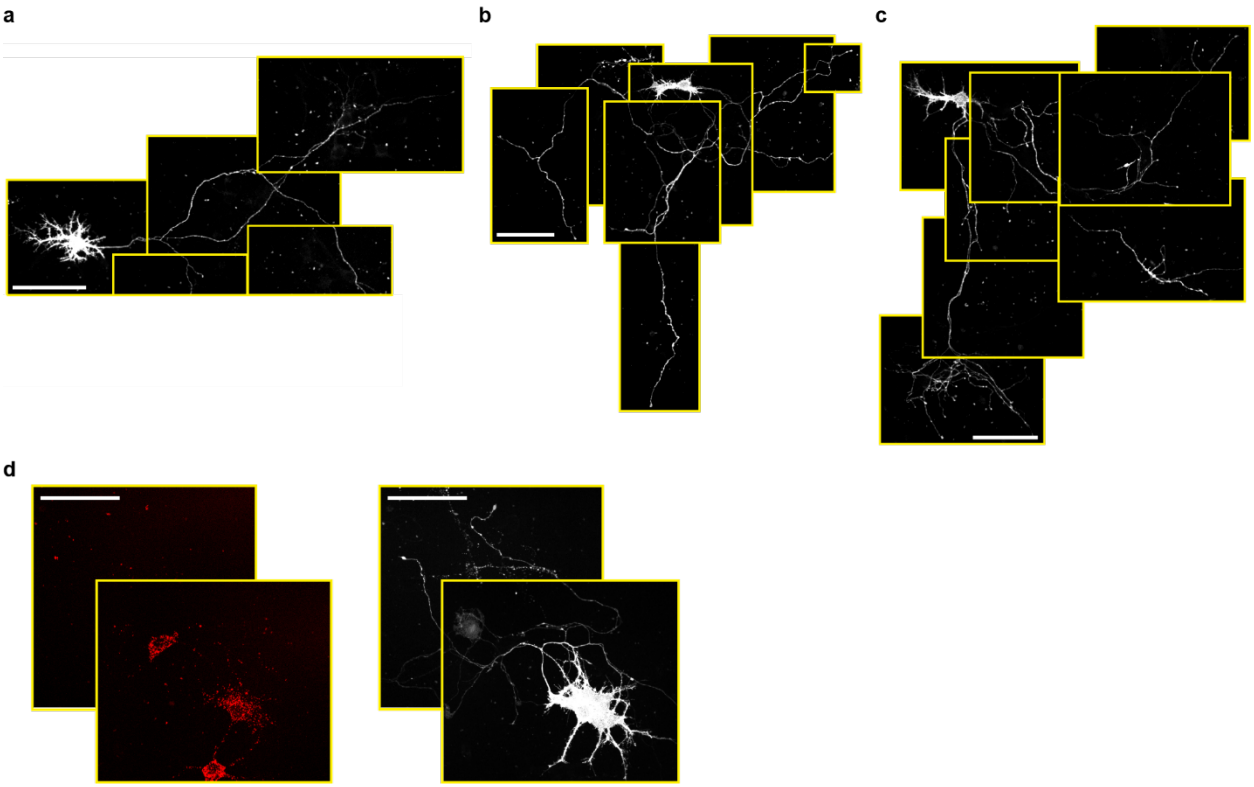

Supplementary Figure 9 | Multiple images were assembled to present the full view of a single neuron. a, Images from five fields of view were assembled to create the image in **Fig. 3b**. **b**, Images from seven fields of view were assembled to create the left image in **Extended Data Fig. 8e**. **c**, Images from eight fields of view were assembled to create the left image in **Extended Data Fig. 8f**. Images were assembled based on the shape of the neuron shown in the CAAX-Crimson channel. Scale bar, 100 µm. **d**, Images from two fields of view were assembled to create the image in **Fig. 5d**. Images were assembled based on the shape of the neuron shown in the CAAX-mNeonGreen channel. Scale bar, 50 µm.

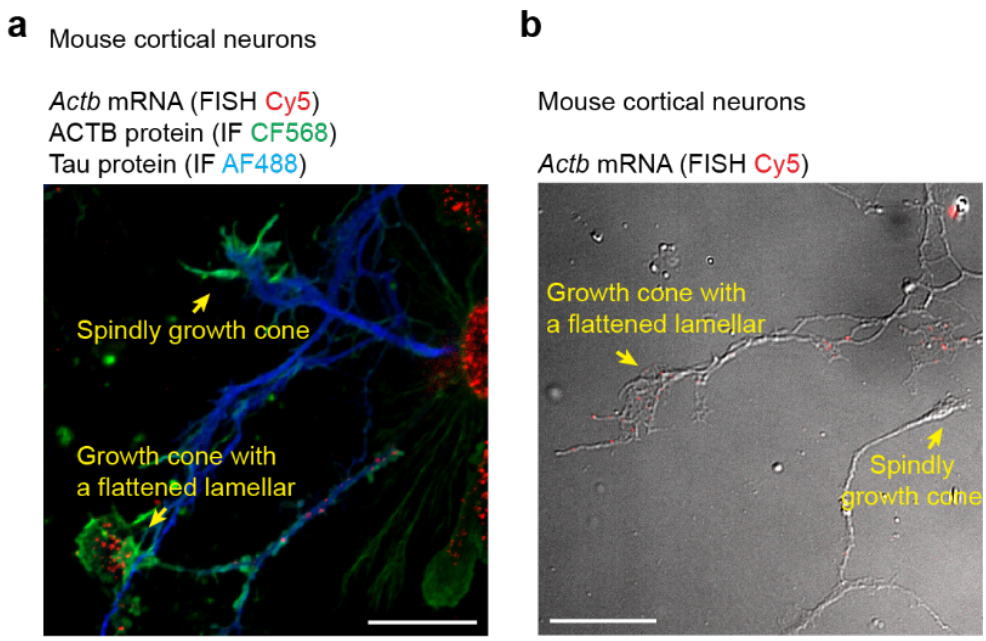

Supplementary Figure 10 | Monitoring *Actb* mRNA localization inside growth cones of mouse cortical neurons. a-b, Representative microscopic images showing the different localization of *Actb* mRNA particles inside two distinct types of growth cones, one with a spindly morphology and one with a flattened lamellar morphology. The growth cone morphology was monitored using immunofluorescence staining of beta-actin protein and Tau (**a**) or differential interference contrast (DIC) microscopy (**b**). Scale bar, 20 µm.

SUPPLEMENTARY NOTES

Designing effective gRNAs for CRISPR-TO. To optimize the perturbation of endogenous mRNA localization via CRISPR-TO, the selection of gRNAs with high binding affinity for dCas13 is crucial. Since existing tools for Cas13 gRNA design[1-3] are primarily exploited for Cas13's ribonuclease functions, they may not always yield the most effective gRNAs for CRISPR-TO applications. A practical approach to pinpoint effective gRNAs for CRISPR-TO involves designing a range of gRNAs, followed by assessing the binding affinity of dCas13 to the target mRNA through RNA immunoprecipitation assays. For instance, in our study targeting the endogenous *GAPDH* mRNA, two of the three designed gRNAs, gG1 and gG2, demonstrated significantly higher binding affinity compared to gG3, as evidenced by RNA immunoprecipitation results (**Supplementary Fig. 7a-b**). This enhanced binding affinity translated into greater CRISPR-TO efficiency for combinations using gG1 and gG2 (**Extended Data Fig. 3h**), underscoring the importance of selecting high-affinity gRNAs. The development of robust, new tools for designing PspCas13b gRNAs will greatly facilitate the application of CRISPR-TO to different mRNAs.

Since most endogenous mRNAs contain non-repetitive sequences, it's important to understand how many binding sites of dCas13 are required for efficient CRISPR-TO activity. By testing reporter mRNA with different GCN4 repeats (**Fig. 1g, Extended Data Fig. 3f-g**) and different combinations of gRNAs targeting the endogenous *GAPDH* mRNA (**Extended Data Fig. 3h**), we found that two effective gRNAs are sufficient for target mRNA localization. Notably, the efficiency of mRNA localization via CRISPR-TO is comparable when using either gG12 or gG123 combinations (**Extended Data Fig. 3h**), suggesting that a less effective gRNA (like gG3) does not significantly impact the functionality of high-affinity gRNAs (gG1 and gG2). This finding allows for the delivery of multiple gRNAs into cells, with the assurance that the presence of at least two high-affinity gRNAs will sustain the functionality of the CRISPR-TO system.

An interesting observation is the notably higher efficiency of CRISPR-TO using the gG12 combination compared to individual gG1 or gG2 (**Extended Data Fig. 3h**), hinting at a potential synergistic effect from multiple dCas13 binding events. A hypothesis is that dCas13's binding to the target mRNA is inherently unstable. With only one binding site, the mRNA may easily dissociate and diffuse away. However, with multiple binding sites, even if the mRNA detaches from one site, it remains anchored by others, thereby reducing diffusion and facilitating re-capture at the released site. This multivalent binding model could explain the observed increased efficiency and highlights the intricate dynamics of dCas13-mRNA interactions in CRISPR-TO applications.

Strategies for localizing mRNA to diverse subcellular compartments using CRISPR-TO. In this study, we explored and reported two strategies for perturbing mRNA localization, via either a diffusion and docking mechanism or active mRNA transport via motor proteins[4]. We employed these two methods in manipulating mRNA localization through CRISPR-TO. Specifically, for

targeting mRNA to subcellular structures such as the OMM, p-bodies, stress granules, telomeres, and nuclear stress bodies, we utilized the passive diffusion and docking strategy (**Fig. 2a-f**). Here, the mRNA-dCas13-ABI ribonucleoprotein (RNP) complex diffuses randomly within the cell until it encounters and is stabilized by PYL1, mediated by ABA, which ensures the bound mRNA localized to specific subcellular compartments.

For the directed anterograde or retrograde transport of mRNA along microtubules, we implemented an active transport strategy using motor proteins. In this case, the mRNA-dCas13-ABI RNP initially undergoes random diffusion before loading onto a PYL1-fused motor protein. Subsequently, the mRNA is actively transported along microtubules in the desired direction depicted by the motor protein activities. This dynamic process was visually validated using a live-cell mRNA imaging technique combined with CRISPR-TO (**Fig. 2k, Extended Data Fig. 7e-j, Supplementary Videos 1-3**).

Our study may expand beyond kinesin proteins (KIF5A, KIF5B, and KIFC1) that we tested. Other motor protein families, such as kinesin, dynein, and myosin, encompassing multiple superfamily proteins[5], could be similarly harnessed for mRNA transport to distinct cellular locales. For instance, myosin might be engineered to facilitate cargo transport in synaptic regions along actin filaments. Similarly, KIF17 offers potential for dendrite-specific cargo transport toward the plus end of microtubules[6,7]. This expansion of applicable motor proteins underscores the versatility and potential of CRISPR-TO in cell biology.

Manipulating mRNA localization in primary neurons. To apply CRISPR-TO into primary neurons, we employed a co-transfection strategy of multiple plasmids encoding dCas13-ABI, motor protein-PYL1 fusion, CAAX-Crimson, and gRNAs into the neurons. One difference between primary neurons and dividing cell lines is their non-dividing nature, which makes their nuclear envelope less favorable for plasmid entry. Despite this, we observed relatively efficient transfection, by pre-mixing multiple plasmids before being combined with the transfection reagent[8], facilitating their co-delivery into individual neurons. To further enhance CRISPR-TO delivery efficiency into primary neurons, one strategy could be to reduce the number of plasmids by engineering single plasmids that encode multiple proteins and gRNAs. This consolidation could simplify the transfection process and increase the uptake of CRISPR-TO components by the neurons.

Influence of transfection amounts / ratios of dCas13:gRNA plasmids on RNA localization efficiency. We tested whether changing the transfection amounts and ratios of dCas13 and gRNA plasmids could affect RNA localization efficiency at the OMM, using a reporter mRNA containing 2xGCN4 repeats as our target. Under our original conditions, cells were transfected with 0.125 µg dCas13 plasmid, 0.125 µg PYL1-MAVS* plasmid, 0.1 µg reporter mRNA plasmid, and 0.15 µg gRNA plasmid. We varied the amounts of transfected dCas13 plasmid (0.05, 0.125, 0.25, and 0.5 µg) while maintaining the other components constant, and measured the RNA localization

efficiency. Surprisingly, we found that increased dCas13 expression decreased RNA localization efficiency (**Supplementary Fig. 6a**). This decrease is likely due to competition between mRNA-bound dCas13 and excess unbound dCas13 for binding to the PYL1 fusion at the OMM. In a separate experiment, we varied the transfected gRNA plasmid amount (0.05, 0.1, 0.15, 0.25, and 0.5 μg). We found that changing gRNA levels moderately influenced RNA localization efficiency, while the percentage of dCas13 localized at the OMM remained unchanged (**Supplementary Fig. 6b**), suggesting gRNA is an important factor. Furthermore, these experiments did show a clear trend regarding the effect of dCas13:gRNA transfection ratios on RNA localization efficiency. These results confirm that fine-tuning transfection conditions can improve CRISPR-TO-mediated RNA localization efficiency.

Different performance of dCas systems on CRISPR-TO-mediated RNA localization control. In **Fig. 1e**, we observed that different dCas effectors display varying performance under the same experimental setting. We considered several potential explanations.

Firstly, we used the same spacer sequence to design gRNAs for all Cas systems. While this spacer sequence works well for PspCas13b, it may not be optimal for the other Cas systems. This is likely not due to the protospacer flanking site (PFS) requirements of each Cas effector, since PFS is not required for RNA interference in mammalian cells for PspCas13b[9,10], RfxCas13d[11], LwaCas13a[12], Cas13bt1[13], and DiCas7-11[14], but rather differences in protein size, structure, and the orientation of the spacer in the gRNA (i.e., 5' or 3'). For example, DiCas7-11 (1,601 aa) is substantially larger than PspCas13b (1,089 aa) and uses a different orientation of the spacer (**Fig. 1d**). It is possible that a target region that works optimally for dPspCas13b may not provide enough space for dDiCas7-11 binding.

Secondly, efficient RNA relocalization via CRISPR-TO requires high binding affinity of dCas to its target RNA. The reported dissociation constant (K_d) varies among effectors. For example, dLwaCas13a has a reported K_d of ~46 nM[15], dDiCas7-11 K_d ~ 161 nM[14], and dBzCas13b K_d ~ 33 nM[16]. While the K_d for dPspCas13b is not known, live-cell RNA imaging comparing different dCas13 proteins (e.g., dCas13a, dCas13b, dCas13d) consistently showed that dPspCas13b exhibited better RNA labeling efficiency[17]. This suggests that dPspCas13b likely has a very strong binding affinity that facilitates efficient RNA localization.

Finally, the ABA-induced ABI/PYL1 heterodimerization system used to recruit dCas proteins may influence the binding function differently across effectors. For each dCas, optimizing the linker between ABI and dCas, considering different N or C-terminal fusions, and exploring alternative heterodimerization systems might be necessary.

To characterize the different performance among dCas effectors, we measured transfection efficiency, expression levels, and cytotoxicity of each dCas effector in HeLa cells. Our results indicate that dPspCas13b exhibits higher transfection efficiency and expression levels compared

with other dCas effectors, while dLwaCas13a, dCas13bt1, and dDiCas7-11 show lower expression (**Supplementary Fig. 5a-b**). Additionally, dLwaCas13a shows increased cytotoxicity (**Supplementary Fig. 5c**). These results suggest that dLwaCas13a, dCas13bt1, and dDiCas7-11 might not be ideal for CRISPR-TO applications due to their lower transfection and expression or higher cytotoxicity, which would require further optimization in future studies.

Natural *Actb* mRNA localization inside neurite tips. We initially observed nearly zero *Actb* mRNA particles in neurite tips of the control group (**Extended Data Fig. 8e-f**), which contradicts reports of *Actb* mRNA localization to axonal growth cones[18]. However, after revisiting the original study on *Actb* mRNA localization in cortical neurons[19], we noted that strong *Actb* mRNA signals were detected only in growth cones with a flattened lamellar morphology, whereas spindly growth cones that predominate in our in vitro studies exhibited very weak signals. To further confirm this observation, we performed *Actb* mRNA FISH on primary mouse cortical neurons and examined the morphology of growth cones using immunofluorescence staining of beta-actin protein and Tau (**Supplementary Fig. 10a**) as well as differential interference contrast (DIC) microscopy (**Supplementary Fig. 10b**). Consistent with the original report[19], *Actb* mRNA was abundant in the growth cones with flattened lamellar morphology but largely absent from spindly growth cones (**Supplementary Fig. 10a-b**).

Stability of ABA in cells. In our study, we performed two time-course experiments. Experiment 1 investigated various ABA treatment durations (**Fig. 2j**, left), and Experiment 2 characterized the reversibility of CRISPR-TO by removing ABA for different periods (**Fig. 2j**, right). It is important to know the stability of ABA in cells for interpreting these results. Previous studies reported that about 60% of ABA activity was retained in culture media after 24 hours of incubation with 100 μM ABA in CHO cells[20], suggesting that ABA is sufficiently stable in mammalian cells despite being actively consumed or degraded. In Experiment 2, we assumed that ABA is rapidly depleted from cells after removal from the culture media through both degradation and rapid diffusion. The protonated form of ABA, a weak acid (pKa = 4.7), is uncharged and more hydrophobic and can readily dissolve within the lipid bilayer to permeate the cell membrane[21]. Therefore, we assumed that intracellular ABA can rapidly diffuse back into the media once external ABA is removed.

SUPPLEMENTARY METHODS

Dissection and culture of primary mouse cortical neurons. Primary mouse cortical neurons were dissected from newborn (P0) pups of C57BL/6J mice (The Jackson Laboratory, 000664) using a modified protocol. Mice were housed and bred in the animal facility in the ChemH/Neuroscience building at Stanford University. All mice were maintained under standard housing conditions, including a 12-hour light/12-hour dark cycle, controlled temperature and humidity, with ad libitum access to food and water. All animal procedures were conducted in accordance with the U.S. National Institutes of Health (NIH) guidelines for the care and use of laboratory animals. Protocols were approved by Stanford University's Administrative Panel on Laboratory Animal Care (APLAC protocol #32070). Cortices were dissected from newborn (P0) C57BL/6J mouse (The Jackson Laboratory, 000664) pups in cold, sterile HBSS buffer (Cytiva, SH30268.01) supplemented with 10 mM HEPES (Thermo Fisher Scientific, 15630130) and 1 mM D-glucose. Tissues were digested in digestion medium containing 9 mL RPMI 1640 medium (Thermo Fisher Scientific, 11835030), 10 mg papain (Worthington Biochemical Corporation, LS003119), which was activated in 1 mL papain activation buffer (1.1 mM EDTA, 0.067 mM mercaptoethanol, 5.5 mM cysteine-HCl, pH 6.2), and 20 µL 10 mg/mL DNase I (Sigma Aldrich, DN25-100MG) for 30 min at 37°C. The digested tissues were triturated with 1 mL pipette tips and resuspended in Neurobasal-A medium (Thermo Fisher Scientific, 10888022) supplemented with 2% B-27 (Thermo Fisher Scientific, 17504044), 1% GlutaMAX (Thermo Fisher Scientific, 35050061), and 10% FBS for plating. For RNA FISH staining, the dissociated neurons were plated onto 12 mm diameter coverslips (Carolina, 633029) pre-treated with poly-D-lysine (PDL) (Thermo Fisher Scientific, A3890401) at a density of 60,000 cells per coverslip in one well of the 24-well plate. For live-cell dynamic imaging, the dissociated neurons were plated in 24-well µ-plates (ibidi, 82426) pre-treated with PDL at a density of 80,000 cells per well. For the microfluidic neuron culture and axotomy assay, the dissociated neurons were plated into the soma chamber of a microfluidic device (Xona, SND450) assembled on a PDL-treated 24 mm × 60 mm coverslip (Globe Scientific, 1419-10) at a density of 100,000 cells per device. Neurons were cultured at 37° C and 5% CO_2 in a humidified incubator for 2 hours. All medium then was removed and replaced with culture medium (Neurobasal-A medium supplemented with 2% B-27 and 1% GlutaMAX). At 3 day *in vitro* (3 DIV), half of the old medium was removed and replaced with fresh culture medium containing Floxuridine (FUDR, 16 µM working concentration). Plasmids were transfected using Lipofectamine 2000 (Thermo Fisher Scientific, 11668030) at 5 DIV.

Transfection of primary mouse cortical neurons. For primary mouse cortical neurons cultured in one well of 24-well plates, 1 µL Lipofectamine 2000 diluted in 100 µL transfection medium (Neurobasal-A medium with 2 mM GlutaMAX) was mixed with 0.5 µg plasmids diluted in 100 µL transfection medium and incubated at room temperature for 15-20 min. The mixture was then incubated with primary neurons at 37°C and 5% CO_2 in a humidified incubator for 60-90 min with

all the culture medium removed. After incubation, the mixture was removed, and the culture medium was added back to neurons for culturing.

RNA FISH staining. For RNA FISH staining of HeLa cells and HEK293T cells, cells were washed with 1xPBS once, fixed with fixation buffer A (3.7% formaldehyde in 1xPBS) at room temperature for 10 min, quenched with 50 mM glycine at room temperature for 5 min, washed with 1xPBS twice, and permeabilized in 70% ethanol at 4°C for 1 hour to overnight. For RNA FISH staining of Neuro-2a cells and primary neurons cultured on coverslips or in microfluidic devices, cells were washed with 1xPBS once, fixed with fixation buffer B (4% PFA, 4% sucrose, 1 mM $MgCl_2$, and 0.1 mM $CaCl_2$ in 1xPBS) at room temperature for 20 min, quenched with 50 mM glycine at room temperature for 5 min, and permeabilized in permeabilization buffer (0.1% Triton X-100, 1 mM $MgCl_2$, and 0.1 mM $CaCl_2$ in 1xPBS) at room temperature for 15 min. Permeabilized cells were incubated with wash buffer A (10% formamide in 2xSSC buffer) at room temperature for 30 min. To be noted, for RNA FISH staining of *Rn28s1* rRNA, the permeabilized cells were incubated with 70% formamide in 2xSSC buffer at 37°C for 30 min to enhance RNA detection.

The cells were then incubated with hybridization system [10% formamide and 0.12 μM FISH probes in Stellaris RNA FISH Hybridization Buffer (Stellaris, SMF-HB1-10)] at 37°C for 4 to 16 hours. Cells were then washed twice with wash buffer B (15% formamide in 2xSSC buffer) at 37°C for 30 min, washed with PBST buffer (0.1% Tween-20 in 1xPBS) once, washed with 2xSSC buffer once, and mounted onto slides with VECTASHIELD PLUS Antifade Mounting Medium (Vector Laboratories, H-1900-10) for imaging.

Immunofluorescence (IF) staining. For IF staining of HeLa cells, cells were washed with 1xPBS once, fixed with cold 100% methanol at -20°C for 10 min, and washed with 1xPBS for another three times. The fixed cells were blocked with 3% BSA at room temperature for 30 min, followed by the incubation with primary antibody in 1xPBS at 37°C for 1 hour. Cells were then washed with PBST buffer twice, washed with 1xPBS once, and incubated with secondary antibody in 1xPBS at room temperature for 30 min. Cells were washed with PBST buffer for three times, stained with DAPI, and mounted onto slides with VECTASHIELD PLUS Antifade Mounting Medium for imaging.

IF-FISH staining. For IF-FISH staining of *Actb* mRNA, *Rn28s1* rRNA, and puromycin, fixed neurons were first stained with mouse anti-puromycin antibody (Kerafast, Kf-Ab02366-1.1, 1:2,500 dilution) in PBS with 1 U/μL RNase inhibitor at room temperature for 1.5 hours. Neurons were then washed with PBST buffer twice, washed with PBS once, and incubated with secondary antibody diluted in PBS with 0.5 U/μL RNase inhibitor at room temperature for 30 min. Neurons were then washed with PBST buffer for three times, washed with PBS once, fixed with fixation buffer B at room temperature for 10 min, quenched with 50 mM glycine at room temperature for

5 min, and washed with PBS once. Neurons were then incubated with 70% formamide in 2xSSC buffer at 37°C for 30 min to enhance RNA detection and incubated with hybridization system [1 U/μL RNase inhibitor, 10% formamide, and 0.12 μM FISH probes in Stellaris RNA FISH Hybridization Buffer (Stellaris, SMF-HB1-10)] at 37°C for 4 hours. Cells were then washed twice with wash buffer B (15% formamide in 2xSSC buffer) at 37°C for 30 min, washed with PBST buffer once, washed with 2xSSC buffer once, and mounted onto slides with buffer containing Tris-HCl (pH=7.5), 100 mM cysteamine (Sigma-Aldrich, M6500), 5% glucose (Sigma-Aldrich, G8270), 0.8 mg/mL glucose oxidase from *Aspergillus niger* (Sigma-Aldrich, G2133-10KU), and 0.04 mg/mL catalase from bovine liver (Sigma-Aldrich, C9322) for STORM microscopy.

Quantitative reverse transcription PCR (RT-qPCR). Total RNA was first extracted from cells using RNeasy Plus Mini Kit (Qiagen, 74136). cDNA was then synthesized from total RNA using iScript™ cDNA Synthesis Kit (Bio-Rad, 1708891). The abundance of mRNA of interest was quantified with RT-qPCR using iTaq Universal SYBR Green Supermix (Bio-Rad, 1725124) and corresponding RT-qPCR primers (**Supplementary Table 8**). Samples were run on a BioRad CFX384 Touch Real-Time PCR Detection System in three technical replicates for each experimental replicate. Gene expression was quantified using the 2-ΔΔCT method using *GAPDH* mRNA (**Extended Data Fig. 6g**) or *ACTB* mRNA (**Extended Data Fig. 6d, Supplementary Fig. 7b**) as an internal control.

RNA immunoprecipitation assay. Lenti-X 293T cells were plated in 6-well plates and transfected with 1.3 μg pSLQ10530 and 1.7 μg gRNA plasmid (pUC-PspCas13b-gG1, gG2, gG3, or gNT) using 9 μL TransIT-LT1 Transfection Reagent. Two days after transfection, cells were washed with PBS once and lysed with 200 μL ice-cold lysis buffer [RIPA lysis and extraction buffer (Thermo, 89900) supplemented with 1× protease inhibitor (Thermo, 87785) and 1 U/μL RNase inhibitor (NxGen, F83923-1)] on ice for 10 min. Cell lysate were centrifuged at 16,000 × g for 10 min at 4°C. 50 μL of supernatant was applied for extracting total RNA using RNeasy Plus Mini Kit and 100 μL of supernatant was applied for RNA immunoprecipitation.

For RNA immunoprecipitation, 50 μL per sample of Pierce Protein G Magnetic Beads (Thermo, 88848) were washed once with wash buffer (PBS with 0.02% Tween-20), resuspended in 100 μL wash buffer with 2 μg mouse anti-Flag IgG (Sigma, F1804), and incubated at room temperature for 10 min on a rotator to allow antibody to conjugate to the beads. The conjugated beads were washed with wash buffer for three times, resuspended in 100 uL ice-cold lysis buffer, and mixed with 100 μL cell lysate to incubate on a rotator at 4°C overnight. Beads were then washed with 200 μL 1xRIPA buffer with 0.02% Tween-20 for three times, washed once with 200 μL DNase buffer [350 mM Tris-HCl (pH 6.5), 50 mM MgCl2, and 5 mM DTT), and incubated with 50 μL DNase buffer containing 0.08 U/μL DNase I (Sigma, DN25-100MG) on a rotator at 37°C for 30 min to remove DNA contamination. After DNase digestion, 50 μL 1xRIPA buffer containing 0.8 U Proteinase K (NEB, P8107S) was added and incubated with beads on a rotator at

37°C for 30 min to digest proteins. After Proteinase K digestion, the supernatant of beads was taken for RNA extraction using TRIzol (Thermo, 15-596-018). Briefly, 100 µL supernatant was mixed with 300 µL Trizol and 60 µL chloroform. After centrifuge at 16,000 × g at 4°C for 10 min, the aqueous phase was collected, supplemented with 0.5 µL 5 mg/mL glycogen (Thermo, AM9510), and precipitated with 250 µL isopropanol on ice for 10 min. The precipitated RNA was pelleted by spinning at 16,000 × g at 4°C for 10 min, washed twice with 75% cold ethanol, and dissolved in 10 µL H_2O.

1/30 of the extracted total RNA and 5 µL immunoprecipitation purified RNA were reverse transcribed to cDNA using iScript cDNA Synthesis Kit. The abundance of *GAPDH* mRNA and *ACTB* mRNA which serves as an internal control was quantified as described in '**Quantitative reverse transcription PCR (RT-qPCR)**'.

Image processing and quantitative analysis. Image processing was performed in Fiji[22] unless otherwise specified. To quantify the percentage of target RNA with high expression level and dCas13 protein localized at the specific subcellular location (OMM, p-bodies, stress granules, telomeres, nuclear stress bodies, and centrosomes) (**Fig. 1c, 1e, 2j, Extended Data Fig. 2b, 2f-g, 2j, 3h, 5b-d, 6a-b, 6i-j, 6l, 7a-b, 7d**), we developed a new MATLAB code (calculate_%_RNA_dCas13_colocalization.m) which enables automatized thresholding of each channel for calculation. In this code, the cut-off value for the colocalization factor is calculated based on the statistics of the pixel values in the image. For the RNA and dCas13 channel, pixels with intensity values greater than the median + 1×STD are considered positive. For the subcellular location channel, we tested factors of 1, 1.5, and 2 (applied as median + factor×STD) and selected the factor that best reflected the subcellular location distribution to generate a mask for each batch (detailed in **Supplementary Table 10**). The percentage of target RNA or dCas13 protein localized at the subcellular location was determined by calculating the percentage of the integrated intensity of RNA or dCas13 channel within the mask to that within the cell.

To quantify the percentage of target RNA with low expression level localized on the OMM (**Extended Data Fig. 2c-e**), we developed a new MATLAB code (colocalization_RNA_OMM.m) which quantifies the percentage of RNA particles detected by ThunderSTORM localized inside the OMM mask generated by MATLAB code (calculate_%_RNA_dCas13_colocalization.m). The two codes are available at the Github (https://github.com/QilabGitHub/CRISPR-TO).

To quantify the percentage of cells with dCas13 or *GAPDH* mRNA enriched around the leading edge of the cell (**Extended Data Fig. 6k**), the number of cells co-expressing dCas13 and PYL1-fusion proteins and cells with dCas13 or *GAPDH* mRNA enriched around cell edge was manually determined without double counting.

To quantify the percentage of dCas13 protein (488 nm channel) or reporter mRNA (647 nm channel) localized on the OMM (405 nm channel) in single cells (**Fig. 1f-g, Extended Data**

Fig. 1i, 3d, 3g), Coloc 2, a plugin in Fiji for colocalization analysis, was used. Briefly, background was first subtracted from all the three channels. Within the region of the target cell, Coloc 2 was used to calculate Mander's overlap coefficient M1[23] of the 488 nm channel with the 405 nm channel to get the percentage of dCas13 protein localized on the OMM, and M1 of the 647 nm channel with the 405 nm channel to get the percentage of target mRNA localized on the OMM.

To estimate the number of reporter mRNA particles labeled by RNA FISH probes per cell within one z-slice (**Fig. 1f, Extended Data Fig. 3c-d**), the fluorescence intensity of single reporter mRNA particles was first measured by fitting the regions containing sparse and well-separated reporter mRNA particles in cells of the gT+DMSO group with ThunderSTORM[24] (**Extended Data Fig. 3b**). The distribution of fluorescence intensity of the isolated reporter mRNA particles displayed a unimodal distribution (**Extended Data Fig. 3b**), suggesting that the analyzed reporter mRNA particles were single molecules[25,26]. Then the total intensity of reporter mRNAs from a given cell of the gT+ABA group was measured by fitting the image of the whole cell using ThunderSTORM and summing the intensities of all obtained peaks. The sum of the intensities was further divided by the median intensity of a single reporter mRNA particle to get the estimated number of reporter mRNA particles within one z-slide of that cell.

To quantify the fluorescence intensity of RNA FISH signals or IF signals in single cells for analyzing the influence of dCas13 binding on mRNA stability and translation (**Fig. 1j, Extended Data Fig. 4g-l**, **4s**, **4v-x**), the z-stack images were first sum projected. Cells expressing dCas13 were manually cropped and the integrated intensity of RNA FISH signals or IF signals in each cell was quantified using the MeasureObjectIntensity module in CellProfiler[27]. Then the background intensity measured from regions without cells were subtracted from the integrated intensity of each cell and the obtained data were normalized such that the minimum value was set to 1 for the purpose of plotting.

To calculate the Polarization Index (PI) and Dispersion Index (DI)[28] for analyzing the impact of dCas13 binding on RNA distribution (**Fig. 1j, Extended Data Fig. 4m-4r**), we developed two pipelines.

Pipeline 1 is for analyzing RNAs with a low expression level (*NDUFS2*, *SDHC*, and *SDHD*) that can be recognized as punctus. The position of each RNA particle ($xRNA_i, yRNA_i$) was first detected using Thunderstorm. The PI was calculated using the equation:

$$\mathrm{PI} = \frac{\sqrt{(\overline{xRNA}-\overline{xcell})2+(\overline{yRNA}-\overline{ycell})2}}{Rgcell} \qquad \text{(Equation 1)}$$

In Equation 1, $\overline{xRNA}$ and $\overline{yRNA}$ are the mean x and y position of all distinct RNA particles, i.e. $\overline{xRNA} = \frac{\sum_{i=1}^{N} xRNA_i}{N}$; $\overline{yRNA} = \frac{\sum_{i=1}^{N} yRNA_i}{N}$. $\overline{xcell}$ and $\overline{ycell}$ are the centroid of the cell determined from the cell outline. Rg is the radius of gyration of the cell.

The second moment of RNA positions was calculated as:

$$\mu 2 = \frac{\sum_{i=1}^{N} \sqrt{(xRNA_i - \overline{xRNA})\text{^}2 + (yRNA_i - \overline{yRNA})\text{^}2}}{N} \qquad \text{(Equation 2)}$$

Here, $(xRNA_i,\ yRNA_i)$ are the position of i[th] RNA particles (total RNA count is N for each cell). Second moment of the hypothetical uniform distribution μ2′ of each cell was calculated as the second moment of each pixel's coordinates using the following equation:

$$\mu'2 = \frac{\sum_{i=1}^{M} \sqrt{(X_i - \overline{xRNA})\text{^}2 + (Y_i - \overline{yRNA})\text{^}2}}{M} \qquad \text{(Equation 3)}$$

Here, (X_i, Y_i) is the position of i[th] pixel. The DI was calculated as:

$$\text{DI} = \frac{\mu 2}{\mu' 2} \qquad \text{(Equation 4)}$$

Pipeline 2 is for analyzing RNAs with a high expression level (*GAPDH*, human *ACTB*, and mouse *Actb*) that cannot be recognized as distinct punctus. The center of all RNA molecules, ($\overline{xRNA}$, $\overline{yRNA}$), was detected using:

$$\overline{xRNA} = \frac{\sum_{i=1}^{M} X_i \times I_i}{\sum_{i=1}^{M} I_i} \qquad \text{(Equation 5)}$$

$$\overline{yRNA} = \frac{\sum_{i=1}^{M} Y_i \times I_i}{\sum_{i=1}^{M} I_i} \qquad \text{(Equation 6)}$$

Here (X_i, Y_i) are the position of i[th] pixel and I_i is the intensity of i[th] pixel.

The PI was calculated using:

$$\text{PI} = \frac{\sqrt{(\overline{xRNA} - \overline{xcell})2 + (\overline{yRNA} - \overline{ycell})2}}{Rgcell} \qquad \text{(Equation 7)}$$

$\overline{xcell}$ and $\overline{ycell}$ are the centroid of the cell determined from the cell outline. Rg is the radius of gyration of the cell.

The corresponding u2 and u2' were calculated as:

$$\mu 2 = \frac{\sum_{ij} I_{ij} * r_{ij}\text{^}2}{\sum_{ij} I_{ij}} \qquad \text{(Equation 8)}$$

Here, r_{ij} is the distance from the centroid of the cell to pixel (i, j) and I_{ij} is the intensity of pixel (i, j).

$$\mu'2 = \frac{\sum_{i=1}^{M} (X_i - \overline{xRNA})\text{^}2 + (Y_i - \overline{yRNA})\text{^}2}{M} \qquad \text{(Equation 9)}$$

Here, (X_i, Y_i) is the position of i[th] pixel and I_i is the intensity of i[th] pixel. The DI was calculated using Equation 4.

To quantify the recruitment of MS2 reporter mRNA labeled with stdMCP-tdTomato to the minus end of microtubules after ABA addition (**Extended Data Fig. 7g**), an ROI of 45 × 45 pixels

was drawn to include the centrosome. The mean intensity of tdTomato per pixel in the ROI and the percentage of tdTomato fluorescence integrated intensity within the ROI relative to the total fluorescence intensity in the entire cell in each frame is measured by Fiji. Trackmate plugin (Fiji) was applied to obtain the RNA trajectories (**Extended Data Fig. 7h**). The trajectories are exhibited with their calculated traversed distance *R* (Equation 10) from smallest to largest:

$$R = \frac{\sqrt{(x(t)_{max} - x(t)_{min})^2 + (y(t)_{max} - y(t)_{min})^2}}{\sqrt{n}} \qquad \text{(Equation 10)}$$

(*x(t), y(t)*) is the position of the RNA particle as a function of time. *n* is the step length of the trajectory.

The ensemble-averaged mean-square displacement (MSD) was calculated as:

$$MSD(\tau) = \langle \left(\vec{R}(t+\tau) - \vec{R}(t) \right)^2 \rangle = \frac{1}{N} \sum_i \frac{1}{m} \sum_m [\vec{R}_i(mt+\tau) - \vec{R}_i(mt)]^2 \qquad \text{(Equation 11)}$$

Here, *N* is the number of trajectories over which the ensemble average is taken (*N* = 20 here for each type). The index m runs from 1 to a specific value given the lag time τ, providing the time average of each trajectory. The final MSD is an average over the ensemble and over time. For RNA imaged every 3 seconds, *m* runs from 1 to 9. The line in MSD plot is the linear fitting of the first 3 points (**Extended Data Fig. 7i**). The distance to ROI was calculated as the distance from the position of an RNA particle at each time point to the center point in ROI (**Extended Data Fig. 7j**).

To quantify the fluorescence intensity of dCas13 (488 nm channel), *Actb* mRNA FISH signals (647 nm channel), and KIF5A*-PYL1 (405 nm channel) in the neurite tips of primary neurons (**Fig. 3d**), the channel-dependent background was first subtracted from all the three channels and an ROI of 30 × 30 pixels was drawn to include a neurite tip to measure its integrated fluorescence intensity for each channel. To calculate the ratio of fluorescence intensity of *Actb* mRNA compared to dCas13 in the neurite tips (**Fig. 3k**), an ROI of 40 × 40 pixels was drawn to include a neurite tip to measure its integrated fluorescence intensity for each channel without removing the background and the ratio was calculated using the measured integrated intensity.

The distance between two mRNA particles in neurites (**Fig. 3g**) was calculated based on the location of mRNA particles detected with ThunderSTORM.

To quantify the number of *Actb* mRNA particles per neurite tip (**Fig. 3e, 3j**), an ROI was first drawn to include a separated *Actb* mRNA particle in the gT+ABA group to measure its fluorescence intensity (**Extended Data Fig. 8g**). The fluorescence intensity of *Actb* mRNA in one neurite tip was divided by the median intensity of a single *Actb* mRNA particle to calculate the number of *Actb* mRNA particles per neurite tip. To quantify the number of *Actb* mRNA particles per neurite tip in **Extended Data Fig. 9m** and the number of *Stmn2* mRNA particles per neurite tip in **Fig. 5e**, the neurite tips were cropped and analyzed using ThunderSTORM to measure the number of mRNA particles.

To quantify the number of *ACTB* mRNA particles per µm in neurites (**Fig. 3f**), the image was first cropped to include a fragment of a neurite. The image of CAAX-Crimson was binarized using a manually set threshold such that the background pixels would have zero values and the pixels corresponding to the neurite membrane would equal to unity. The positions of mRNA particles were detected with subpixel precision in ThunderSTORM. Further processing was done in MATLAB. The coordinates of the centers of the pixels positive for CAAX-Crimson were converted to nanometers and the distances between them and the mRNA particles were calculated using the pdist2 function. An mRNA particle was counted as associated with a neurite if the particle was found within 195 nm from the center of a closest CAAX-Crimson pixel.

To quantify the number of *Actb* mRNA particles per µm in microfluidic channels (**Extended Data Fig. 9q**), a fragment of a microfluidic channel was cropped and the number of *Actb* mRNA particles were measured using ThunderSTORM.

Neuroanatomy/SNT plugin (Fiji)[29] was used to measure the length of neurites (**Fig. 3f**) and regenerated axons (**Fig. 4k-4l**) based on the CAAX-Crimson signals.

To quantify the number of protrusions at the neurite tip (**Fig. 4i**), a custom pipeline was generated in CellProfiler[27,30]. A ROI which only contains the neurite tip was manually cropped out from the image for analysis in CellProfiler. The position of the neurite tip (primary object) was identified based on the signal of KIF5A*-PYL1 using the IdentifyPrimaryObjects module. Neurites indicated by CAAX-mNeonGreen were then enhanced using the EnhanceOrSuppressFeatures module, converted into a binary image using the Threshold module, identified as secondary objects based on the primary object location using the IdentifySecondaryObjects module, and skeletonized using the Morph (skelpe) module. Finally, the skeletonized neurites were automatically measured using the MeasureObjectSkeleton module to get the value of NumberTrunks and the number of protrusions at the neurite tip was calculated by subtracting 1 from the value of NumberTrunks.

To quantify the percentage of neurite tips growing out dynamic protrusions after DMSO or ABA treatment (**Fig. 4j**), the number of neurite tips which did not have protrusions before DMSO or ABA treatment but grew out dynamic protrusions after DMSO or ABA treatment was manually determined without double counting.

To quantify the percentage of *Actb* mRNA particles colocalized with *Rn28s1* rRNA in the neurites (**Extended Data Fig. 9e**), a fragment of neurite containing well separated *Actb* mRNA particles and with CAAX-mNeonGreen signal was first cropped out from the image. The locations of *Actb* mRNA particles were then detected with ThunderSTORM. The fluorescence intensity of *Rn28s1* rRNA at the location of the *Actb* mRNA particle was quantified using a custom MATLAB script. Specifically, for each *Actb* mRNA position (x0, y0), a 3 pixel x 3 pixel box region was chosen (pixel size = 162.5 nm) and the mean intensity within the box region in the rRNA channel

were calculated. The distribution of the intensity of rRNA was plotted in **Extended Data Fig. 9e**. We also calculated the rRNA intensity distribution for 38 *Actb* mRNA particles that do not colocalize with rRNA (**Extended Data Fig. 9e**, black), as judged manually (**Extended Data Fig. 9d, 9f**), and used the maximum intensity value as a cutoff intensity to quantify the percentage of *Actb* mRNA particles colocalized with *Rn28s1* rRNA.

Statistics analysis. For the dose response curves to ABA (**Extended Data Fig. 7a**), we assumed the percentage of dCas13-ABI or *GAPDH* mRNA localized on the OMM follows a saturation binding curve with Hill equation:

$$F([ABA]) = A_0 + A_m \cdot \frac{[ABA]^n}{K_d + [ABA]^n} \qquad \text{(Equation 12)}$$

Here, K_d represents the apparent dissociation constant, and n represents the Hill coefficient. We constrained A_0 as the mean of the observed fractions under the 0 μM ABA condition.

For *GAPDH* mRNA localization to the OMM under different ABA treatment time (**Fig. 2j**, left), we assumed a simple exponential model:

$$F_{mRNA}(t) = A_0^{mRNA} + A_m^{mRNA} \cdot (1 - e^{-t/\tau_{mRNA}}) \qquad \text{(Equation 13)}$$

Here, τ_{mRNA} is the characteristic time of the colocalization.

For dCas13-ABI localization to the OMM under different ABA treatment time (**Extended Data Fig. 7b-c**), we assumed a "two-phase exponential" model, in which the observed curve is the combined effect of two molecule species: free dCas13-ABI (fast) and mRNA bound dCas13-ABI (slow). Based on this assumption, the slower phase can be described using the above result about the mRNA dynamics (F_{mRNA}). Therefore, the dynamic of dCas13-ABI can be described as below:

$$F_{dCas}(t) = A_0^{dCas} + A_m^{dCas} \cdot (1 - r) \cdot \left(1 - e^{-t/\tau_{dCas}}\right) + r \cdot F_{mRNA}(t) \qquad \text{(Equation 14)}$$

Here, r represents the mRNA-bound dCas13-ABI's contribution to the observed localization.

For the dissociation curves (**Fig. 2j**, right; **Extended Data Fig. 7d**), a simple exponential decay curve is used:

$$F(t) = A_0 + A_m \cdot e^{-t/\tau} \qquad \text{(Equation 15)}$$

Here, τ is the characteristic time of the dissociation. We further constrained A_0 (equivalent to $F_{t\to\infty}$) to be mean of the fractions from the DMSO group (released for infinite amount of time).

For all the regression analysis above, we used the curve_fit function from the SciPy package, which utilizes a least square method for curve fitting. The code for the above analysis is available at the Github (https://github.com/QilabGitHub/CRISPR-TO).

SUPPLEMENTARY TABLES

Supplementary Table 1 | Plasmids information. Description, plasmid number, and source of all the plasmids used in this study.

Description	Plasmid #	Source
pHR-EF1a-NES-dPspCas13b-EGFP-ABI	pSLQ10530	Cloned in this study
pHR-EF1a-NLS-dPspCas13b-EGFP-ABI	pSLQ10531	Cloned in this study
pHR-EF1a-NLS-ABI-dPspCas13b-BFP	pSLQ10524	Cloned in this study
pHR-EF1a-NLS-dPspCas13b-Linker1-BFP-ABI	pSLQ10527	Cloned in this study
pHR-EF1a-NLS-dPspCas13b-Linker2-BFP-ABI	pSLQ10529	Cloned in this study
pHR-EF1a-NES-dPspCas13b-Linker1-BFP-ABI	pSLQ10526	Cloned in this study
pHR-SFFV-NES-dPspCas13b-EGFP-ABI	pSLQ10608	Cloned in this study
pHR-TRE3G-3xFlag-IRES-NES-dPspCas13b-EGFP-ABI	pSLQ14222	Cloned in this study
pHR-PspCas13b-mU6-G1-hU6-G2-7SK-G3-PGK-PuroR	pSLQ14233	Cloned in this study
pHR-EF1a-PYL1-BFP-MAVS (aa510-540)	pSLQ10680	Cloned in this study
pHR-PGK-PYL1-BFP-MAVS(aa510-540)	pSLQ10550	Cloned in this study
pHR-SFFV-PYL1-BFP-DDX6	pSLQ10539	Cloned in this study
pHR-PGK-PYL1-BFP-G3BP1	pSLQ10552	Cloned in this study
pHR-PGK-PYL1-BFP-KIFC1(aa125-673)	pSLQ10622	Cloned in this study
pHR-PGK-KIF5B(aa1-555)-BFP-PYL1	pSLQ10554	Cloned in this study
pHR-PGK-HSF1-BFP-PYL1	pSLQ14806	Cloned in this study
pUC-CMV-TRF1-BFP-PYL1	pSLQ14566	Cloned in this study
PGK-mRuby3-1xGCN4	pSLQ10666	Cloned in this study
PGK-mRuby3-2xGCN4	pSLQ10667	Cloned in this study
PGK-mRuby3-3xGCN4	pSLQ10668	Cloned in this study
PGK-mRuby3-7xGCN4	pSLQ10669	Cloned in this study
CMV-BFP-24xGCN4	pSLQ14274	Cloned in this study
pHR-PGK-PYL1-HaloTag-MAVS(aa510-540)	pSLQ10623	Cloned in this study
pHR-PGK-PYL1-HaloTag-KIFC1(aa125-673)	pSLQ10650	Cloned in this study
pCAGGS-CAG-NES-dPspCas13b-EGFP-ABI	pSLQ10625	Cloned in this study
pHR-CAG-KIF5A(aa1-559)-BFP-PYL1	pSLQ14256	Cloned in this study
pHR-CAG-Crimson-CAAX	pSLQ14264	Cloned in this study
pHR-PGK-mKIF5A(aa1-559)-HaloTag-PYL1	pSLQ14826	Cloned in this study
pHR-EF1a-NES-dPspCas13b-EGFP-ABI_CMV-puro	pSLQ10671	Cloned in this study
pUC-CMV-Flag-NLS-dPspCas13b-Linker-EGFP-ABI-V5	pSLQ14565	Cloned in this study
pUC-CMV-TRF1-BFP-PYL1	pSLQ14566	Cloned in this study
pCAGGS-CAG-Crimson-CAAX	pSLQ14827	Cloned in this study

pCAGGS-CAG-NES-dPspCas13b-HaloTag-ABI	pSLQ14828	Cloned in this study
pCAGGS-CAG-mNeonGreen-CAAX	pSLQ14829	Cloned in this study
pCAGGS-CAG-NES-dPspCas13b-ABI	pSLQ14811	Cloned in this study
pHR-CAG-HaloTag-CAAX	pSLQ14266	Cloned in this study
CMV-Dendra2-24xGCN4	pSLQ14848	Cloned in this study
pHR-CAG-mKIF5A(aa1-559)-mCherry-PYL1	pSLQ14253	Cloned in this study
pHR-CAG-mKIF5A(aa1-559)-mNeonGreen-PYL1	pSLQ14837	Cloned in this study
pUC-CAG-mScarlet-I-CAAX	pSLQ14568	Cloned in this study
pCAGGS-CAG-PYL1-BFP-hKIFC1(aa125-673)	pSLQ10628	Cloned in this study
pCXX37-EF1a-Flag-NES-dCasRx-Linker-EGFP-ABI-V5	pSLQ14206	Cloned in this study
pCXX37-EF1a-Flag-NES-dLwaCas13a-Linker-EGFP-ABI-V5	pSLQ14830	Cloned in this study
pCXX37-EF1a-Flag-NES-Di-dCas7-11-Linker-EGFP-ABI-V5	pSLQ14831	Cloned in this study
pCXX37-EF1a-Flag-NES-dCas13bt1-Linker-EGFP-ABI-V5	pSLQ14832	Cloned in this study
pCXX37-EF1a-Flag-NLS-dLwaCas13a-Linker-EGFP-ABI-V5	pSLQ14870	Cloned in this study
pCXX37-EF1a-Flag-NLS-Di-dCas7-11-Linker-EGFP-ABI-V5	pSLQ14871	Cloned in this study
pCXX37-EF1a-Flag-NLS-dCas13bt1-Linker-EGFP-ABI-V5	pSLQ14872	Cloned in this study
pCXX37-EF1a-Flag-NLS-dCasRx-Linker-EGFP-ABI-V5	pSLQ14873	Cloned in this study
pCAGGS-CAG-mScarlet3-CAAX	pSLQ14857	Cloned in this study
pCAGGS-TRE3G-BFP-7xGCN4-CMV-rtta	pSLQ14860	Cloned in this study
pHR-SFFV-PYL1-mCherry-hDDX6	pSLQ14861	Cloned in this study
pcDNA3_CMV-FLAG-24xSuntagV4-oxEBFP-AID-baUTR1-MS2x24	pSLQ14862	Cloned in this study
pCAGGS-CAG-HaloTag-CAAX	pSLQ14863	Cloned in this study
pUbC-OsTIR1-myc-IRES-scFv-sfGFP	pSLQ10562	Addgene plasmid 84563
RG6	pSLQ10471	Addgene plasmid 80167
pmRuby3-24xGCN4	pSLQ10461	Addgene plasmid 132413
PHY23-phage-ubc-nls-ha-stdMCP-tdTomato	pSLQ10573	Addgene plasmid 164044
pHR-EF1alpha-Tet3G-2A	pSLQ1709	From reference [31]
pUC-PspCas13b-gRNA-backbone	pSLQ10481	Cloned in this study
pUC-pspcas13b-gNT	N/A	Spacer sequence from reference [9]
pUC-pspcas13b-gNT2	N/A	Cloned in this study

pUC-pspcas13b-gNT3	N/A	Spacer sequence from reference [32]
pUC-PspCas13b-gSA	N/A	Spacer sequence from reference [11]
pUC-PspCas13b-gGCN4	N/A	Spacer sequence from reference [17]
pUC-PspCas13b-gMS2	N/A	Cloned in this study
pUC-PspCas13b-gTERRA	N/A	Cloned in this study
pUC-PspCas13b-hGAPDH-gRNA1	N/A	Cloned in this study
pUC-PspCas13b-hGAPDH-gRNA2	N/A	Cloned in this study
pUC-PspCas13b-hGAPDH-gRNA3	N/A	Cloned in this study
pUC-PspCas13b-hACTB-gRNA1	N/A	Cloned in this study
pUC-PspCas13b-hACTB-gRNA2	N/A	Cloned in this study
pUC-PspCas13b-hACTB-gRNA3	N/A	Cloned in this study
pUC-PspCas13b-hSDHC-gRNA1	N/A	Cloned in this study
pUC-PspCas13b-hSDHC-gRNA2	N/A	Cloned in this study
pUC-PspCas13b-hSDHC-gRNA3	N/A	Cloned in this study
pUC-PspCas13b-hSDHD-gRNA1	N/A	Cloned in this study
pUC-PspCas13b-hSDHD-gRNA2	N/A	Cloned in this study
pUC-PspCas13b-hSDHD-gRNA3	N/A	Cloned in this study
pUC-PspCas13b-hNDUFS2-gRNA1	N/A	Cloned in this study
pUC-PspCas13b-hNDUFS2-gRNA2	N/A	Cloned in this study
pUC-PspCas13b-hNDUFS2-gRNA3	N/A	Cloned in this study
pUC-PspCas13b-mActb-gRNA1	N/A	Cloned in this study
pUC-PspCas13b-mActb-gRNA2	N/A	Cloned in this study
pUC-PspCas13b-mActb-gRNA3	N/A	Cloned in this study
pUC-PspCas13b-mActb-gRNA4	N/A	Cloned in this study
pUC-PspCas13b-mActb-gRNA5	N/A	Cloned in this study
pUC-PspCas13b-mActb-gRNA6	N/A	Cloned in this study
pUC-PspCas13b-mActb-gRNA7	N/A	Cloned in this study
pUC-PspCas13b-mGap43-gRNA1	N/A	Cloned in this study
pUC-PspCas13b-mGap43-gRNA2	N/A	Cloned in this study
pUC-PspCas13b-mGap43-gRNA3	N/A	Cloned in this study
pUC-PspCas13b-mGap43-gRNA4	N/A	Cloned in this study
pUC-PspCas13b-mGap43-gRNA5	N/A	Cloned in this study
pUC-PspCas13b-mGap43-gRNA6	N/A	Cloned in this study
pUC-PspCas13b-mGap43-gRNA7	N/A	Cloned in this study
pUC-PspCas13b-mGap43-gRNA8	N/A	Cloned in this study
pUC-PspCas13b-mGap43-gRNA9	N/A	Cloned in this study
pUC-PspCas13b-mGap43-gRNA10	N/A	Cloned in this study
pUC-PspCas13b-mGap43-gRNA11	N/A	Cloned in this study

pUC-PspCas13b-mGap43-gRNA12	N/A	Cloned in this study
pUC-PspCas13b-mGap43-gRNA13	N/A	Cloned in this study
pUC-PspCas13b-mGap43-gRNA14	N/A	Cloned in this study
pUC-PspCas13b-mImpa1-gRNA1	N/A	Cloned in this study
pUC-PspCas13b-mImpa1-gRNA2	N/A	Cloned in this study
pUC-PspCas13b-mImpa1-gRNA3	N/A	Cloned in this study
pUC-PspCas13b-mImpa1-gRNA4	N/A	Cloned in this study
pUC-PspCas13b-mImpa1-gRNA5	N/A	Cloned in this study
pUC-PspCas13b-mKpnb1-gRNA1	N/A	Cloned in this study
pUC-PspCas13b-mKpnb1-gRNA2	N/A	Cloned in this study
pUC-PspCas13b-mKpnb1-gRNA3	N/A	Cloned in this study
pUC-PspCas13b-mKpnb1-gRNA4	N/A	Cloned in this study
pUC-PspCas13b-mKpnb1-gRNA5	N/A	Cloned in this study
pUC-PspCas13b-mMtor-gRNA1	N/A	Cloned in this study
pUC-PspCas13b-mMtor-gRNA2	N/A	Cloned in this study
pUC-PspCas13b-mMtor-gRNA3	N/A	Cloned in this study
pUC-PspCas13b-mMtor-gRNA4	N/A	Cloned in this study
pUC-PspCas13b-mMtor-gRNA5	N/A	Cloned in this study
pUC-PspCas13b-mTdp43-gRNA1	N/A	Cloned in this study
pUC-PspCas13b-mTdp43-gRNA2	N/A	Cloned in this study
pUC-PspCas13b-mTdp43-gRNA3	N/A	Cloned in this study
pUC-PspCas13b-mTdp43-gRNA4	N/A	Cloned in this study
pUC-PspCas13b-mTdp43-gRNA5	N/A	Cloned in this study
pUC-PspCas13b-mStmn2-gRNA1	N/A	Cloned in this study
pUC-PspCas13b-mStmn2-gRNA2	N/A	Cloned in this study
pUC-PspCas13b-mStmn2-gRNA3	N/A	Cloned in this study
pUC-PspCas13b-mStmn2-gRNA4	N/A	Cloned in this study
pUC-PspCas13b-mStmn2-gRNA5	N/A	Cloned in this study
pUC-PspCas13b-mRhoA-gRNA1	N/A	Cloned in this study
pUC-PspCas13b-mRhoA-gRNA2	N/A	Cloned in this study
pUC-PspCas13b-mRhoA-gRNA3	N/A	Cloned in this study
pUC-PspCas13b-mRhoA-gRNA4	N/A	Cloned in this study
pUC-PspCas13b-mRhoA-gRNA5	N/A	Cloned in this study
pUC-PspCas13b-mPum2-gRNA1	N/A	Cloned in this study
pUC-PspCas13b-mPum2-gRNA2	N/A	Cloned in this study
pUC-PspCas13b-mPum2-gRNA3	N/A	Cloned in this study
pUC-PspCas13b-mPum2-gRNA4	N/A	Cloned in this study
pUC-PspCas13b-mPum2-gRNA5	N/A	Cloned in this study
pUC-PspCas13b-mPten-gRNA1	N/A	Cloned in this study
pUC-PspCas13b-mPten-gRNA2	N/A	Cloned in this study
pUC-PspCas13b-mPten-gRNA3	N/A	Cloned in this study

pUC-PspCas13b-mPten-gRNA4	N/A	Cloned in this study
pUC-PspCas13b-mPten-gRNA5	N/A	Cloned in this study
pUC-PspCas13b-mTmsb4x-gRNA1	N/A	Cloned in this study
pUC-PspCas13b-mTmsb4x-gRNA2	N/A	Cloned in this study
pUC-PspCas13b-mTmsb4x-gRNA3	N/A	Cloned in this study
pUC-PspCas13b-mTmsb4x-gRNA4	N/A	Cloned in this study
pUC-PspCas13b-mTmsb4x-gRNA5	N/A	Cloned in this study
pUC-PspCas13b-mSmn1-gRNA1	N/A	Cloned in this study
pUC-PspCas13b-mSmn1-gRNA2	N/A	Cloned in this study
pUC-PspCas13b-mSmn1-gRNA3	N/A	Cloned in this study
pUC-PspCas13b-mSmn1-gRNA4	N/A	Cloned in this study
pUC-PspCas13b-mSmn1-gRNA5	N/A	Cloned in this study
pUC-PspCas13b-mMap1b-gRNA1	N/A	Cloned in this study
pUC-PspCas13b-mMap1b-gRNA2	N/A	Cloned in this study
pUC-PspCas13b-mMap1b-gRNA3	N/A	Cloned in this study
pUC-PspCas13b-mMap1b-gRNA4	N/A	Cloned in this study
pUC-PspCas13b-mMap1b-gRNA5	N/A	Cloned in this study
pUC-PspCas13b-mL1cam-gRNA1	N/A	Cloned in this study
pUC-PspCas13b-mL1cam-gRNA2	N/A	Cloned in this study
pUC-PspCas13b-mL1cam-gRNA3	N/A	Cloned in this study
pUC-PspCas13b-mL1cam-gRNA4	N/A	Cloned in this study
pUC-PspCas13b-mL1cam-gRNA5	N/A	Cloned in this study
pUC-PspCas13b-mGsk3b-gRNA1	N/A	Cloned in this study
pUC-PspCas13b-mGsk3b-gRNA2	N/A	Cloned in this study
pUC-PspCas13b-mGsk3b-gRNA3	N/A	Cloned in this study
pUC-PspCas13b-mGsk3b-gRNA4	N/A	Cloned in this study
pUC-PspCas13b-mGsk3b-gRNA5	N/A	Cloned in this study
pUC-PspCas13b-mFmr1-gRNA1	N/A	Cloned in this study
pUC-PspCas13b-mFmr1-gRNA2	N/A	Cloned in this study
pUC-PspCas13b-mFmr1-gRNA3	N/A	Cloned in this study
pUC-PspCas13b-mFmr1-gRNA4	N/A	Cloned in this study
pUC-PspCas13b-mFmr1-gRNA5	N/A	Cloned in this study
pUC-PspCas13b-mEif4b-gRNA1	N/A	Cloned in this study
pUC-PspCas13b-mEif4b-gRNA2	N/A	Cloned in this study
pUC-PspCas13b-mEif4b-gRNA3	N/A	Cloned in this study
pUC-PspCas13b-mEif4b-gRNA4	N/A	Cloned in this study
pUC-PspCas13b-mEif4b-gRNA5	N/A	Cloned in this study
pUC-PspCas13b-mDixdc1-gRNA1	N/A	Cloned in this study
pUC-PspCas13b-mDixdc1-gRNA2	N/A	Cloned in this study
pUC-PspCas13b-mDixdc1-gRNA3	N/A	Cloned in this study
pUC-PspCas13b-mDixdc1-gRNA4	N/A	Cloned in this study

pUC-PspCas13b-mDixdc1-gRNA5	N/A	Cloned in this study
pUC-PspCas13b-mAkt3-gRNA1	N/A	Cloned in this study
pUC-PspCas13b-mAkt3-gRNA2	N/A	Cloned in this study
pUC-PspCas13b-mAkt3-gRNA3	N/A	Cloned in this study
pUC-PspCas13b-mAkt3-gRNA4	N/A	Cloned in this study
pUC-PspCas13b-mAkt3-gRNA5	N/A	Cloned in this study
pUC-PspCas13b-mRictor-gRNA1	N/A	Cloned in this study
pUC-PspCas13b-mRictor-gRNA2	N/A	Cloned in this study
pUC-PspCas13b-mRictor-gRNA3	N/A	Cloned in this study
pUC-PspCas13b-mRictor-gRNA4	N/A	Cloned in this study
pUC-PspCas13b-mRictor-gRNA5	N/A	Cloned in this study
pUC-PspCas13b-mCamk2a-gRNA1	N/A	Cloned in this study
pUC-PspCas13b-mCamk2a-gRNA2	N/A	Cloned in this study
pUC-PspCas13b-mCamk2a-gRNA3	N/A	Cloned in this study
pUC-PspCas13b-mCamk2a-gRNA4	N/A	Cloned in this study
pUC-PspCas13b-mCamk2a-gRNA5	N/A	Cloned in this study
pUC-PspCas13b-mRptor-gRNA1	N/A	Cloned in this study
pUC-PspCas13b-mRptor-gRNA2	N/A	Cloned in this study
pUC-PspCas13b-mRptor-gRNA3	N/A	Cloned in this study
pUC-PspCas13b-mRptor-gRNA4	N/A	Cloned in this study
pUC-PspCas13b-mRptor-gRNA5	N/A	Cloned in this study
pUC-PspCas13b-mAlkbh5-gRNA1	N/A	Cloned in this study
pUC-PspCas13b-mAlkbh5-gRNA2	N/A	Cloned in this study
pUC-PspCas13b-mAlkbh5-gRNA3	N/A	Cloned in this study
pUC-PspCas13b-mAlkbh5-gRNA4	N/A	Cloned in this study
pUC-PspCas13b-mAlkbh5-gRNA5	N/A	Cloned in this study
pUC-RfxCas13d-hGAPDH-gRNA1	N/A	Cloned in this study
pUC-RfxCas13d-hGAPDH-gRNA2	N/A	Cloned in this study
pUC-RfxCas13d-gNT	N/A	Cloned in this study
pUC-LwaCas13a-hGAPDH-gRNA1	N/A	Cloned in this study
pUC-LwaCas13a-hGAPDH-gRNA2	N/A	Cloned in this study
pUC-LwaCas13a-gNT	N/A	Cloned in this study
pUC-Cas13bt1-hGAPDH-gRNA1	N/A	Cloned in this study
pUC-Cas13bt1-hGAPDH-gRNA2	N/A	Cloned in this study
pUC-Cas13bt1-gNT	N/A	Cloned in this study
pUC-DiCas7-11-hGAPDH-gRNA1	N/A	Cloned in this study
pUC-DiCas7-11-hGAPDH-gRNA2	N/A	Cloned in this study
pUC-DiCas7-11-gNT	N/A	Cloned in this study
pUC-PspCas13b-gG1-SM1	N/A	Cloned in this study
pUC-PspCas13b-gG1-SM2	N/A	Cloned in this study
pUC-PspCas13b-gG1-SM3	N/A	Cloned in this study

pUC-PspCas13b-gG1-SM4	N/A	Cloned in this study
pUC-PspCas13b-gG1-SM5	N/A	Cloned in this study
pUC-PspCas13b-gG1-SM6	N/A	Cloned in this study
pUC-PspCas13b-gG1-SM7	N/A	Cloned in this study
pUC-PspCas13b-gG1-SM8	N/A	Cloned in this study
pUC-PspCas13b-gG1-SM9	N/A	Cloned in this study
pUC-PspCas13b-gG1-SM10	N/A	Cloned in this study
pUC-PspCas13b-gG1-DM1	N/A	Cloned in this study
pUC-PspCas13b-gG1-DM2	N/A	Cloned in this study
pUC-PspCas13b-gG1-DM3	N/A	Cloned in this study
pUC-PspCas13b-gG1-DM4	N/A	Cloned in this study
pUC-PspCas13b-gG1-DM5	N/A	Cloned in this study
pUC-PspCas13b-gG1-DM6	N/A	Cloned in this study
pUC-PspCas13b-gG1-DM7	N/A	Cloned in this study
pUC-PspCas13b-gG1-DM8	N/A	Cloned in this study
pUC-PspCas13b-gG1-DM9	N/A	Cloned in this study
pUC-PspCas13b-gG1-DM10	N/A	Cloned in this study
pUC-PspCas13b-gG1-TM1	N/A	Cloned in this study
pUC-PspCas13b-gG1-TM2	N/A	Cloned in this study
pUC-PspCas13b-gG1-TM3	N/A	Cloned in this study
pUC-PspCas13b-gG1-TM4	N/A	Cloned in this study
pUC-PspCas13b-gG1-TM5	N/A	Cloned in this study
pUC-PspCas13b-gG1-TM6	N/A	Cloned in this study
pUC-PspCas13b-gG1-TM7	N/A	Cloned in this study
pUC-PspCas13b-gG1-TM8	N/A	Cloned in this study
pUC-PspCas13b-gG1-TM9	N/A	Cloned in this study
pUC-PspCas13b-gG1-TM10	N/A	Cloned in this study

Supplementary Table 2 | gRNA sequence. Spacer sequence of all gRNAs used in this study.

gRNA plasmid description	Short name	Target RNA	Spacer sequence
pUC-pspcas13b-gNT, pUC-RfxCas13d-gNT, pUC-LwaCas13a-gNT, pUC-Cas13bt1-gNT, pUC-DiCas7-11-gNT	gNT or gNT1	Non-targeting	gcagggttttcccagtcacgacgttgtaaaa
pUC-pspcas13b-gNT2	gNT2	Non-targeting	gtaactactcgagacgcctatt
pUC-pspcas13b-gNT3	gNT3	Non-targeting	ggtaatgcctggcttgtcgacgcatagtctg
pUC-PspCas13b-gSA	gSA	Splice reporter mRNA	gatatcgcctggatcctgagcca
pUC-PspCas13b-gGCN4	gGCN4	GCN4 reporter mRNA	gcagttcttctccactgccagaa
pUC-PspCas13b-gMS2	gMS2	MS2 reporter mRNA	ggtaccttaggatctaatgaacccgggaat
pUC-PspCas13b-gTERRA	gTERRA	Human *TERRA* lncRNA	gtaaccctaaccctaaccctaaccctaaccc
pUC-PspCas13b-hGAPDH-gRNA1, pUC-RfxCas13d-hGAPDH-gRNA1, pUC-LwaCas13a-hGAPDH-gRNA1, pUC-Cas13bt1-hGAPDH-gRNA1, pUC-DiCas7-11-hGAPDH-gRNA1	gG1	Human *GAPDH* mRNA	gggtactttattgatggtacatgacaaggt
pUC-PspCas13b-hGAPDH-gRNA2, pUC-RfxCas13d-hGAPDH-gRNA2, pUC-LwaCas13a-hGAPDH-gRNA3, pUC-Cas13bt1-hGAPDH-gRNA4, pUC-DiCas7-11-hGAPDH-gRNA5	gG2	Human *GAPDH* mRNA	gtctacatggcaactgtgaggaggggagat
pUC-PspCas13b-hGAPDH-gRNA3	gG3	Human *GAPDH* mRNA	gtctctctcttcctcttgtgctcttgctgg

pUC-PspCas13b-hACTB-gRNA1	ghA1	Human *ACTB* mRNA	gcaatcaaagtcctcggccacattgtgaac
pUC-PspCas13b-hACTB-gRNA2	ghA2	Human *ACTB* mRNA	gaaagcaatgctatcacctcccctgtgtgg
pUC-PspCas13b-hACTB-gRNA3	ghA3	Human *ACTB* mRNA	gccctggctgcctccacccactcccaggga
pUC-PspCas13b-hSDHC-gRNA1	gSDHC1	Human *SDHC* mRNA	gaattgtcctttaagccagcaacccacagg
pUC-PspCas13b-hSDHC-gRNA2	gSDHC2	Human *SDHC* mRNA	gaaagcataaaattaagaggcttttctgga
pUC-PspCas13b-hSDHC-gRNA3	gSDHC3	Human *SDHC* mRNA	gactaattcccctccacccccacctctctt
pUC-PspCas13b-hSDHD-gRNA1	gSDHD1	Human *SDHD* mRNA	ggcatgacaaagcagaggcaaagaggcata
pUC-PspCas13b-hSDHD-gRNA2	gSDHD2	Human *SDHD* mRNA	gcaaccccattaactcaccagaatatagaa
pUC-PspCas13b-hSDHD-gRNA3	gSDHD3	Human *SDHD* mRNA	gagattgataaattgaaaggcaaaagctga
pUC-PspCas13b-hNDUFS2-gRNA1	gN1	Human *NDUFS2* mRNA	gcacagaaagcctgacagccaagtgtacat
pUC-PspCas13b-hNDUFS2-gRNA2	gN2	Human *NDUFS2* mRNA	gctccacagaagaagctgataggcaggggg
pUC-PspCas13b-hNDUFS2-gRNA3	gN3	Human *NDUFS2* mRNA	gcacacacacacacacacagaggccaatt
pUC-PspCas13b-mActb-gRNA1	gmA1	Mouse *Actb* mRNA	gtgtgcacttttattggtctcaagtcagtg
pUC-PspCas13b-mActb-gRNA2	gmA2	Mouse *Actb* mRNA	gtacaaagtcctcagccacatttgtagaac
pUC-PspCas13b-mActb-gRNA3	gmA3	Mouse *Actb* mRNA	gggaggcctcagacctgggccattcagaaa
pUC-PspCas13b-mActb-gRNA4	gmA4	Mouse *Actb* mRNA	gcagtacataatttacacagaagcaatgct
pUC-PspCas13b-mActb-gRNA5	gmA5	Mouse *Actb* mRNA	gctccaaccaactgctgtcgccttcaccgt
pUC-PspCas13b-mActb-gRNA6	gmA6	Mouse *Actb* mRNA	gcctcaacacctcaacccccctcccagggag
pUC-PspCas13b-mActb-gRNA7	gmA7	Mouse *Actb* mRNA	gtaaccacttatttcatggatacttggaat
pUC-PspCas13b-mGap43-gRNA1	gGap43_1	Mouse *Gap43* mRNA	gaaacaaatgtttaagccacactgttggac

pUC-PspCas13b-mGap43-gRNA2	gGap43_2	Mouse *Gap43* mRNA	gaacggaacattgcacacacacacttggaa
pUC-PspCas13b-mGap43-gRNA3	gGap43_3	Mouse *Gap43* mRNA	gtacagtgcaagaatttcccaagatgactg
pUC-PspCas13b-mGap43-gRNA4	gGap43_4	Mouse *Gap43* mRNA	ggaaacttcagagtggagctgagaagggca
pUC-PspCas13b-mGap43-gRNA5	gGap43_5	Mouse *Gap43* mRNA	gccacacagagagagagggctcataggtag
pUC-PspCas13b-mGap43-gRNA6	gGap43_6	Mouse *Gap43* mRNA	gagaagggcaggagagacagggttcaggtg
pUC-PspCas13b-mGap43-gRNA7	gGap43_7	Mouse *Gap43* mRNA	gacaggctcacacacgtgagcaggacagga
pUC-PspCas13b-mGap43-gRNA8	gGap43_8	Mouse *Gap43* mRNA	ttttttttctttaaatgtttgccacacaga
pUC-PspCas13b-mGap43-gRNA9	gGap43_9	Mouse *Gap43* mRNA	gccacactgttggacttgggatctttcctg
pUC-PspCas13b-mGap43-gRNA10	gGap43_10	Mouse *Gap43* mRNA	gcatcatcattaccaaaaactcgccataac
pUC-PspCas13b-mGap43-gRNA11	gGap43_11	Mouse *Gap43* mRNA	gggccacacgcaccagatcaaaaaaccggg
pUC-PspCas13b-mGap43-gRNA12	gGap43_12	Mouse *Gap43* mRNA	gaacagagagaaatagagaggaaagtggac
pUC-PspCas13b-mGap43-gRNA13	gGap43_13	Mouse *Gap43* mRNA	ggactcctcagaacggaacattgcacacac
pUC-PspCas13b-mGap43-gRNA14	gGap43_14	Mouse *Gap43* mRNA	gttcattccatcacattgaaaatgaggaaa
pUC-PspCas13b-mImpa1-gRNA1	gImpa1_1	Mouse *Impa1* mRNA	gcattatatgtgacaccgccaagacttcca
pUC-PspCas13b-mImpa1-gRNA2	gImpa1_2	Mouse *Impa1* mRNA	gatatagtcattacagtgcccaaatctgag
pUC-PspCas13b-mImpa1-gRNA3	gImpa1_3	Mouse *Impa1* mRNA	gacttagtcctacagccagtggcttgcaca
pUC-PspCas13b-mImpa1-gRNA4	gImpa1_4	Mouse *Impa1* mRNA	gaccttatagagagagcatctagagttagc
pUC-PspCas13b-mImpa1-gRNA5	gImpa1_5	Mouse *Impa1* mRNA	tagtacactgctgtatgttgtaggttctgc
pUC-PspCas13b-mKpnb1-gRNA1	gKpnb1_1	Mouse *Kpnb1* mRNA	gacagtaccaagtgcaacggtacagtgaag
pUC-PspCas13b-mKpnb1-gRNA2	gKpnb1_2	Mouse *Kpnb1* mRNA	gcctttcacaacacagccccacaggtgaac

pUC-PspCas13b-mKpnb1-gRNA3	gKpnb1_3	Mouse *Kpnb1* mRNA	gaaccatagtacaggaaaggcgccttgatg
pUC-PspCas13b-mKpnb1-gRNA4	gKpnb1_4	Mouse *Kpnb1* mRNA	gaaaccaaaccaaacctaaacagcgtcttt
pUC-PspCas13b-mKpnb1-gRNA5	gKpnb1_5	Mouse *Kpnb1* mRNA	gcaagagaccaataccgcattgcagtcagt
pUC-PspCas13b-mMtor-gRNA1	gMtor_1	Mouse *Mtor* mRNA	gcaaatacagcatatccctccctcactgaa
pUC-PspCas13b-mMtor-gRNA2	gMtor_2	Mouse *Mtor* mRNA	gcccatcctgcaaatgtcgccactgcatcc
pUC-PspCas13b-mMtor-gRNA3	gMtor_3	Mouse *Mtor* mRNA	gcacaaaatttactcagatacaacgtggtg
pUC-PspCas13b-mMtor-gRNA4	gMtor_4	Mouse *Mtor* mRNA	gacagtgtcttttcaacagcagctaggagg
pUC-PspCas13b-mMtor-gRNA5	gMtor_5	Mouse *Mtor* mRNA	gcttataactcacaacctgctctagtgtgt
pUC-PspCas13b-mTdp43-gRNA1	gTdp43_1	Mouse *Tdp43* mRNA	gagaaaaacaagcagctcagggtgtggtga
pUC-PspCas13b-mTdp43-gRNA2	gTdp43_2	Mouse *Tdp43* mRNA	gcaaaattcagatgcacagggtttggaaat
pUC-PspCas13b-mTdp43-gRNA3	gTdp43_3	Mouse *Tdp43* mRNA	gaccaccaaaaatgtaccgccgtgtatgaa
pUC-PspCas13b-mTdp43-gRNA4	gTdp43_4	Mouse *Tdp43* mRNA	gaaaatcaaatgcacagaggcactcagaac
pUC-PspCas13b-mTdp43-gRNA5	gTdp43_5	Mouse *Tdp43* mRNA	gccattgacaagtaacttaccccaggactc
pUC-PspCas13b-mStmn2-gRNA1	gStmn2_1	Mouse *Stmn2* mRNA	gcaaaacattctgcaaagagaccgcattga
pUC-PspCas13b-mStmn2-gRNA2	gStmn2_2	Mouse *Stmn2* mRNA	gacgaagagtaaatatgcaggcagtttggg
pUC-PspCas13b-mStmn2-gRNA3	gStmn2_3	Mouse *Stmn2* mRNA	gcttccaaaagaacagacctagcaaatcca
pUC-PspCas13b-mStmn2-gRNA4	gStmn2_4	Mouse *Stmn2* mRNA	gcacccacagataagccacccgacatgtca
pUC-PspCas13b-mStmn2-gRNA5	gStmn2_5	Mouse *Stmn2* mRNA	gaccagcttgagtaaaagtccacagtgctt
pUC-PspCas13b-mRhoA-gRNA1	gRhoA_1	Mouse *RhoA* mRNA	ggtaactaacatgagaccacagaactgtaa
pUC-PspCas13b-mRhoA-gRNA2	gRhoA_2	Mouse *RhoA* mRNA	gtacagaaaaatgtttagtcagctggagag

pUC-PspCas13b-mRhoA-gRNA3	gRhoA_3	Mouse *RhoA* mRNA	gttagttataaagtagttacagcctaattc
pUC-PspCas13b-mRhoA-gRNA4	gRhoA_4	Mouse *RhoA* mRNA	gagcactgtgacttagagccagaccctgca
pUC-PspCas13b-mRhoA-gRNA5	gRhoA_5	Mouse *RhoA* mRNA	gaaattctttgaattagcgcctggtgtcag
pUC-PspCas13b-mPum2-gRNA1	gPum2_1	Mouse *Pum2* mRNA	gcaatcatgcgtaaatgctgagctatcact
pUC-PspCas13b-mPum2-gRNA2	gPum2_2	Mouse *Pum2* mRNA	ggaaatgtacataaggccgcttgtaaatgt
pUC-PspCas13b-mPum2-gRNA3	gPum2_3	Mouse *Pum2* mRNA	gagccaataagagccaggacttagacaaac
pUC-PspCas13b-mPum2-gRNA4	gPum2_4	Mouse *Pum2* mRNA	gagaattattctacatgagcgagaatactg
pUC-PspCas13b-mPum2-gRNA5	gPum2_5	Mouse *Pum2* mRNA	gtcactatgaaattagcaaggcttccataa
pUC-PspCas13b-mPten-gRNA1	gPten_1	Mouse *Pten* mRNA	gaaaaatattaacagtgcaacagcccattg
pUC-PspCas13b-mPten-gRNA2	gPten_2	Mouse *Pten* mRNA	ggtatatacatgacacagctacacaacctt
pUC-PspCas13b-mPten-gRNA3	gPten_3	Mouse *Pten* mRNA	gaagtaaaattgaagccctaatcccaactc
pUC-PspCas13b-mPten-gRNA4	gPten_4	Mouse *Pten* mRNA	gaccacagctagtgaacaatttcagcacca
pUC-PspCas13b-mPten-gRNA5	gPten_5	Mouse *Pten* mRNA	gagcaactacatttagagtcagaggactgt
pUC-PspCas13b-mTmsb4x-gRNA1	gTmsb4x_1	Mouse *Tmsb4x* mRNA	gtaaaataagaaggcaatgctcgtggaatg
pUC-PspCas13b-mTmsb4x-gRNA2	gTmsb4x_2	Mouse *Tmsb4x* mRNA	gtcatttaaacttgatccaacctctttgca
pUC-PspCas13b-mTmsb4x-gRNA3	gTmsb4x_3	Mouse *Tmsb4x* mRNA	gattaaactgcattttacatcctgcaggac
pUC-PspCas13b-mTmsb4x-gRNA4	gTmsb4x_4	Mouse *Tmsb4x* mRNA	gctttttccttcaccaacatgcaagttctt
pUC-PspCas13b-mTmsb4x-gRNA5	gTmsb4x_5	Mouse *Tmsb4x* mRNA	gaggccttcctgctcagtagttctgattct
pUC-PspCas13b-mSmn1-gRNA1	gSmn1_1	Mouse *Smn1* mRNA	gacaccacttagccaagagtccactgatga
pUC-PspCas13b-mSmn1-gRNA2	gSmn1_2	Mouse *Smn1* mRNA	gtagactgccttccgacacgcacactccac

pUC-PspCas13b-mSmn1-gRNA3	gSmn1_3	Mouse *Smn1* mRNA	ggcacgctctgctgctgacttaggatggat
pUC-PspCas13b-mSmn1-gRNA4	gSmn1_4	Mouse *Smn1* mRNA	gacatgctaagaaaatgacaattgcacatt
pUC-PspCas13b-mSmn1-gRNA5	gSmn1_5	Mouse *Smn1* mRNA	gttcttgtcgaccagggacaccgacacccc
pUC-PspCas13b-mMap1b-gRNA1	gMap1b_1	Mouse *Map1b* mRNA	gaactagcaagatcagattagccacacagg
pUC-PspCas13b-mMap1b-gRNA2	gMap1b_2	Mouse *Map1b* mRNA	gattcacagcattaagtagactgcatgggt
pUC-PspCas13b-mMap1b-gRNA3	gMap1b_3	Mouse *Map1b* mRNA	gccaatgcaagacaaaggaaggcagatgct
pUC-PspCas13b-mMap1b-gRNA4	gMap1b_4	Mouse *Map1b* mRNA	gacatagtatagcatctggcaggtaataac
pUC-PspCas13b-mMap1b-gRNA5	gMap1b_5	Mouse *Map1b* mRNA	gagtaaaagagcagtgcgaaacatacgctt
pUC-PspCas13b-mL1cam-gRNA1	gL1cam_1	Mouse *L1cam* mRNA	gaccaagcaaaagcatacagggaagccaca
pUC-PspCas13b-mL1cam-gRNA2	gL1cam_2	Mouse *L1cam* mRNA	gtaagaaagagactcgaagccacagttcct
pUC-PspCas13b-mL1cam-gRNA3	gL1cam_3	Mouse *L1cam* mRNA	ggcaaagaaaagggagcagatggtgggga c
pUC-PspCas13b-mL1cam-gRNA4	gL1cam_4	Mouse *L1cam* mRNA	gctataaaatggagaaaccacctagagact
pUC-PspCas13b-mL1cam-gRNA5	gL1cam_5	Mouse *L1cam* mRNA	gtgagagaagccacttcgatgttgtctgat
pUC-PspCas13b-mGsk3b-gRNA1	gGsk3b_1	Mouse *Gsk3b* mRNA	gacacagtaaccaaagacagcagcttatac
pUC-PspCas13b-mGsk3b-gRNA2	gGsk3b_2	Mouse *Gsk3b* mRNA	gcaatagtttgtatacaacccacagtcctt
pUC-PspCas13b-mGsk3b-gRNA3	gGsk3b_3	Mouse *Gsk3b* mRNA	gagtatataaggcccacaaagacaccaacc
pUC-PspCas13b-mGsk3b-gRNA4	gGsk3b_4	Mouse *Gsk3b* mRNA	gcacggcaattatctgagaagcgctttacc
pUC-PspCas13b-mGsk3b-gRNA5	gGsk3b_5	Mouse *Gsk3b* mRNA	gttattgttacaataatacaggccggtacc
pUC-PspCas13b-mFmr1-gRNA1	gFmr1_1	Mouse *Fmr1* mRNA	gtacagagaatattgcccaagagcagttac
pUC-PspCas13b-mFmr1-gRNA2	gFmr1_2	Mouse *Fmr1* mRNA	gacacaggacatgaaatggcacagcatttc

pUC-PspCas13b-mFmr1-gRNA3	gFmr1_3	Mouse *Fmr1* mRNA	gttgaaattcgtcatcaggccaaagagcag
pUC-PspCas13b-mFmr1-gRNA4	gFmr1_4	Mouse *Fmr1* mRNA	gtaaaatcctgccctgaagtgttaagtgta
pUC-PspCas13b-mFmr1-gRNA5	gFmr1_5	Mouse *Fmr1* mRNA	gtaattcacatttaagcaagttagcgcctt
pUC-PspCas13b-mEif4b-gRNA1	gEif4b_1	Mouse *Eif4b* mRNA	gtcacatacattataaacaagcaccagcgt
pUC-PspCas13b-mEif4b-gRNA2	gEif4b_2	Mouse *Eif4b* mRNA	ggcagaaatcaaagatagcacagagaaaac
pUC-PspCas13b-mEif4b-gRNA3	gEif4b_3	Mouse *Eif4b* mRNA	gcacatcaaagcagacaggtcaagctacag
pUC-PspCas13b-mEif4b-gRNA4	gEif4b_4	Mouse *Eif4b* mRNA	gctactagccaatcaaatccaccggagaag
pUC-PspCas13b-mEif4b-gRNA5	gEif4b_5	Mouse *Eif4b* mRNA	ggattttacatctcaagacatctcccaagt
pUC-PspCas13b-mDixdc1-gRNA1	gDixdc1_1	Mouse *Dixdc1* mRNA	gagattcgaagtaccagatacgccaggcac
pUC-PspCas13b-mDixdc1-gRNA2	gDixdc1_2	Mouse *Dixdc1* mRNA	gctctgaatttaaagagtccccagtgaaaa
pUC-PspCas13b-mDixdc1-gRNA3	gDixdc1_3	Mouse *Dixdc1* mRNA	gacaaataagactgtgcagtcatgatacgg
pUC-PspCas13b-mDixdc1-gRNA4	gDixdc1_4	Mouse *Dixdc1* mRNA	gactcttattaaagaggcagacattgaagg
pUC-PspCas13b-mDixdc1-gRNA5	gDixdc1_5	Mouse *Dixdc1* mRNA	gtcttcaacagaagaccaggacagcgtgca
pUC-PspCas13b-mAkt3-gRNA1	gAkt3_1	Mouse *Akt3* mRNA	gctataatagtaagacagtagcagcaacag
pUC-PspCas13b-mAkt3-gRNA2	gAkt3_2	Mouse *Akt3* mRNA	gattctaaccaacagatacagtcccagagc
pUC-PspCas13b-mAkt3-gRNA3	gAkt3_3	Mouse *Akt3* mRNA	gaaaaagacaatgcagtaccactgtgtcac
pUC-PspCas13b-mAkt3-gRNA4	gAkt3_4	Mouse *Akt3* mRNA	gctaaactcttacatacacacaccaccacc
pUC-PspCas13b-mAkt3-gRNA5	gAkt3_5	Mouse *Akt3* mRNA	gtttcctaagattttccagccaaatgtcag
pUC-PspCas13b-mRictor-gRNA1	gRictor_1	Mouse *Rictor* mRNA	gcatagacaatttcccccagtatactgatc
pUC-PspCas13b-mRictor-gRNA2	gRictor_2	Mouse *Rictor* mRNA	gaacctccaaaaatgtagcagcgtattact

pUC-PspCas13b-mRictor-gRNA3	gRictor_3	Mouse *Rictor* mRNA	gataccagcagttacagcccacggggtaac
pUC-PspCas13b-mRictor-gRNA4	gRictor_4	Mouse *Rictor* mRNA	gctcttgtaaagactagtgcagactcctgt
pUC-PspCas13b-mRictor-gRNA5	gRictor_5	Mouse *Rictor* mRNA	gcaacaacctgaagcgacagaggacaagta
pUC-PspCas13b-mCamk2a-gRNA1	gCamk2a_1	Mouse *Camk2a* mRNA	gcaaagaaaacagtgcagacaggagatccc
pUC-PspCas13b-mCamk2a-gRNA2	gCamk2a_2	Mouse *Camk2a* mRNA	gcaaaatccaaaggagaaccagcagccaca
pUC-PspCas13b-mCamk2a-gRNA3	gCamk2a_3	Mouse *Camk2a* mRNA	gcaagcacaatagagcgcacaccaggccaa
pUC-PspCas13b-mCamk2a-gRNA4	gCamk2a_4	Mouse *Camk2a* mRNA	gtaacaaagaagccagcacggggcctggca
pUC-PspCas13b-mCamk2a-gRNA5	gCamk2a_5	Mouse *Camk2a* mRNA	gctgtaaaaaggcatgcgtccaagtagaag
pUC-PspCas13b-mRptor-gRNA1	gRptor_1	Mouse *Rptor* mRNA	gcttcatgattgaatttccgcatcagactt
pUC-PspCas13b-mRptor-gRNA2	gRptor_2	Mouse *Rptor* mRNA	gtaaaacctcagaagaaaacagggcaggaa
pUC-PspCas13b-mRptor-gRNA3	gRptor_3	Mouse *Rptor* mRNA	gcacacagacacatgtcggacacacgggga
pUC-PspCas13b-mRptor-gRNA4	gRptor_4	Mouse *Rptor* mRNA	gacatacacaatgtgctggactgcctcggt
pUC-PspCas13b-mRptor-gRNA5	gRptor_5	Mouse *Rptor* mRNA	gtcctctcttgcctgtgcacgcagacacgt
pUC-PspCas13b-mAlkbh5-gRNA1	gAlkbh5_1	Mouse *Alkbh5* mRNA	gccaagaacaaaagaacccaggtcttttac
pUC-PspCas13b-mAlkbh5-gRNA2	gAlkbh5_2	Mouse *Alkbh5* mRNA	gtagcatacaaaaagaggccatgtgactat
pUC-PspCas13b-mAlkbh5-gRNA3	gAlkbh5_3	Mouse *Alkbh5* mRNA	gcttcctaccaaagtcttaaggagagcaca
pUC-PspCas13b-mAlkbh5-gRNA4	gAlkbh5_4	Mouse *Alkbh5* mRNA	gaacaaaagaaatgaagccctaccacacac
pUC-PspCas13b-mAlkbh5-gRNA5	gAlkbh5_5	Mouse *Alkbh5* mRNA	gtaacaatttctgaagaaagagcagcatcg
pUC-PspCas13b-gG1-SM1	gSM1	Mismatch gRNA for gG1	gggtactttattgatggtacatgacaaggA
pUC-PspCas13b-gG1-SM2	gSM2	Mismatch gRNA for gG1	gggtactttattgatggtacatgacaTggt

pUC-PspCas13b-gG1-SM3	gSM3	Mismatch gRNA for gG1	gggtactttattgatggtacatgTcaaggt
pUC-PspCas13b-gG1-SM4	gSM4	Mismatch gRNA for gG1	gggtactttattgatggtacTtgacaaggt
pUC-PspCas13b-gG1-SM5	gSM5	Mismatch gRNA for gG1	gggtactttattgatggAacatgacaaggt
pUC-PspCas13b-gG1-SM6	gSM6	Mismatch gRNA for gG1	gggtactttattgaAggtacatgacaaggt
pUC-PspCas13b-gG1-SM7	gSM7	Mismatch gRNA for gG1	gggtactttatAgatggtacatgacaaggt
pUC-PspCas13b-gG1-SM8	gSM8	Mismatch gRNA for gG1	gggtacttAattgatggtacatgacaaggt
pUC-PspCas13b-gG1-SM9	gSM9	Mismatch gRNA for gG1	gggtaGtttattgatggtacatgacaaggt
pUC-PspCas13b-gG1-SM10	gSM10	Mismatch gRNA for gG1	ggCtactttattgatggtacatgacaaggt
pUC-PspCas13b-gG1-DM1	gDM1	Mismatch gRNA for gG1	gggtactttattgatggtacatgacaagCA
pUC-PspCas13b-gG1-DM2	gDM2	Mismatch gRNA for gG1	gggtactttattgatggtacatgacTTggt
pUC-PspCas13b-gG1-DM3	gDM3	Mismatch gRNA for gG1	gggtactttattgatggtacatCTcaaggt
pUC-PspCas13b-gG1-DM4	gDM4	Mismatch gRNA for gG1	gggtactttattgatggtaGTtgacaaggt
pUC-PspCas13b-gG1-DM5	gDM5	Mismatch gRNA for gG1	gggtactttattgatgCAacatgacaaggt
pUC-PspCas13b-gG1-DM6	gDM6	Mismatch gRNA for gG1	gggtactttattgTAggtacatgacaaggt
pUC-PspCas13b-gG1-DM7	gDM7	Mismatch gRNA for gG1	gggtactttaAAgatggtacatgacaaggt
pUC-PspCas13b-gG1-DM8	gDM8	Mismatch gRNA for gG1	gggtactAAattgatggtacatgacaaggt
pUC-PspCas13b-gG1-DM9	gDM9	Mismatch gRNA for gG1	gggtTGtttattgatggtacatgacaaggt
pUC-PspCas13b-gG1-DM10	gDM10	Mismatch gRNA for gG1	gCCtactttattgatggtacatgacaaggt
pUC-PspCas13b-gG1-TM1	gTM1	Mismatch gRNA for gG1	gggtactttattgatggtacatgacaaCCA
pUC-PspCas13b-gG1-TM2	gTM2	Mismatch gRNA for gG1	gggtactttattgatggtacatgaGTTggt

pUC-PspCas13b-gG1-TM3	gTM3	Mismatch gRNA for gG1	gggtactttattgatggtacaACTcaaggt
pUC-PspCas13b-gG1-TM4	gTM4	Mismatch gRNA for gG1	gggtactttattgatggtTGTtgacaaggt
pUC-PspCas13b-gG1-TM5	gTM5	Mismatch gRNA for gG1	gggtactttattgatCCAacatgacaaggt
pUC-PspCas13b-gG1-TM6	gTM6	Mismatch gRNA for gG1	gggtactttattCTAggtacatgacaaggt
pUC-PspCas13b-gG1-TM7	gTM7	Mismatch gRNA for gG1	gggtactttTAAgatggtacatgacaaggt
pUC-PspCas13b-gG1-TM8	gTM8	Mismatch gRNA for gG1	gggtacAAAattgatggtacatgacaaggt
pUC-PspCas13b-gG1-TM9	gTM9	Mismatch gRNA for gG1	gggATGtttattgatggtacatgacaaggt
pUC-PspCas13b-gG1-TM10	gTM10	Mismatch gRNA for gG1	gCCCtactttattgatggtacatgacaaggt

Supplementary Table 3 | Transfection and drug treatment conditions. Plasmids used for transfection, cell type and culture plate, and drug treatment conditions for each figure. Each transfection reaction was given a number in the first column.

No.	Plasmid used	Cell type and culture plate	Drug treatment	Related to Figures
1	0.1 μg pSLQ10530 + 0.1 μg pSLQ10550 + 0.3 μg gG123/gNT	HeLa, 24-well plate	250 μM ABA/DMSO, 4 h	Fig. 1b-c, Supplementary Fig. 2c
2	0.1 μg pSLQ10530/14206/14830/14831/14832 + 0.1 μg pSLQ10550 + 0.3 μg gG12/gNT (cloned in the gRNA backbone of the corresponding dCas system)	HeLa, 24-well plate	500 μM ABA, 24 h	Fig. 1e, Supplementary Fig. 4b
3	0.125 μg pSLQ10530 + 0.125 μg pSLQ10550 + 0.1 μg pSLQ10461 + 0.15 μg gGCN4/gNT	HeLa, 24-well plate	250 μM ABA/DMSO, 4 h	Fig. 1f, Extended Data Fig. 1h-i, 3a-e
4	0.125 μg pSLQ10530 + 0.125 μg pSLQ10550 + 0.1 μg pSLQ10666/10667/10668/10669 + 0.15 μg gGCN4	HeLa, 24-well plate	250 μM ABA, 4 h	Fig. 1g, Extended Data Fig. 3g
5	0.05 μg pSLQ10671 + 0.45 μg gG123/ghA123/gSDHC123/gSDHD123/gN123/gmA123/gNT	HeLa and Neuro-2a cells, 24-well plate	N/A	Fig. 1j, Extended Data Fig. 4
6	0.1 μg pSLQ10530 + 0.1 μg pSLQ10539 + 0.3 μg gG123/gNT	HeLa, 24-well plate	250 μM ABA/DMSO, 4 h	Fig. 2b, Extended Data Fig. 6a
7	0.1 μg pSLQ10530 + 0.1 μg pSLQ10552 + 0.3 μg gG123/gNT	HeLa, 24-well plate	250 μM ABA/DMSO, 4 h; 50 μM NaAsO2, 6h	Fig. 2c, Extended Data Fig. 6b
8	0.1 μg pSLQ14565 + 0.1 μg pSLQ14566 + 0.3 μg gTERRA/gNT	HeLa, 24-well plate	500 μM ABA/DMSO, 24 h	Fig. 2e, Extended Data Fig. 6i
9	0.125 μg pSLQ10531 + 0.125 μg pSLQ14806 + 0.1 μg pSLQ10461 + 0.15 μg gGCN4/gNT	HeLa, 24-well plate	500 μM ABA/DMSO, 24 h; 100 μM NaAsO2, 6 h	Fig. 2f, Extended Data Fig. 6j, Supplementary Fig. 8b
10	0.1 μg pSLQ10608 + 0.1 μg pSLQ10554 + 0.3 μg gG123/gNT	HeLa, 24-well plate	1 mM ABA/DMSO, 4 h	Fig. 2h, Extended Data Fig. 6k
11	0.1 μg pSLQ10530 + 0.1 μg pSLQ10622 + 0.3 μg gG123/gNT	HeLa, 24-well plate	1 mM ABA/DMSO, 4 h	Fig. 2i, Extended Data Fig. 6l
12	0.1 μg pSLQ10530 + 0.1 μg pSLQ10550 + 0.3 μg gG123/gNT	HeLa, 24-well plate	See Methods 'Characterization of ABA concentration, treatment time, and ABA removal for CRISPR-TO'	Fig. 2j, Extended Data Fig. 7a-d

13	0.4 µg pSLQ10530 + 0.4 µg pSLQ10650 + 1.2 µg gMS2	Engineered U2OS-2-6-3 stable cells	See Methods 'Live-cell tracking of MS2 mRNA repositioned by CRISPR-TO'	Fig. 2k, Extended Data Fig. 7f-j, Supplementary Videos 1-2
14	0.4 µg pSLQ10530 + 0.4 µg pSLQ14826 + 1.2 µg gMS2	Engineered U2OS-2-6-3 stable cells	See Methods 'Live-cell tracking of MS2 mRNA repositioned by CRISPR-TO'	Supplementary Video 3
15	0.05 µg pSLQ10625 + 0.1 µg pSLQ14256 + 0.3 µg gmA123/gNT + 0.05 µg pSLQ14264	Mouse cortical neurons (P0), 24-well plate	250 µM ABA/DMSO, 24 h	Fig. 3b-g, Extended Data Fig. 8e-g, Supplementary Fig. 9a-c
16	0.05 µg pSLQ10625 + 0.1 µg pSLQ14256 + 0.3 µg gmA123 + 0.05 µg pSLQ14827	Mouse cortical neurons (P0), 24-well plate	Neurons were first treated with 250 µM ABA for 24 h, washed with fresh media for three times to remove ABA, and cultured for another 1 h, 4 h, or 24 h.	Fig. 3i-3k
17	0.05 µg pSLQ14828 + 0.1 µg pSLQ14256 + 0.2 µg gmA123 + 0.2 µg gGap43_11,13,14 + 0.05 µg pSLQ14829, 0.05 µg pSLQ14828 + 0.1 µg pSLQ14256 + 0.3 µg gmA123/gGap43_11,13,14/gNT + 0.05 µg pSLQ14829	Mouse cortical neurons (P0), 24-well plate	250 µM ABA, 24 h	Fig. 3h, Extended Data Fig. 8h
18	0.05 µg pSLQ14811 + 0.05 µg pSLQ14256 + 0.2 µg gGCN4 + 0.05 µg pSLQ14266 + 0.15 µg pSLQ14848	Mouse cortical neurons (P0), 24-well plate	250 µM ABA/DMSO, 6 h; 40 µM Anisomycin, 1 h; 200 µM puromycin, 1 h	Fig. 4a-c, Extended Data Fig. 9c, Supplementary Video 4
19	0.05 µg pSLQ14811 + 0.1 µg pSLQ14256 + 0.3 µg gmA123 + 0.05 µg pSLQ14863	Mouse cortical neurons (P0), 24-well plate	250 µM ABA, 24 hours, then 355 µM cycloheximide, 30 min, followed by 3 µM puromycin for 15 min	Fig. 4e-g, Extended Data Fig. 9g-i
20	0.05 µg pSLQ14811 + 0.1 µg pSLQ14256 + 0.3 µg gmA123 + 0.05 µg pSLQ14863	Mouse cortical neurons (P0), 24-well plate	250 µM ABA, 24 h, then 355 µM cycloheximide, 30 min, followed by 3 µM puromycin for 15 min. Also stain with 1 µM HaloTag Oregon Green Ligand (Promega,	Extended Data Fig. 9j

			G2802) for 15 min before fixation.	
21	0.05 µg pSLQ14828 + 0.1 µg pSLQ14256 + 0.3 µg gmA123 + 0.05 µg pSLQ14829	Mouse cortical neurons (P0), 24-well plate	250 µM ABA, 24 h	Extended Data Fig. 9d-f
22	0.05 µg pSLQ14828 + 0.1 µg pSLQ14253 + 0.3 µg gmA123/gNT + 0.05 µg pSLQ14829	Mouse cortical neurons (P0), 24-well plate	Neurons were treated with 250 µM ABA and imaged immediately.	Fig. 4i-j
23	0.2 µg pSLQ10625 + 0.4 µg pSLQ14256 + 1.2 µg gmA123 + 0.2 µg pSLQ14264	Mouse cortical neurons (P0), microfluidic device	250 µM ABA/DMSO, 2 days	Extended Data Fig. 9p-q
24	0.2 µg pSLQ10625 + 0.4 µg pSLQ14256 + 1.2 µg gmA123 + 0.2 µg pSLQ14264	Mouse cortical neurons (P0), microfluidic device	Neurons were treated with 250 µM ABA/DMSO for 1.5 days after axotomy.	Fig. 4k-l
25	0.05 µg pSLQ14828 + 0.05 µg pSLQ14837 + 0.3 µg gRNA + 0.1 µg pSLQ14568	Mouse cortical neurons (P0), 24-well plate	Neurons were treated with 250 µM ABA and imaged immediately for 12 h.	Fig. 5b-c, Extended Data Fig. 10c, 10e
26	0.05 µg pSLQ14828 + 0.1 µg pSLQ14256 + 0.3 µg gStmn2_1-5/gNT + 0.05 µg pSLQ14829	Mouse cortical neurons (P0), 24-well plate	250 µM ABA, 24 h	Fig. 5d-e, Supplementary Fig. 9d
27	0.05 µg pSLQ14828 + 0.05 µg pSLQ14837 + 0.3 µg gStmn2_1-5/gNT + 0.1 µg pSLQ14568	Mouse cortical neurons (P0), 24-well plate	Neurons were treated with 250 µM ABA/DMSO and imaged immediately for 12 h.	Fig. 5f-g, 5i
28	0.05 µg pSLQ14828 + 0.05 µg pSLQ10628 + 0.3 µg gStmn2_1-5/gNT + 0.1 µg pSLQ14568	Mouse cortical neurons (P0), 24-well plate	Neurons were treated with 250 µM ABA and imaged immediately for 12 h.	Fig. 5h-i
29	0.3 µg pSLQ10524/pSLQ10527 + 0.1 µg pSLQ10471 + 0.3 µg gSA/gNT	HEK293T, 24-well plate	N/A	Extended Data Fig. 1b
30	0.3 µg pSLQ10527/pSLQ10529 + 0.1 µg pSLQ10471 + 0.3 µg gSA/gNT	HEK293T, 24-well plate	N/A	Extended Data Fig. 1c
31	0.5 µg pSLQ10526/pSLQ10527/ pSLQ10530/pSLQ10531	HeLa, 24-well plate	N/A	Extended Data Fig. 1d
32	0.5 µg pSLQ10550	HeLa, 24-well plate	100 nM MitoTracker Red CMXRos (Cell Signaling Technologies, 9082), 30 min	Extended Data Fig. 1g

33	0.1 µg pSLQ10530 + 0.1 µg pSLQ10550 + 0.3 µg gG1/gG2/gG3/gG12/gG13/gG23	HeLa, 24-well plate	250 µM ABA/DMSO, 4 h	Extended Data Fig. 3h
34	0.1 µg pSLQ10530 + 0.1 µg pSLQ10550 + 0.3 µg ghA123/gNT	HeLa, 24-well plate	250 µM ABA/DMSO, 4 h	Extended Data Fig. 2b
35	0.1 µg pSLQ10530 + 0.1 µg pSLQ10550 + 0.3 µg gSDHC123/gNT	HeLa, 24-well plate	250 µM ABA/DMSO, 4 h	Extended Data Fig. 2c
36	0.1 µg pSLQ10530 + 0.1 µg pSLQ10550 + 0.3 µg gSDHD123/gNT	HeLa, 24-well plate	250 µM ABA/DMSO, 4 h	Extended Data Fig. 2d
37	0.1 µg pSLQ10530 + 0.1 µg pSLQ10550 + 0.3 µg gN123/gNT	HeLa, 24-well plate	250 µM ABA/DMSO, 4 h	Extended Data Fig. 2e
38	0.1 µg pSLQ10530 + 0.1 µg pSLQ10550 + 0.3 µg gG123/gNT	HEK293T, 24-well plate	250 µM ABA, 4 h	Extended Data Fig. 2f
39	0.1 µg pSLQ10530 + 0.1 µg pSLQ10550 + 0.3 µg gmA123/gNT	Neuro-2a, 24-well plate	250 µM ABA, 4 h	Extended Data Fig. 2g
40	0.1 µg pSLQ10530 + 0.1 µg pSLQ10550 + 0.3 µg gGap43_8,13,14/gNT	Neuro-2a, 24-well plate	250 µM ABA, 4 h	Extended Data Fig. 3j
41	0.1 µg pSLQ10530 + 0.1 µg pSLQ10550 + 0.6 µg gG1/gNT/mismatch gRNA	HeLa, 24-well plate	250 µM ABA, 4 h	Extended Data Fig. 5a-c
42	0.1 µg pSLQ10530 + 0.1 µg pSLQ10550 + 0.3 µg gG1 + 0.3 µg gG2	HeLa, 24-well plate	250 µM ABA/DMSO, 4 h	Extended Data Fig. 5d
43	0.25 µg pSLQ10530 + 0.75 µg pSLQ14861 + 0.5 µg pSLQ14860 + 1 µg gGCN4/gNT	HeLa, 6-well plate	First treated with 200 ng/µL Dox for 24 h and 250 µM ABA/DMSO for 2 h. Then change to media without Dox but with 250 µM ABA/DMSO. Collect cells after 0, 4, 6, 24, and 48 h.	Extended Data Fig. 6g-h
44	0.05 µg pSLQ10625 + 0.1 µg pSLQ14256 + 0.3 µg gmA123 + 0.05 µg pSLQ14857 or 0.5 µg pSLQ14857	Mouse cortical neurons (P0), 24-well plate	250 µM DMSO, 24 h	Extended Data Fig. 8a-b
45	0.3 µg gmA123/gNT + 0.2 µg pSLQ14857	Mouse cortical neurons (P0), 24-well plate	No treatment	Extended Data Fig. 8i

46	0.05 µg pSLQ10625 + 0.3 µg gmA123/gNT + 0.15 µg pSLQ14857	Mouse cortical neurons (P0), 24-well plate	N/A	Extended Data Fig. 8j
47	0.05 µg pSLQ10625 + 0.1 µg pSLQ14256 + 0.3 µg gmA123/gNT + 0.05 µg pSLQ14857	Mouse cortical neurons (P0), 24-well plate	250 µM ABA/DMSO, 24 h	Extended Data Fig. 8k-l
48	0.05 µg pSLQ14811 + 0.05 µg pSLQ14256 + 0.2 µg gGCN4 + 0.05 µg pSLQ14266 + 0.15 µg pSLQ14848	Mouse cortical neurons (P0), 24-well plate	250 µM DMSO, 6 h	Extended Data Fig. 9b
49	0.05 µg pSLQ14811 + 0.05 µg pSLQ14256 + 0.2 µg gMS2 + 0.25 µg pSLQ14862 + 0.05 µg pSLQ10562 + 0.05 µg pSLQ10573 + 0.05 µg pSLQ14863	Mouse cortical neurons (P0), 24-well plate	250 µM ABA and 500 µg/mL IAA, 24 h; 10 nM JF646, 15 min	Extended Data Fig. 9l
50	0.05 µg pSLQ10625 + 0.1 µg pSLQ14256 + 0.3 µg gmA123 + 0.05 µg pSLQ14827	Mouse cortical neurons (P0), 24-well plate	250 µM ABA, 0 h, 1 h, 2 h, and 3 h	Extended Data Fig. 9m
51	0.05 µg pSLQ10625 + 0.1 µg pSLQ14256 + 0.3 µg gmA123 + 0.05 µg pSLQ14827	Mouse cortical neurons (P0), 24-well plate	250 µM ABA, 3 h	Extended Data Fig. 9n
52	0.05 µg pSLQ14828 + 0.05 µg pSLQ14837 + 0.3 µg gNT + 0.1 µg pSLQ14568	Mouse cortical neurons (P0), 24-well plate	N/A	Extended Data Fig. 10a-b
53	1.3 µg pSLQ10530 + 1.7 µg gG1/gG2/gG3/gNT	Lenti-X 293T cells, 24-well plate	N/A	Supplementary Fig. 7b
54	0.5 µg pSLQ10531/14870/14871/14872/14873 or 0.1 µg pSLQ10531/14870/14871/14872/14873 + 0.4 µg gNT	HeLa, 24-well plate	N/A	Supplementary Fig. 8a
55	1) 0.125 µg pSLQ10530 + 0.125 µg pSLQ10550 + 0.1 µg pSLQ10667 + 0.15 µg gGCN4 2) 0.05 µg pSLQ10530 + 0.125 µg pSLQ10550 + 0.1 µg pSLQ10667 + 0.15 µg gGCN4 3) 0.25 µg pSLQ10530 + 0.125 µg pSLQ10550 + 0.1 µg pSLQ10667 + 0.15 µg gGCN4	HeLa, 24-well plate	250 µM ABA, 4h	Supplementary Fig. 6

	4) 0.5 µg pSLQ10530 + 0.125 µg pSLQ10550 + 0.1 µg pSLQ10667 + 0.15 µg gGCN4 5) 0.125 µg pSLQ10530 + 0.125 µg pSLQ10550 + 0.1 µg pSLQ10667 + 0.05 µg gGCN4 6) 0.125 µg pSLQ10530 + 0.125 µg pSLQ10550 + 0.1 µg pSLQ10667 + 0.1 µg gGCN4 7) 0.125 µg pSLQ10530 + 0.125 µg pSLQ10550 + 0.1 µg pSLQ10667 + 0.25 µg gGCN4 8) 0.125 µg pSLQ10530 + 0.125 µg pSLQ10550 + 0.1 µg pSLQ10667 + 0.5 µg gGCN4			
56	0.5 µg pSLQ10530/14206/14830/ 14831/14832	HeLa, 24-well plate	All cells were stained with 0.1 µg/mL Hoechst 33342 for 5 min at 37C. Dead cells were stained with 5 nM SYTOX™ Red Dead Cell Stain (Thermo, S34854) for 15 min at room temperature	Supplementary Fig. 5
57	0.1 µg pSLQ10530 + 0.1 µg pSLQ10550 + 0.3 µg gRNA	Neuro-2a, 24-well plate	250 µM ABA, 4 h	Supplementary Table 5

Supplementary Table 4 | RNA FISH probes used in the study. Name, probe sequence, target RNA, and source of all the smiFISH probes used in this study.

RNA FISH probe	Probe sequence	Target RNA	Source
mActb_smi-Y1	atagtgatgacctggccgtcagttacactcggacctcgtcgacatgcatt	Mouse *Actb* mRNA	From reference [33]
mActb_smi-Y2	catcggaaccgctcgttgccttacactcggacctcgtcgacatgcatt	Mouse *Actb* mRNA	From reference [33]
mActb_smi-Y3	acccaagaaggaaggctggaattacactcggacctcgtcgacatgcatt	Mouse *Actb* mRNA	From reference [33]
mActb_smi-Y4	tcatggatgccacaggattccttacactcggacctcgtcgacatgcatt	Mouse *Actb* mRNA	From reference [33]
mActb_smi-Y5	cggatgtcaacgtcacacttcattacactcggacctcgtcgacatgcatt	Mouse *Actb* mRNA	From reference [33]
mActb_smi-Y6	ccagacagcactgtgttggcatttacactcggacctcgtcgacatgcatt	Mouse *Actb* mRNA	From reference [33]
mActb_smi-Y7	atgcctgggtacatggtggtacttacactcggacctcgtcgacatgcatt	Mouse *Actb* mRNA	From reference [33]
mActb_smi-Y8	tctccttctgcatcctgtcagcttacactcggacctcgtcgacatgcatt	Mouse *Actb* mRNA	From reference [33]
mActb_smi-Y9	catggtgctaggagccagagcttacactcggacctcgtcgacatgcatt	Mouse *Actb* mRNA	From reference [33]
mActb_smi-Y10	cagagtacttgcgctcaggaggttacactcggacctcgtcgacatgcatt	Mouse *Actb* mRNA	From reference [33]
mActb_smi-Y11	ccaggatggagccaccgatcttacactcggacctcgtcgacatgcatt	Mouse *Actb* mRNA	From reference [33]
mActb_smi-Y12	atctgctggaaggtggacagtgttacactcggacctcgtcgacatgcatt	Mouse *Actb* mRNA	From reference [33]
mActb_smi-Y13	cgtactcctgcttgctgatccattacactcggacctcgtcgacatgcatt	Mouse *Actb* mRNA	From reference [33]
mActb_smi-Y14	cttgcggtgcacgatggagggttacactcggacctcgtcgacatgcatt	Mouse *Actb* mRNA	From reference [33]
mActb_smi-Y15	cgcagctcagtaacagtccgcttacactcggacctcgtcgacatgcatt	Mouse *Actb* mRNA	From reference [33]
mActb_smi-Y16	tcaaagaaagggtgtaaaacttacactcggacctcgtcgacatgcatt	Mouse *Actb* mRNA	From reference [33]
mActb_smi-Y17	ttttttttttttctgcgcaagttagttacactcggacctcgtcgacatgcatt	Mouse *Actb* mRNA	From reference [33]
mActb_smi-Y18	aaagccatgccaatgttgtcttacactcggacctcgtcgacatgcatt	Mouse *Actb* mRNA	From reference [33]

mActb_smi-Y19	gcgccaaaacaaaacaaaaaaacttattacactcggacctcgtcgacatgcatt	Mouse *Actb* mRNA	From reference [33]
mActb_smi-Y20	tcaccgttccagtttttaaattacactcggacctcgtcgacatgcatt	Mouse *Actb* mRNA	From reference [33]
mActb_smi-Y21	atgtttgctccaaccaactgttacactcggacctcgtcgacatgcatt	Mouse *Actb* mRNA	From reference [33]
mActb_smi-Y22	ccacatttgtagaactttggttacactcggacctcgtcgacatgcatt	Mouse *Actb* mRNA	From reference [33]
mActb_smi-Y23	caaaacaatgtacaaagtccttacactcggacctcgtcgacatgcatt	Mouse *Actb* mRNA	From reference [33]
mActb_smi-Y24	ggaatgactattaaaaaaagacttacactcggacctcgtcgacatgcatt	Mouse *Actb* mRNA	From reference [33]
mActb_smi-Y25	accacttatttcatggatacttacactcggacctcgtcgacatgcatt	Mouse *Actb* mRNA	From reference [33]
mActb_smi-Y26	aggagtgggggtggcttttgttacactcggacctcgtcgacatgcatt	Mouse *Actb* mRNA	From reference [33]
mActb_smi-Y27	ggacgcgaccatcctcctctttacactcggacctcgtcgacatgcatt	Mouse *Actb* mRNA	From reference [33]
mActb_smi-Y28	accttccccggggtggactttacactcggacctcgtcgacatgcatt	Mouse *Actb* mRNA	From reference [33]
mActb_smi-Y29	atttttgcagtacataatttacacttacactcggacctcgtcgacatgcatt	Mouse *Actb* mRNA	From reference [33]
mActb_smi-Y30	ttaaggcggaagatttaaaaaaattacactcggacctcgtcgacatgcatt	Mouse *Actb* mRNA	From reference [33]
mActb_smi-Y31	acctgggccattcagaaattttacactcggacctcgtcgacatgcatt	Mouse *Actb* mRNA	From reference [33]
mActb_smi-Y32	gggacaaaaaaaagggaggcttacactcggacctcgtcgacatgcatt	Mouse *Actb* mRNA	From reference [33]
mActb_smi-Y33	ctcccagggagaccaaagccttacactcggacctcgtcgacatgcatt	Mouse *Actb* mRNA	From reference [33]
mActb_smi-Y34	ggctgcctcaacacctcaacttacactcggacctcgtcgacatgcatt	Mouse *Actb* mRNA	From reference [33]
mActb_smi-Y35	gtcagtgtacaggccagcccttacactcggacctcgtcgacatgcatt	Mouse *Actb* mRNA	From reference [33]
mActb_smi-Y36	ggtgtgcacttttattggtcttacactcggacctcgtcgacatgcatt	Mouse *Actb* mRNA	From reference [33]
mActb_smi-Y37	tgcaaagaagctgtgctcgcttacactcggacctcgtcgacatgcatt	Mouse *Actb* mRNA	Designed via Stellaris Probe Designer in this study

mActb_smi-Y38	tgtggaccggcaacgaaggattacactcggacctcgtcgacatgcatt	Mouse *Actb* mRNA	Designed via Stellaris Probe Designer in this study
mActb_smi-Y39	atatcgtcatccatggcgaattacactcggacctcgtcgacatgcatt	Mouse *Actb* mRNA	Designed via Stellaris Probe Designer in this study
mActb_smi-Y40	gagagcatagccctcgtagatgggcattacactcggacctcgtcgacatgcatt	Mouse *Actb* mRNA	Designed via Oligostan in this study
mActb_smi-Y41	agcctggatggctacgtacatggctgttacactcggacctcgtcgacatgcatt	Mouse *Actb* mRNA	Designed via Oligostan in this study
mActb_smi-Y42	aggtgtggtgccagatcttctccatgtttacactcggacctcgtcgacatgcatt	Mouse *Actb* mRNA	Designed via Oligostan in this study
mActb_smi-Y43	tcccagttggtaacaatgccatgttcaatgttacactcggacctcgtcgacatgcatt	Mouse *Actb* mRNA	Designed via Oligostan in this study
mActb_smi-Y44	gtacttcagggtcaggatacctctcttgttacactcggacctcgtcgacatgcatt	Mouse *Actb* mRNA	Designed via Oligostan in this study
mActb_smi-Y45	ttctctttgatgtcacgcacgatttcccttacactcggacctcgtcgacatgcatt	Mouse *Actb* mRNA	Designed via Oligostan in this study
mActb_smi-Y46	tcagctgtggtggtgaagctgtagccattacactcggacctcgtcgacatgcatt	Mouse *Actb* mRNA	Designed via Oligostan in this study
mActb_smi-Y47	ctcggtcaggatcttcatgaggtagtctgtttacactcggacctcgtcgacatgcatt	Mouse *Actb* mRNA	Designed via Oligostan in this study
mActb_smi-Y48	cgtctccggagtccatcacaatgcctttacactcggacctcgtcgacatgcatt	Mouse *Actb* mRNA	Designed via Oligostan in this study
mActb_smi-Y49	gtgttgaaggtctcaaacatgatctgggtcatttacactcggacctcgtcgacatgcatt	Mouse *Actb* mRNA	Designed via Oligostan in this study
mActb_smi-Y50	tttcacggttggccttagggttcaggggttacactcggacctcgtcgacatgcatt	Mouse *Actb* mRNA	Designed via Oligostan in this study
mActb_smi-Y51	tcaggggccacacgcagctcattgtattacactcggacctcgtcgacatgcatt	Mouse *Actb* mRNA	Designed via Oligostan in this study
mActb_smi-Y52	cctcgtcacccacataggagtccttcttacactcggacctcgtcgacatgcatt	Mouse *Actb* mRNA	Designed via Oligostan in this study
NDUFS2_smi-Y1	caaactgctgtgcccattccacatctttacactcggacctcgtcgacatgcatt	Human *NDUFS2* mRNA	Designed via Oligostan in this study
NDUFS2_smi-Y2	gctgtttctttgcttgggtacataacagctttacactcggacctcgtcgacatgcatt	Human *NDUFS2* mRNA	Designed via Oligostan in this study
NDUFS2_smi-Y3	acatcattccaaggtggaggcttccagtttacactcggacctcgtcgacatgcatt	Human *NDUFS2* mRNA	Designed via Oligostan in this study

NDUFS2_smi-Y4	aatgttcttcacaattgtgtcctttggagggtttacactcggacctcgtcgacatgcatt	Human *NDUFS2* mRNA	Designed via Oligostan in this study
NDUFS2_smi-Y5	aggagcccgatgtgaggatcacacttcttacactcggacctcgtcgacatgcatt	Human *NDUFS2* mRNA	Designed via Oligostan in this study
NDUFS2_smi-Y6	tattcaatgagcttctcagtgcctcggtttacactcggacctcgtcgacatgcatt	Human *NDUFS2* mRNA	Designed via Oligostan in this study
NDUFS2_smi-Y7	gggcatgtgtggtcacagccatgatgtttacactcggacctcgtcgacatgcatt	Human *NDUFS2* mRNA	Designed via Oligostan in this study
NDUFS2_smi-Y8	attcgggctccagacactcgctcgtattacactcggacctcgtcgacatgcatt	Human *NDUFS2* mRNA	Designed via Oligostan in this study
NDUFS2_smi-Y9	gtgcactcctcctggccggatataagttacactcggacctcgtcgacatgcatt	Human *NDUFS2* mRNA	Designed via Oligostan in this study
NDUFS2_smi-Y10	ttgttggtcagcaactcctccaactcatttacactcggacctcgtcgacatgcatt	Human *NDUFS2* mRNA	Designed via Oligostan in this study
NDUFS2_smi-Y11	caatgtcaattgtccgatttcgccagatccttacactcggacctcgtcgacatgcatt	Human *NDUFS2* mRNA	Designed via Oligostan in this study
NDUFS2_smi-Y12	ccatagttaagtgcttcttctgctgttacaacttacactcggacctcgtcgacatgcatt	Human *NDUFS2* mRNA	Designed via Oligostan in this study
NDUFS2_smi-Y13	ccacccggcacaggtacctatcatagttacactcggacctcgtcgacatgcatt	Human *NDUFS2* mRNA	Designed via Oligostan in this study
NDUFS2_smi-Y14	tcttgtttagacactgtgcgataattctcaggttacactcggacctcgtcgacatgcatt	Human *NDUFS2* mRNA	Designed via Oligostan in this study
NDUFS2_smi-Y15	atctctgctcgcttaggtggagacactttacactcggacctcgtcgacatgcatt	Human *NDUFS2* mRNA	Designed via Oligostan in this study
NDUFS2_smi-Y16	tgtggctcctggaggaacttggtagccttacactcggacctcgtcgacatgcatt	Human *NDUFS2* mRNA	Designed via Oligostan in this study
NDUFS2_smi-Y17	ctcccttgggagcctcaatggcagtattacactcggacctcgtcgacatgcatt	Human *NDUFS2* mRNA	Designed via Oligostan in this study

NDUFS2_smi-Y18	gccttgatcttgcatcgataagggcggttacactcggacctcgtcgacatgcatt	Human *NDUFS2* mRNA	Designed via Oligostan in this study
NDUFS2_smi-Y19	ctgccaacatgtgtcccttagacatcttttacactcggacctcgtcgacatgcatt	Human *NDUFS2* mRNA	Designed via Oligostan in this study
NDUFS2_smi-Y20	cctgctcaccgatctacttctccaaattacactcggacctcgtcgacatgcatt	Human *NDUFS2* mRNA	Designed via Oligostan in this study
NDUFS2_smi-Y21	actcaacctggtcgtaaacatcatagggcttacactcggacctcgtcgacatgcatt	Human *NDUFS2* mRNA	Designed via Oligostan in this study
NDUFS2_smi-Y22	catctccccactcaattccatcactattacactcggacctcgtcgacatgcatt	Human *NDUFS2* mRNA	Designed via Oligostan in this study
NDUFS2_smi-Y23	ttcgttacacatcatggacacatagtctagcttacactcggacctcgtcgacatgcatt	Human *NDUFS2* mRNA	Designed via Oligostan in this study
NDUFS2_smi-Y24	aaactgataaatgtcatccataagcccaagggttacactcggacctcgtcgacatgcatt	Human *NDUFS2* mRNA	Designed via Oligostan in this study
SDHC_smi-Y1	cggaggcaatgacgaccaacgtgtctcattacactcggacctcgtcgacatgcatt	Human *SDHC* mRNA	Designed via Oligostan in this study
SDHC_smi-Y2	ttctgatacagagctgagggctaaagtgggttacactcggacctcgtcgacatgcatt	Human *SDHC* mRNA	Designed via Oligostan in this study
SDHC_smi-Y3	ctttggccgtggttcccaaaggaacagcttacactcggactcgtcgacatgcatt	Human *SDHC* mRNA	Designed via Oligostan in this study
SDHC_smi-Y4	tattcttattccagaaccgctccatctcttacactcggacctcgtcgacatgcatt	Human *SDHC* mRNA	Designed via Oligostan in this study
SDHC_smi-Y5	gtaatgtggggagacagaggacggtttgaaccttacactcggacctcgtcgacatgcatt	Human *SDHC* mRNA	Designed via Oligostan in this study
SDHC_smi-Y6	gacatcgccatgggaagagaccaactgtttacactcggacctcgtcgacatgcatt	Human *SDHC* mRNA	Designed via Oligostan in this study
SDHC_smi-Y7	aaagcaataccagtgccacggtggcagattacactcggacctcgtcgacatgcatt	Human *SDHC* mRNA	Designed via Oligostan in this study
SDHC_smi-Y8	ataagactcaaagttcccagggagtaacagggttacactcggacctcgtcgacatgcatt	Human *SDHC* mRNA	Designed via Oligostan in this study
SDHC_smi-Y9	acatgagagggaagacaagtgcaaacttagctttacactcggacctcgtcgacatgcatt	Human *SDHC* mRNA	Designed via Oligostan in this study
SDHC_smi-Y10	ggtcccacatcaagtgtcggatcccattacactcggacctcgtcgacatgcatt	Human *SDHC* mRNA	Designed via Oligostan in this study

SDHC_smi-Y11	tagctggggaatcttcaggccttttccttacactcggacctcgtcgacatgcatt	Human *SDHC* mRNA	Designed via Oligostan in this study
SDHC_smi-Y12	aagaaccaggacaaccactccagactggttacactcggacctcgtcgacatgcatt	Human *SDHC* mRNA	Designed via Oligostan in this study
SDHC_smi-Y13	taataatgtgtaggaagatgatgctgggagccttacactcggacctcgtcgacatgcatt	Human *SDHC* mRNA	Designed via Oligostan in this study
SDHC_smi-Y14	aacaaataaggagaacttttcccaggctggagttacactcggacctcgtcgacatgcatt	Human *SDHC* mRNA	Designed via Oligostan in this study
SDHC_smi-Y15	ttatggtctaccaggtactctactgctcttacactcggacctcgtcgacatgcatt	Human *SDHC* mRNA	Designed via Oligostan in this study
SDHC_smi-Y16	agaaacaaggggaaaactagacccttttccacttacactcggacctcgtcgacatgcatt	Human *SDHC* mRNA	Designed via Oligostan in this study
SDHC_smi-Y17	agctgtgggcaaaaaaggggagtttttgcagcttacactcggacctcgtcgacatgcatt	Human *SDHC* mRNA	Designed via Oligostan in this study
SDHC_smi-Y18	gagagagaataactgcttctaggccgagagtattacactcggacctcgtcgacatgcatt	Human *SDHC* mRNA	Designed via Oligostan in this study
SDHC_smi-Y19	gaccctcagcacaaatcaaagcccaatattacactcggacctcgtcgacatgcatt	Human *SDHC* mRNA	Designed via Oligostan in this study
SDHC_smi-Y20	tttccactgtctcaggaagaaggagccaaaagttacactcggacctcgtcgacatgcatt	Human *SDHC* mRNA	Designed via Oligostan in this study
SDHC_smi-Y21	atgaagagaattgtcctttaagccagcaaccttacactcggacctcgtcgacatgcatt	Human *SDHC* mRNA	Designed via Oligostan in this study
SDHC_smi-Y22	gtaggtgttaatggcctgggctctcacttacactcggacctcgtcgacatgcatt	Human *SDHC* mRNA	Designed via Oligostan in this study
SDHC_smi-Y23	caagaactaactagccctctttatctcccttacactcggacctcgtcgacatgcatt	Human *SDHC* mRNA	Designed via Oligostan in this study
SDHC_smi-Y24	gctatatattttctcctcaaaagcagctgcttacactcggacctcgtcgacatgcatt	Human *SDHC* mRNA	Designed via Oligostan in this study
SDHD_smi-Y1	agcaggtctgaccactggagttcgaagcttacactcggacctcgtcgacatgcatt	Human *SDHD* mRNA	Designed via Oligostan in this study
SDHD_smi-Y2	ggataggtcggtcctgaagaaatgctgagatattacactcggacctcgtcgacatgcatt	Human *SDHD* mRNA	Designed via Oligostan in this study
SDHD_smi-Y3	tgtatgtgctgcactccacaccattcttacactcggacctcgtcgacatgcatt	Human *SDHD* mRNA	Designed via Oligostan in this study
SDHD_smi-Y4	ttggagccagaatggtggctcggtgacattacactcggacctcgtcgacatgcatt	Human *SDHD* mRNA	Designed via Oligostan in this study
SDHD_smi-Y5	tctcgctagtccagtggagagatgcagttacactcggacctcgtcgacatgcatt	Human *SDHD* mRNA	Designed via Oligostan in this study
SDHD_smi-Y6	gcagacccaggagcaaaacactgacaacttacactcggacctcgtcgacatgcatt	Human *SDHD* mRNA	Designed via Oligostan in this study

SDHD_smi-Y7	cgcagagcaaggattcaaataagcagccggttacactcggacctcgtcgacatgcatt	Human *SDHD* mRNA	Designed via Oligostan in this study
SDHD_smi-Y8	ttgtccaaggccccagtgaccatgaagttacactcggacctcgtcgacatgcatt	Human *SDHD* mRNA	Designed via Oligostan in this study
SDHD_smi-Y9	aaggcatccccatgaacatagtcagtaacattacactcggacctcgtcgacatgcatt	Human *SDHD* mRNA	Designed via Oligostan in this study
SDHD_smi-Y10	caaaagccctgccttggcagctttctttacactcggacctcgtcgacatgcatt	Human *SDHD* mRNA	Designed via Oligostan in this study
SDHD_smi-Y11	agcaaagcccagcaaaggttaaagctgaaagtttacactcggacctcgtcgacatgcatt	Human *SDHD* mRNA	Designed via Oligostan in this study
SDHD_smi-Y12	ggcaacagctttgcagatgcccacatttacactcggacctcgtcgacatgcatt	Human *SDHD* mRNA	Designed via Oligostan in this study
SDHD_smi-Y13	tatgaagtcaaaaaggtcagagcttccacagcttacactcggacctcgtcgacatgcatt	Human *SDHD* mRNA	Designed via Oligostan in this study
SDHD_smi-Y14	aagcagaggcaaagaggcatacatcaattcttttacactcggacctcgtcgacatgcatt	Human *SDHD* mRNA	Designed via Oligostan in this study
SDHD_smi-Y15	atcttgtgattaagagaagaaggctgtccaccttacactcggacctcgtcgacatgcatt	Human *SDHD* mRNA	Designed via Oligostan in this study
SDHD_smi-Y16	ccccattaactcaccagaatatagaactcagttacactcggacctcgtcgacatgcatt	Human *SDHD* mRNA	Designed via Oligostan in this study
SDHD_smi-Y17	tatactgtgagtcttataagaagctgggaggcttacactcggacctcgtcgacatgcatt	Human *SDHD* mRNA	Designed via Oligostan in this study
SDHD_smi-Y18	gtattttgatacatctacagggaaacttgcccttacactcggacctcgtcgacatgcatt	Human *SDHD* mRNA	Designed via Oligostan in this study
hGAPDH_smi-Y1	cccagccttctccatggtggtgaagattacactcggacctcgtcgacatgcatt	Human *GAPDH* mRNA	Designed via Oligostan in this study
hGAPDH_smi-Y2	taccaaagttgtcatggatgaccttggccttacactcggacctcgtcgacatgcatt	Human *GAPDH* mRNA	Designed via Oligostan in this study
hGAPDH_smi-Y3	cctgcttcaccaccttcttgatgtcattacactcggacctcgtcgacatgcatt	Human *GAPDH* mRNA	Designed via Oligostan in this study
hGAPDH_smi-Y4	cttgacggtgccatggaatttgccatggttacactcggacctcgtcgacatgcatt	Human *GAPDH* mRNA	Designed via Oligostan in this study
hGAPDH_smi-Y5	cttggaggccatgtgggccatgaggtttacactcggacctcgtcgacatgcatt	Human *GAPDH* mRNA	Designed via Oligostan in this study
hGAPDH_smi-Y6	tctcatggttcacacccatgacgaacatttacactcggacctcgtcgacatgcatt	Human *GAPDH* mRNA	Designed via Oligostan in this study

hGAPDH_smi-Y7	cagcatcgccccacttgattttggaggttacactcggacctcgtcgacatgcatt	Human *GAPDH* mRNA	Designed via Oligostan in this study
hGAPDH_smi-Y8	tccattgatgacaagcttcccgttctcattacactcggacctcgtcgacatgcatt	Human *GAPDH* mRNA	Designed via Oligostan in this study
hGAPDH_smi-Y9	cacggaaggccatgccagtgagcttcttacactcggacctcgtcgacatgcatt	Human *GAPDH* mRNA	Designed via Oligostan in this study
hGAPDH_smi-Y10	ccagtggactccacgacgtactcagcttacactcggacctcgtcgacatgcatt	Human *GAPDH* mRNA	Designed via Oligostan in this study
hGAPDH_smi-Y11	atccacagtcttctgggtggcagtgatttacactcggacctcgtcgacatgcatt	Human *GAPDH* mRNA	Designed via Oligostan in this study
hGAPDH_smi-Y12	ggagtgggtgtcgctgttgaagtcagaggagttacactcggacctcgtcgacatgcatt	Human *GAPDH* mRNA	Designed via Oligostan in this study
hGAPDH_smi-Y13	ctcggctggcgacgcaaaagaagatgcgttacactcggacctcgtcgacatgcatt	Human *GAPDH* mRNA	Designed via Oligostan in this study
hGAPDH_smi-Y14	gggcatcagcagaggggcagagatgttacactcggacctcgtcgacatgcatt	Human *GAPDH* mRNA	Designed via Oligostan in this study
hGAPDH_smi-Y15	tctcgctcctggaagatggtgatgggattacactcggacctcgtcgacatgcatt	Human *GAPDH* mRNA	Designed via Oligostan in this study
hGAPDH_smi-Y16	caatatccactttaccagagttaaaagcagccttacactcggacctcgtcgacatgcatt	Human *GAPDH* mRNA	Designed via Oligostan in this study
hGAPDH_smi-Y17	cttggcagcgccagtagaggcagggattacactcggacctcgtcgacatgcatt	Human *GAPDH* mRNA	Designed via Oligostan in this study
hGAPDH_smi-Y18	atatttggcaggtttttctagacggcaggtcattacactcggacctcgtcgacatgcatt	Human *GAPDH* mRNA	Designed via Oligostan in this study
hGAPDH_smi-Y19	gggtgctaagcagttggtggtgcaggagttacactcggacctcgtcgacatgcatt	Human *GAPDH* mRNA	Designed via Oligostan in this study
hGAPDH_smi-Y20	catggactgtggtcatgagtccttccacttacactcggacctcgtcgacatgcatt	Human *GAPDH* mRNA	Designed via Oligostan in this study

hGAPDH_smi-Y21	cctggtgctcagtgtagcccaggatgttacactcggacctcgtcgacatgcatt	Human *GAPDH* mRNA	Designed via Oligostan in this study
hGAPDH_smi-Y22	accaccctgttgctgtagccaaattcgttacactcggacctcgtcgacatgcatt	Human *GAPDH* mRNA	Designed via Oligostan in this study
hGAPDH_smi-Y23	tccaccactgacacgttggcagtgggttacactcggacctcgtcgacatgcatt	Human *GAPDH* mRNA	Designed via Oligostan in this study
hGAPDH_smi-Y24	caatgccagccccagcgtcaaaggtgttacactcggacctcgtcgacatgcatt	Human *GAPDH* mRNA	Designed via Oligostan in this study
hGAPDH_smi-Y25	ccttccccatggtgtctgagcgatgtttacactcggacctcgtcgacatgcatt	Human *GAPDH* mRNA	Designed via Oligostan in this study
hGAPDH_smi-Y26	attgctgatgatcttgaggctgttgtcatattacactcggacctcgtcgacatgcatt	Human *GAPDH* mRNA	Designed via Oligostan in this study
hGAPDH_smi-Y27	aaccatgtagttgaggtcaatgaaggggtcatttacactcggacctcgtcgacatgcatt	Human *GAPDH* mRNA	Designed via Oligostan in this study
hGAPDH_smi-Y28	catcacgccacagtttcccggaggggttacactcggacctcgtcgacatgcatt	Human *GAPDH* mRNA	Designed via Oligostan in this study
hGAPDH_smi-Y29	gtcataccaggaaatgagcttgacaaagtggtttacactcggacctcgtcgacatgcatt	Human *GAPDH* mRNA	Designed via Oligostan in this study
hGAPDH_smi-Y30	gttcagctcagggatgaccttgcccattacactcggacctcgtcgacatgcatt	Human *GAPDH* mRNA	Designed via Oligostan in this study
hGAPDH_smi-Y31	ggtgaccaggcgcccaatacgaccaattacactcggacctcgtcgacatgcatt	Human *GAPDH* mRNA	Designed via Oligostan in this study
hGAPDH_smi-Y32	gactgagtgtggcagggactccccagttacactcggacctcgtcgacatgcatt	Human *GAPDH* mRNA	Designed via Oligostan in this study
GCN4_smi-Y	gctacctcattttccaggtggttacactcggacctcgtcgacatgcatt	GCN4 reporter mRNA	From reference [17]
mRuby3-smi-Y1	ttccttgatcagctcttcgttacactcggacctcgtcgacatgcatt	GCN4 reporter mRNA	From reference [17]
mRuby3-smi-Y2	accaccttcatacgcatatttacactcggacctcgtcgacatgcatt	GCN4 reporter mRNA	From reference [17]

mRuby3-smi-Y3	cgttgaccgaaccttccatttacactcggacctcgtcgacatgcatt	GCN4 reporter mRNA	From reference [17]
mRuby3-smi-Y4	tccctcgatgactttgatcttacactcggacctcgtcgacatgcatt	GCN4 reporter mRNA	From reference [17]
mRuby3-smi-Y5	aaggcaaatggcaggggtcttacactcggacctcgtcgacatgcatt	GCN4 reporter mRNA	From reference [17]
mRuby3-smi-Y6	acgacgtggcaagaatgtcttacactcggacctcgtcgacatgcatt	GCN4 reporter mRNA	From reference [17]
mRuby3-smi-Y7	aaaggtacggctgccatacttacactcggacctcgtcgacatgcatt	GCN4 reporter mRNA	From reference [17]
mRuby3-smi-Y8	gaaatcagggatgtcggccttacactcggacctcgtcgacatgcatt	GCN4 reporter mRNA	From reference [17]
mRuby3-smi-Y9	accatcttcgtatctcgtattacactcggacctcgtcgacatgcatt	GCN4 reporter mRNA	From reference [17]
mRuby3-smi-Y10	tgcgtgacggtgacgactcttacactcggacctcgtcgacatgcatt	GCN4 reporter mRNA	From reference [17]
mRuby3-smi-Y11	catcctcaaggctggtgtcttacactcggacctcgtcgacatgcatt	GCN4 reporter mRNA	From reference [17]
mRuby3-smi-Y12	gacgttgtagacgagctcgttacactcggacctcgtcgacatgcatt	GCN4 reporter mRNA	From reference [17]
mRuby3-smi-Y13	gaaagtttacccctctgacttacactcggacctcgtcgacatgcatt	GCN4 reporter mRNA	From reference [17]
mRuby3-smi-Y14	ttggtcttcttctgcatcattacactcggacctcgtcgacatgcatt	GCN4 reporter mRNA	From reference [17]
mRuby3-smi-Y15	tctgtattaggctcccaacttacactcggacctcgtcgacatgcatt	GCN4 reporter mRNA	From reference [17]
mRuby3-smi-Y16	catctgctggatacatcatttacactcggacctcgtcgacatgcatt	GCN4 reporter mRNA	From reference [17]
mRuby3-smi-Y17	tcagtgcgatgtcagtgtattacactcggacctcgtcgacatgcatt	GCN4 reporter mRNA	From reference [17]
mRuby3-smi-Y18	acggtctttttgacctgtttacactcggacctcgtcgacatgcatt	GCN4 reporter mRNA	From reference [17]
mRuby3-smi-Y19	accgggcatcttgatgttcttacactcggacctcgtcgacatgcatt	GCN4 reporter mRNA	From reference [17]
mRuby3-smi-Y20	cggtgatcaacggcatggattacactcggacctcgtcgacatgcatt	GCN4 reporter mRNA	From reference [17]
mRuby3-smi-Y21	cactctcctcgatcctttcttacactcggacctcgtcgacatgcatt	GCN4 reporter mRNA	From reference [17]
mRuby3-smi-Y22	gcactacgtaggtttcattttacactcggacctcgtcgacatgcatt	GCN4 reporter mRNA	From reference [17]

mRuby3-smi-Y23	tggcaactgccacttctctttacactcggacctcgtcgacatgcatt	GCN4 reporter mRNA	From reference [17]
mRuby3-smi-Y24	accaccaaggttgctgtatttacactcggacctcgtcgacatgcatt	GCN4 reporter mRNA	From reference [17]
mRuby3-smi-Y25	ttgtacagctcgtccatgcttacactcggacctcgtcgacatgcatt	GCN4 reporter mRNA	From reference [17]
hTERRA-smi-Y1	taaccctaaccctaaccctaaccctaaccctaaccctacactcggacctcgtcgacatgcatt	Human *TERRA* lncRNA	From reference [17]
mGap43-smi-Y1	tcttggtcagcctcggggtcttctttattacactcggacctcgtcgacatgcatt	Mouse *Gap43* mRNA	Designed via Oligostan in this study
mGap43-smi-Y2	agcagcaggcacatcggcttgtttaggttacactcggacctcgtcgacatgcatt	Mouse *Gap43* mRNA	Designed via Oligostan in this study
mGap43-smi-Y3	tgggccatcttcagccttggaggacgttacactcggacctcgtcgacatgcatt	Mouse *Gap43* mRNA	Designed via Oligostan in this study
mGap43-smi-Y4	tggtcctcatcattcttttcaacctgtttgttacactcggacctcgtcgacatgcatt	Mouse *Gap43* mRNA	Designed via Oligostan in this study
mGap43-smi-Y5	tcttctcatacagcacagcatggtggtattacactcggacctcgtcgacatgcatt	Mouse *Gap43* mRNA	Designed via Oligostan in this study
mGap43-smi-Y6	ctcatcctgtcgggcactttccttagttacactcggacctcgtcgacatgcatt	Mouse *Gap43* mRNA	Designed via Oligostan in this study
mGap43-smi-Y7	ttggcttcgtctacagcgtctttctccttacactcggacctcgtcgacatgcatt	Mouse *Gap43* mRNA	Designed via Oligostan in this study
mGap43-smi-Y8	ctcagcttggctgctttctgcagtctttacactcggacctcgtcgacatgcatt	Mouse *Gap43* mRNA	Designed via Oligostan in this study
mGap43-smi-Y9	caggggtggtggcagcagcatcagtgttacactcggacctcgtcgacatgcatt	Mouse *Gap43* mRNA	Designed via Oligostan in this study
mGap43-smi-Y10	gagttatcagtggtagctttagcagcactttcttacactcggacctcgtcgacatgcatt	Mouse *Gap43* mRNA	Designed via Oligostan in this study
mGap43-smi-Y11	tggtggctggggctgcatcggtagtattacactcggacctcgtcgacatgcatt	Mouse *Gap43* mRNA	Designed via Oligostan in this study
mGap43-smi-Y12	ctccttcttctccacaccatcagcaattacactcggacctcgtcgacatgcatt	Mouse *Gap43* mRNA	Designed via Oligostan in this study
mGap43-smi-Y13	tttttccttgttatgtgtccacggaagctagcttacactcggacctcgtcgacatgcatt	Mouse *Gap43* mRNA	Designed via Oligostan in this study
mGap43-smi-Y14	gaattttggtcgcagccttatgagccttatttacactcggacctcgtcgacatgcatt	Mouse *Gap43* mRNA	Designed via Oligostan in this study
mGap43-smi-Y15	tccggcttgacaccatcttgttcaatctttacactcggacctcgtcgacatgcatt	Mouse *Gap43* mRNA	Designed via Oligostan in this study
mGap43-smi-Y16	gagaaatagagaggaaagtggactcccacaggttacactcggacctcgtcgacatgcatt	Mouse *Gap43* mRNA	Designed via Oligostan in this study

mGap43-smi-Y17	gaggacaggctcacacacgtgagcaggacaggttacactcggacctcgtcgacatgcatt	Mouse *Gap43* mRNA	Designed via Oligostan in this study
mGap43-smi-Y18	gagaagggcaggagagacagggttcaggtgttacactcggacctcgtcgacatgcatt	Mouse *Gap43* mRNA	Designed via Oligostan in this study
mGap43-smi-Y19	acgtggaaagccatttcttaaagttcaggcatttacactcggacctcgtcgacatgcatt	Mouse *Gap43* mRNA	Designed via Oligostan in this study
mGap43-smi-Y20	cccttcacccttcttctcctcagaagttacactcggacctcgtcgacatgcatt	Mouse *Gap43* mRNA	Designed via Oligostan in this study
mGap43-smi-Y21	tgcatcacccttcttctcgcctttgattacactcggacctcgtcgacatgcatt	Mouse *Gap43* mRNA	Designed via Oligostan in this study
mGap43-smi-Y22	ctctcctttcctcctctcttccttatttacactcggacctcgtcgacatgcatt	Mouse *Gap43* mRNA	Designed via Oligostan in this study
mGap43-smi-Y23	catcattaccaaaaactcgccataacaacaccttacactcggacctcgtcgacatgcatt	Mouse *Gap43* mRNA	Designed via Oligostan in this study
mGap43-smi-Y24	cacacgcaccagatcaaaaaaccggggtattacactcggacctcgtcgacatgcatt	Mouse *Gap43* mRNA	Designed via Oligostan in this study
mStmn2-smi-Y1	tgatcagcacgttggaaggttcagcctttcttacactcggacctcgtcgacatgcatt	Mouse *Stmn2* mRNA	Designed via Oligostan in this study
mStmn2-smi-Y2	ggctttgccgcttctaggcaggaagcttacactcggacctcgtcgacatgcatt	Mouse *Stmn2* mRNA	Designed via Oligostan in this study
mStmn2-smi-Y3	acgctcagagattacggagtcatctaggtcttacactcggacctcgtcgacatgcatt	Mouse *Stmn2* mRNA	Designed via Oligostan in this study
mStmn2-smi-Y4	gcggctccgggtagaagcaggagcagttacactcggactcgtcgacatgcatt	Mouse *Stmn2* mRNA	Designed via Oligostan in this study
mStmn2-smi-Y5	cagtgacagcatagacagctccttcatttttacactcggacctcgtcgacatgcatt	Mouse *Stmn2* mRNA	Designed via Oligostan in this study
mStmn2-smi-Y6	ccttgtaggccattgctgttttagccattttacactcggacctcgtcgacatgcatt	Mouse *Stmn2* mRNA	Designed via Oligostan in this study
mStmn2-smi-Y7	gtgtctgctgattcttatacttggcacaaatttacactcggacctcgtcgacatgcatt	Mouse *Stmn2* mRNA	Designed via Oligostan in this study
mStmn2-smi-Y8	agtggtttggtcttgtttataggcaggattgcttacactcggacctcgtcgacatgcatt	Mouse *Stmn2* mRNA	Designed via Oligostan in this study
mStmn2-smi-Y9	ttgtttgtgtttttaatgcagcaaccagctcattacactcggacctcgtcgacatgcatt	Mouse *Stmn2* mRNA	Designed via Oligostan in this study
mStmn2-smi-Y10	gagaaataagcccacttcatgaagaacaatccttacactcggacctcgtcgacatgcatt	Mouse *Stmn2* mRNA	Designed via Oligostan in this study
mStmn2-smi-Y11	ctgcttgaaccctctggctttgcgttttacactcggacctcgtcgacatgcatt	Mouse *Stmn2* mRNA	Designed via Oligostan in this study
mStmn2-smi-Y12	gtgtagcgcgtaatccatgaggagcagacttacactcggacctcgtcgacatgcatt	Mouse *Stmn2* mRNA	Designed via Oligostan in this study

mStmn2-smi-Y13	aagtgctatgactggtagattcccttagcttacactcggacctcgtcgacatgcatt	Mouse *Stmn2* mRNA	Designed via Oligostan in this study
mStmn2-smi-Y14	cagtacccacgatctaggtgtggtcttggttacactcggacctcgtcgacatgcatt	Mouse *Stmn2* mRNA	Designed via Oligostan in this study
mStmn2-smi-Y15	taggcaatggtgggtttctagcaccatagattacactcggacctcgtcgacatgcatt	Mouse *Stmn2* mRNA	Designed via Oligostan in this study
mStmn2-smi-Y16	gtctactgacctcatttttcggttggaatgaattacactcggacctcgtcgacatgcatt	Mouse *Stmn2* mRNA	Designed via Oligostan in this study
mStmn2-smi-Y17	gagttctttttaaaccatgtcatacacttcccttacactcggacctcgtcgacatgcatt	Mouse *Stmn2* mRNA	Designed via Oligostan in this study
mStmn2-smi-Y18	ggggatttactatgggaggggcttgccttacactcggacctcgtcgacatgcatt	Mouse *Stmn2* mRNA	Designed via Oligostan in this study
mStmn2-smi-Y19	cctgcagttccttgttcctgcgaaccttacactcggacctcgtcgacatgcatt	Mouse *Stmn2* mRNA	Designed via Oligostan in this study
mStmn2-smi-Y20	ccttaatctgttccatcttcaggatcagcttacactcggacctcgtcgacatgcatt	Mouse *Stmn2* mRNA	Designed via Oligostan in this study
mStmn2-smi-Y21	tgcttcagcacctgagcctcttgagattacactcggacctcgtcgacatgcatt	Mouse *Stmn2* mRNA	Designed via Oligostan in this study
mStmn2-smi-Y22	ctctgcagcctccagctttttctgaatttacactcggacctcgtcgacatgcatt	Mouse *Stmn2* mRNA	Designed via Oligostan in this study
mStmn2-smi-Y23	cctccagagacaggtctttcttctttggagttacactcggacctcgtcgacatgcatt	Mouse *Stmn2* mRNA	Designed via Oligostan in this study
mStmn2-smi-Y24	gctagagttcgtggagcttctgagatgggattacactcggacctcgtcgacatgcatt	Mouse *Stmn2* mRNA	Designed via Oligostan in this study
mStmn2-smi-Y25	tggtggcttcaagatcagctcaaaagcctttacactcggacctcgtcgacatgcatt	Mouse *Stmn2* mRNA	Designed via Oligostan in this study
mStmn2-smi-Y26	ccagaggcccgcttgttgatctgcttttacactcggacctcgtcgacatgcatt	Mouse *Stmn2* mRNA	Designed via Oligostan in this study
mStmn2-smi-Y27	agggatgtgcacgcacggagtggtggttacactcggacctcgtcgacatgcatt	Mouse *Stmn2* mRNA	Designed via Oligostan in this study
mStmn2-smi-Y28	gttcacagaactccaattctttattcatcacattacactcggacctcgtcgacatgcatt	Mouse *Stmn2* mRNA	Designed via Oligostan in this study
mStmn2-smi-Y29	cccttcactgcgtcagcatcacagatttacactcggacctcgtcgacatgcatt	Mouse *Stmn2* mRNA	Designed via Oligostan in this study
mStmn2-smi-Y30	aacgttcagtagcattatgtgcttgtactacattacactcggacctcgtcgacatgcatt	Mouse *Stmn2* mRNA	Designed via Oligostan in this study
mStmn2-smi-Y31	ttctaccctgactgagctcagatttgtcttacactcggacctcgtcgacatgcatt	Mouse *Stmn2* mRNA	Designed via Oligostan in this study
mStmn2-smi-Y32	attacgagcaaatgtggaggttcacatggacattacactcggacctcgtcgacatgcatt	Mouse *Stmn2* mRNA	Designed via Oligostan in this study

mStmn2-smi-Y33	acacaacgtcaaaagcctgttacaggacatgttacactcggacctcgtcgacatgcatt	Mouse *Stmn2* mRNA	Designed via Oligostan in this study
mStmn2-smi-Y34	actgatatcgcatgatccattataatataggcttacactcggacctcgtcgacatgcatt	Mouse *Stmn2* mRNA	Designed via Oligostan in this study
mStmn2-smi-Y35	ccgccattgcttcagccagacagttcttacactcggacctcgtcgacatgcatt	Mouse *Stmn2* mRNA	Designed via Oligostan in this study
mStmn2-smi-Y36	catgcctctccttttcctgcagacgtttacactcggacctcgtcgacatgcatt	Mouse *Stmn2* mRNA	Designed via Oligostan in this study
mStmn2-smi-Y37	aatgatagcagctagattagcctcacggttttacactcggacctcgtcgacatgcatt	Mouse *Stmn2* mRNA	Designed via Oligostan in this study
mStmn2-smi-Y38	ctcctccgccatcttgctgaagttgtttacactcggacctcgtcgacatgcatt	Mouse *Stmn2* mRNA	Designed via Oligostan in this study
mStmn2-smi-Y39	cctccatgtcgtcgtaggtgtagatgttgatttacactcggacctcgtcgacatgcatt	Mouse *Stmn2* mRNA	Designed via Oligostan in this study
mStmn2-smi-Y40	aaggcaaaggagaagggtccagctgtagcttacactcggacctcgtcgacatgcatt	Mouse *Stmn2* mRNA	Designed via Oligostan in this study
mStmn2-smi-Y41	acaacttcaaaactgcaataggtacgtatgctttacactcggacctcgtcgacatgcatt	Mouse *Stmn2* mRNA	Designed via Oligostan in this study
mStmn2-smi-Y42	cacatgcacctgtttctaaaacccaaacacttacactcggacctcgtcgacatgcatt	Mouse *Stmn2* mRNA	Designed via Oligostan in this study
mActb-smi-X1	atagtgatgacctggccgtcagcctcctaagtttcgagctggactcagtg	Mouse *Actb* mRNA	From reference [33]
mActb-smi-X2	catcggaaccgctcgttgcccctcctaagtttcgagctggactcagtg	Mouse *Actb* mRNA	From reference [33]
mActb-smi-X3	acccaagaaggaaggctggaacctcctaagtttcgagctggactcagtg	Mouse *Actb* mRNA	From reference [33]
mActb-smi-X4	tcatggatgccacaggattcccctcctaagtttcgagctggactcagtg	Mouse *Actb* mRNA	From reference [33]
mActb-smi-X5	cggatgtcaacgtcacacttcacctcctaagtttcgagctggactcagtg	Mouse *Actb* mRNA	From reference [33]
mActb-smi-X6	ccagacagcactgtgttggcatcctcctaagtttcgagctggactcagtg	Mouse *Actb* mRNA	From reference [33]
mActb-smi-X7	atgcctgggtacatggtggtaccctcctaagtttcgagctggactcagtg	Mouse *Actb* mRNA	From reference [33]
mActb-smi-X8	tctccttctgcatcctgtcagccctcctaagtttcgagctggactcagtg	Mouse *Actb* mRNA	From reference [33]
mActb-smi-X9	catggtgctaggagccagagccctcctaagtttcgagctggactcagtg	Mouse *Actb* mRNA	From reference [33]
mActb-smi-X10	cagagtacttgcgctcaggaggcctcctaagtttcgagctggactcagtg	Mouse *Actb* mRNA	From reference [33]

mActb-smi-X11	ccaggatggagccaccgatccctcctaagtttcgagctggactcagtg	Mouse *Actb* mRNA	From reference [33]
mActb-smi-X12	atctgctggaaggtggacagtgcctcctaagtttcgagctggactcagtg	Mouse *Actb* mRNA	From reference [33]
mActb-smi-X13	cgtactcctgcttgctgatccacctcctaagtttcgagctggactcagtg	Mouse *Actb* mRNA	From reference [33]
mActb-smi-X14	cttgcggtgcacgatggagggcctcctaagtttcgagctggactcagtg	Mouse *Actb* mRNA	From reference [33]
mActb-smi-X15	cgcagctcagtaacagtccgccctcctaagtttcgagctggactcagtg	Mouse *Actb* mRNA	From reference [33]
mActb-smi-X16	tcaaagaaagggtgtaaaaccctcctaagtttcgagctggactcagtg	Mouse *Actb* mRNA	From reference [33]
mActb-smi-X17	ttttttttttttctgcgcaagttagcctcctaagtttcgagctggactcagtg	Mouse *Actb* mRNA	From reference [33]
mActb-smi-X18	aaagccatgccaatgttgtccctcctaagtttcgagctggactcagtg	Mouse *Actb* mRNA	From reference [33]
mActb-smi-X19	gcgccaaaacaaaacaaaaaaacttacctcctaagtttcgagctggactcagtg	Mouse *Actb* mRNA	From reference [33]
mActb-smi-X20	tcaccgttccagtttttaaacctcctaagtttcgagctggactcagtg	Mouse *Actb* mRNA	From reference [33]
mActb-smi-X21	atgtttgctccaaccaactgcctcctaagtttcgagctggactcagtg	Mouse *Actb* mRNA	From reference [33]
mActb-smi-X22	ccacatttgtagaactttggcctcctaagtttcgagctggactcagtg	Mouse *Actb* mRNA	From reference [33]
mActb-smi-X23	caaaacaatgtacaaagtcccctcctaagtttcgagctggactcagtg	Mouse *Actb* mRNA	From reference [33]
mActb-smi-X24	ggaatgactattaaaaaaagaccctcctaagtttcgagctggactcagtg	Mouse *Actb* mRNA	From reference [33]
mActb-smi-X25	accacttatttcatggataccctcctaagtttcgagctggactcagtg	Mouse *Actb* mRNA	From reference [33]
mActb-smi-X26	aggagtgggggtggcttttgcctcctaagtttcgagctggactcagtg	Mouse *Actb* mRNA	From reference [33]
mActb-smi-X27	ggacgcgaccatcctcctctcctcctaagtttcgagctggactcagtg	Mouse *Actb* mRNA	From reference [33]
mActb-smi-X28	accttccccggggtggactcctcctaagtttcgagctggactcagtg	Mouse *Actb* mRNA	From reference [33]
mActb-smi-X29	atttttgcagtacataatttacaccctcctaagtttcgagctggactcagtg	Mouse *Actb* mRNA	From reference [33]
mActb-smi-X30	ttaaggcggaagatttaaaaaaacctcctaagtttcgagctggactcagtg	Mouse *Actb* mRNA	From reference [33]

mActb-smi-X31	acctgggccattcagaaattcctcctaagtttcgagctggactcagtg	Mouse *Actb* mRNA	From reference [33]
mActb-smi-X32	gggacaaaaaaaagggaggccctcctaagtttcgagctggactcagtg	Mouse *Actb* mRNA	From reference [33]
mActb-smi-X33	ctcccagggagaccaaagcccctcctaagtttcgagctggactcagtg	Mouse *Actb* mRNA	From reference [33]
mActb-smi-X34	ggctgcctcaacacctcaaccctcctaagtttcgagctggactcagtg	Mouse *Actb* mRNA	From reference [33]
mActb-smi-X35	gtcagtgtacaggccagccccctcctaagtttcgagctggactcagtg	Mouse *Actb* mRNA	From reference [33]
mActb-smi-X36	ggtgtgcacttttattggtccctcctaagtttcgagctggactcagtg	Mouse *Actb* mRNA	From reference [33]
mActb-smi-X37	tgcaaagaagctgtgctcgccctcctaagtttcgagctggactcagtg	Mouse *Actb* mRNA	Designed via Stellaris Probe Designer in this study
mActb-smi-X38	tgtggaccggcaacgaaggacctcctaagtttcgagctggactcagtg	Mouse *Actb* mRNA	Designed via Stellaris Probe Designer in this study
mActb-smi-X39	atatcgtcatccatggcgaacctcctaagtttcgagctggactcagtg	Mouse *Actb* mRNA	Designed via Stellaris Probe Designer in this study
mActb-smi-X40	gagagcatagccctcgtagatgggcacctcctaagtttcgagctggactcagtg	Mouse *Actb* mRNA	Designed via Oligostan in this study
mActb-smi-X41	agcctggatggctacgtacatggctgcctcctaagtttcgagctggactcagtg	Mouse *Actb* mRNA	Designed via Oligostan in this study
mActb-smi-X42	aggtgtggtgccagatcttctccatgtcctcctaagtttcgagctggactcagtg	Mouse *Actb* mRNA	Designed via Oligostan in this study
mActb-smi-X43	tcccagttggtaacaatgccatgttcaatgcctcctaagtttcgagctggactcagtg	Mouse *Actb* mRNA	Designed via Oligostan in this study
mActb-smi-X44	gtacttcagggtcaggatacctctcttgcctcctaagtttcgagctggactcagtg	Mouse *Actb* mRNA	Designed via Oligostan in this study
mActb-smi-X45	ttctctttgatgtcacgcacgatttcccctcctaagtttcgagctggactcagtg	Mouse *Actb* mRNA	Designed via Oligostan in this study
mActb-smi-X46	tcagctgtggtggtgaagctgtagccacctcctaagtttcgagctggactcagtg	Mouse *Actb* mRNA	Designed via Oligostan in this study
mActb-smi-X47	ctcggtcaggatcttcatgaggtagtctgtcctcctaagtttcgagctggactcagtg	Mouse *Actb* mRNA	Designed via Oligostan in this study
mActb-smi-X48	cgtctccggagtccatcacaatgcctcctcctaagtttcgagctggactcagtg	Mouse *Actb* mRNA	Designed via Oligostan in this study
mActb-smi-X49	gtgttgaaggtctcaaacatgatctgggtcatcctcctaagtttcgagctggactcagtg	Mouse *Actb* mRNA	Designed via Oligostan in this study

mActb-smi-X50	tttcacggttggccttagggttcaggggcctcctaagtttcgagctggactcagtg	Mouse *Actb* mRNA	Designed via Oligostan in this study
mActb-smi-X51	tcaggggccacacgcagctcattgtacctcctaagtttcgagctggactcagtg	Mouse *Actb* mRNA	Designed via Oligostan in this study
mActb-smi-X52	cctcgtcacccacataggagtccttccctcctaagtttcgagctggactcagtg	Mouse *Actb* mRNA	Designed via Oligostan in this study
Rn28s1_smi-X1	atgcttaaattcagcgggtccctcctaagtttcgagctggactcagtg	Mouse *Rn28s1* rRNA	From reference [34]
Rn28s1_smi-X2	cggtatttagccttagatggcctcctaagtttcgagctggactcagtg	Mouse *Rn28s1* rRNA	From reference [34]
Rn28s1_smi-X3	tacctcttaacggtttcacgcctcctaagtttcgagctggactcagtg	Mouse *Rn28s1* rRNA	From reference [34]
Rn28s1_smi-X4	agggaaccagctactagatgcctcctaagtttcgagctggactcagtg	Mouse *Rn28s1* rRNA	From reference [34]
Rn28s1_smi-X5	ttctgcttaccaaaagtggccctcctaagtttcgagctggactcagtg	Mouse *Rn28s1* rRNA	From reference [34]
Rn28s1_smi-X6	gagttgttacacactccttacctcctaagtttcgagctggactcagtg	Mouse *Rn28s1* rRNA	From reference [34]
Rn28s1_smi-X7	ttatcccgaagttacggatccctcctaagtttcgagctggactcagtg	Mouse *Rn28s1* rRNA	From reference [34]
Rn28s1_smi-X8	cgcgcttcattgaatttcttcctcctaagtttcgagctggactcagtg	Mouse *Rn28s1* rRNA	From reference [34]
Rn28s1_smi-X9	atagtaggtagggacagtggcctcctaagtttcgagctggactcagtg	Mouse *Rn28s1* rRNA	From reference [34]
Rn28s1_smi-X10	agagtagtggtatttcaccgcctcctaagtttcgagctggactcagtg	Mouse *Rn28s1* rRNA	From reference [34]
Rn28s1_smi-X11	gtggtaacttttctgacacccctcctaagtttcgagctggactcagtg	Mouse *Rn28s1* rRNA	From reference [34]
Rn28s1_smi-X12	ctcgtactgagcaggattaccctcctaagtttcgagctggactcagtg	Mouse *Rn28s1* rRNA	From reference [34]
Rn28s1_smi-X13	attctgacttagaggcgttccctcctaagtttcgagctggactcagtg	Mouse *Rn28s1* rRNA	From reference [34]
Rn28s1_smi-X14	ggtcgtctacgaatggtttacctcctaagtttcgagctggactcagtg	Mouse *Rn28s1* rRNA	From reference [34]
Rn28s1_smi-X15	tcgagggctgactttcaatacctcctaagtttcgagctggactcagtg	Mouse *Rn28s1* rRNA	From reference [34]
hGAPDH_smi-X1	cccagccttctccatggtggtgaagacctcctaagtttcgagctggactcagtg	Human *GAPDH* mRNA	Designed via Oligostan in this study
hGAPDH_smi-X2	taccaaagttgtcatggatgaccttggcccctcctaagtttcgagctggactcagtg	Human *GAPDH* mRNA	Designed via Oligostan in this study

hGAPDH_smi-X3	cctgcttcaccaccttcttgatgtcacctcctaagtttcgagctggactcagtg	Human *GAPDH* mRNA	Designed via Oligostan in this study
hGAPDH_smi-X4	cttgacggtgccatggaatttgccatggcctcctaagtttcgagctggactcagtg	Human *GAPDH* mRNA	Designed via Oligostan in this study
hGAPDH_smi-X5	cttggaggccatgtgggccatgaggtcctcctaagtttcgagctggactcagtg	Human *GAPDH* mRNA	Designed via Oligostan in this study
hGAPDH_smi-X6	tctcatggttcacacccatgacgaacatcctcctaagtttcgagctggactcagtg	Human *GAPDH* mRNA	Designed via Oligostan in this study
hGAPDH_smi-X7	cagcatcgccccacttgattttggaggcctcctaagtttcgagctggactcagtg	Human *GAPDH* mRNA	Designed via Oligostan in this study
hGAPDH_smi-X8	tccattgatgacaagcttcccgttctcacctcctaagtttcgagctggactcagtg	Human *GAPDH* mRNA	Designed via Oligostan in this study
hGAPDH_smi-X9	cacggaaggccatgccagtgagcttccctcctaagtttcgagctggactcagtg	Human *GAPDH* mRNA	Designed via Oligostan in this study
hGAPDH_smi-X10	ccagtggactccacgacgtactcagccctcctaagtttcgagctggactcagtg	Human *GAPDH* mRNA	Designed via Oligostan in this study
hGAPDH_smi-X11	atccacagtcttctgggtggcagtgatcctcctaagtttcgagctggactcagtg	Human *GAPDH* mRNA	Designed via Oligostan in this study
hGAPDH_smi-X12	ggagtgggtgtcgctgttgaagtcagaggagcctcctaagtttcgagctggactcagtg	Human *GAPDH* mRNA	Designed via Oligostan in this study
hGAPDH_smi-X13	ctcggctggcgacgcaaaagaagatgcgcctcctaagttttcgagctggactcagtg	Human *GAPDH* mRNA	Designed via Oligostan in this study
hGAPDH_smi-X14	gggcatcagcagaggggcagagatgcctcctaagtttcgagctggactcagtg	Human *GAPDH* mRNA	Designed via Oligostan in this study
hGAPDH_smi-X15	tctcgctcctggaagatggtgatgggacctcctaagtttcgagctggactcagtg	Human *GAPDH* mRNA	Designed via Oligostan in this study
hGAPDH_smi-X16	caatatccactttaccagagttaaaagcagcccctcctaagtttcgagctggactcagtg	Human *GAPDH* mRNA	Designed via Oligostan in this study

Supplementary Table 5 | Scoring of different gRNA combinations based on CRISPR-TO performance for exploring gRNA design principles. Different combinations of gRNAs were used for CRISPR-TO perturbation in Neuro-2a cells to recruit *Actb* or *Gap43* mRNA to the OMM. Each set of gRNAs were scored from 0 to 4 based on the efficiency of mRNA relocalization: 0 (not working), 1 (probably working), 2 (working), 3 (working well), and 4 (working very well).

Target RNA	gRNA combination	Score
Mouse *Actb* mRNA	1,2,3,4,5,6,7	3
Mouse *Actb* mRNA	2,3,4,5,6,7	1
Mouse *Actb* mRNA	1,3,4,5,6,7	2
Mouse *Actb* mRNA	1,2,4,5,6,7	3
Mouse *Actb* mRNA	1,2,3,5,6,7	2
Mouse *Actb* mRNA	1,2,3,4,6,7	2
Mouse *Actb* mRNA	1,2,3,4,5,7	4
Mouse *Actb* mRNA	1,2,3,4,5,6	3
Mouse *Actb* mRNA	1,2,4,5,	2
Mouse *Actb* mRNA	1,2,4	3
Mouse *Actb* mRNA	1,2,3	3
Mouse *Actb* mRNA	1,2	2
Mouse *Gap43* mRNA	1,2,3,4,5	0
Mouse *Gap43* mRNA	6, 8, 10, 12	0
Mouse *Gap43* mRNA	2, 6, 8, 14	3
Mouse *Gap43* mRNA	5, 12, 14	0
Mouse *Gap43* mRNA	9, 11, 13, 14	3
Mouse *Gap43* mRNA	7, 10, 14	0
Mouse *Gap43* mRNA	2, 3, 4, 8	3
Mouse *Gap43* mRNA	2, 4, 8, 11	1
Mouse *Gap43* mRNA	2, 3, 11	0
Mouse *Gap43* mRNA	1, 7, 11	0
Mouse *Gap43* mRNA	5, 10, 12	0
Mouse *Gap43* mRNA	3, 9, 13	0
Mouse *Gap43* mRNA	4, 8	0
Mouse *Gap43* mRNA	6, 8, 10, 12, 14	1
Mouse *Gap43* mRNA	6 ,8, 11, 13, 14, 2	2
Mouse *Gap43* mRNA	6, 9, 11, 13, 14	1
Mouse *Gap43* mRNA	6, 10, 12, 14, 5	2
Mouse *Gap43* mRNA	7, 9, 11, 13, 14	2
Mouse *Gap43* mRNA	7, 10, 12, 14, 1	0
Mouse *Gap43* mRNA	8, 10, 12, 14, 2, 3, 4	2
Mouse *Gap43* mRNA	8, 11, 13, 14, 2, 4	2
Mouse *Gap43* mRNA	9, 11, 13, 14, 2, 3, 4	2
Mouse *Gap43* mRNA	10, 12, 14, 2, 4, 5	2
Mouse *Gap43* mRNA	2, 6, 8	0
Mouse *Gap43* mRNA	2, 8, 14	3

Mouse *Gap43* mRNA	2, 6, 14	1
Mouse *Gap43* mRNA	6, 8, 14	1
Mouse *Gap43* mRNA	11, 13, 14	4
Mouse *Gap43* mRNA	2, 8, 11, 14	1
Mouse *Gap43* mRNA	8, 11, 13, 14	3
Mouse *Gap43* mRNA	2, 8, 11	3
Mouse *Gap43* mRNA	2, 11, 14	3
Mouse *Gap43* mRNA	8 ,11, 14	3
Mouse *Gap43* mRNA	8, 13, 14	4
Mouse *Gap43* mRNA	8, 11, 13	3
Mouse *Gap43* mRNA	1,2,3,4,5	0
Mouse *Gap43* mRNA	6, 8, 10, 12	0
Mouse *Gap43* mRNA	2, 6, 8, 14	3
Mouse *Gap43* mRNA	5, 12, 14	0
Mouse *Gap43* mRNA	9, 11, 13, 14	3
Mouse *Gap43* mRNA	7, 10, 14	0
Mouse *Gap43* mRNA	2, 3, 4, 8	3
Mouse *Gap43* mRNA	2, 4, 8, 11	1
Mouse *Gap43* mRNA	2, 3, 11	0
Mouse *Gap43* mRNA	1, 7, 11	0
Mouse *Gap43* mRNA	5, 10, 12	0
Mouse *Gap43* mRNA	3, 9, 13	0
Mouse *Gap43* mRNA	4, 8	0
Mouse *Gap43* mRNA	6, 8, 10, 12, 14	1
Mouse *Gap43* mRNA	6 ,8, 11, 13, 14, 2	2
Mouse *Gap43* mRNA	6, 9, 11, 13, 14	1
Mouse *Gap43* mRNA	6, 10, 12, 14, 5	2
Mouse *Gap43* mRNA	7, 9, 11, 13, 14	2
Mouse *Gap43* mRNA	7, 10, 12, 14, 1	0
Mouse *Gap43* mRNA	8, 10, 12, 14, 2, 3, 4	2
Mouse *Gap43* mRNA	8, 11, 13, 14, 2, 4	2
Mouse *Gap43* mRNA	9, 11, 13, 14, 2, 3, 4	2
Mouse *Gap43* mRNA	10, 12, 14, 2, 4, 5	2
Mouse *Gap43* mRNA	2, 6, 8	0
Mouse *Gap43* mRNA	2, 8, 14	3
Mouse *Gap43* mRNA	2, 6, 14	1
Mouse *Gap43* mRNA	6, 8, 14	1
Mouse *Gap43* mRNA	11, 13, 14	4
Mouse *Gap43* mRNA	2, 8, 11, 14	1
Mouse *Gap43* mRNA	8, 11, 13, 14	3
Mouse *Gap43* mRNA	2, 8, 11	3
Mouse *Gap43* mRNA	2, 11, 14	3
Mouse *Gap43* mRNA	8 ,11, 14	3
Mouse *Gap43* mRNA	8, 13, 14	4
Mouse *Gap43* mRNA	8, 11, 13	3

Supplementary Table 6 | Motor proteins used in the study. The sequence and amino acid regions of the truncated motor proteins used in this study.

Truncated motor protein	Amino acid region	Amino acid sequence
KIF5B*	aa1-555	MADPAECNIKVMCRFRPLNESEVNRGDKYVAKFQGEDTVM IASKPYAFDRVFQSSTSQEQVYNDCAKKIVKDVLEGYNGTIF AYGQTSSGKTHTMEGKLHDPEGMGIIPRIVQDIFNYIYSMDE NLEFHIKVSYFEIYLDKIRDLLDVSKTNLSVHEDKNRVPYVK GCTERFVCSPDEVMDTIDEGKSNRHVAVTNMNEHSSRSHSIF LINVKQENTQTEQKLSGKLYLVDLAGSEKVSKTGAEGAVLD EAKNINKSLSALGNVISALAEGSTYVPYRDSKMTRILQDSLG GNCRTTIVICCSPSSYNESETKSTLLFGQRAKTIKNTVCVNVE LTAEQWKKKYEKEKEKNKTLRNTIQWLENELNRWRNGETV PIDEQFDKEKANLEAFTADKDIAITSDKPAAAVGMAGSFTDA ERRKCEEELAKLYKQLDDKDEEINQQSQLVEKLKTQMLDQE ELLASTRRDQDNMQAELNRLQAENDASKEEVKEVLQALEE LAVNYDQKSQEVEDKTKEYELLSDELNQKSATLASIDAELQ KLKEMTNHQKKRAAEMM
KIFC1*	aa125-673	MAGGKKPSKRPAWDLKGQLCDLNAELKRCRERTQTLDQEN QQLQDQLRDAQQQVKALGTERTTLEGHLAKVQAQAEQGQ QELKNLRACVLELEERLSTQEGLVQELQKKQVELQEERRGL MSQLEEKERRLQTSEAALSSSQAEVASLRQETVAQAALLTER EERLHGLEMERRRLHNQLQELKGNIRVFCRVRPVLPGEPTPP PGLLLFPSGPGGPSDPPTRLSLSRSDERRGTLSGAPAPPTRHD FSFDRVFPPGSGQDEVFEEIAMLVQSALDGYPVCIFAYGQTG SGKTFTMEGGPGGDPQLEGLIPRALRHLFSVAQELSGQGWT YSFVASYVEIYNETVRDLLATGTRKGQGGECEIRRAGPGSEE LTVTNARYVPVSCEKEVDALLHLARQNRAVARTAQNERSSR SHSVFQLQISGEHSSRGLQCGAPLSLVDLAGSERLDPGLALG PGERERLRETQAINSSLSTLGLVIMALSNKESHVPYRNSKLT YLLQNSLGGSAKMLMFVNISPLEENVSESLNSLRFASKVNQ CVIGTAQANRK
KIF5A*	aa1-559	MAETNNECSIKVLCRFRPLNQAEILRGDKFIPIFQGDDSVIIG GKPYVFDRVFPPNTTQEQVYHACAMQIVKDVLAGYNGTIFA YGQTSSGKTHTMEGKLHDPQLMGIIPRIARDIFNHIYSMDEN LEFHIKVSYFEIYLDKIRDLLDVTKTNLSVHEDKNRVPFVKG CTERFVSSPEEILDVIDEGKSNRHVAVTNMNEHSSRSHSIFLI

		NIKQENVETEQKLSGKLYLVDLAGSEKVSKTGAEGAVLDEA KNINKSLSALGNVISALAEGTKSYVPYRDSKMTRILQDSLGG NCRTTMFICCSPSSYNDAETKSTLMFGQRAKTIKNTASVNLE LTAEQWKKKYEKEKEKTKAQKETIAKLEAELSRWRNGENV PETERLAGEDSALGAELCEETPVNDNSSIVVRIAPEERQKYE EEIRRLYKQLDDKDDEINQQSQLIEKLKQQMLDQEELLVSTR GDNEKVQRELSHLQSENDAAKDEVKEVLQALEELAVNYDQ KSQEVEEKSQQNQLLVDELSQKVATMLSLESELQRLQEVSG HQRKRIAEVLNGLMRDLS

Supplementary Table 7 | Literature sources for selection of 21 mRNA candidates for screening. The 21 mRNA candidates were selected based on literature indicating their protein functions are related to neurite outgrowth or regeneration.

mRNA	Reported function (quoting the reference)	Reference
Impa1	Blocking axonal transport or translation of IMPA-1 mRNA results in degeneration of the axons.	[35]
Kpnb1	Axonal knockout of Importin b1 attenuates cell body transcriptional responses to nerve injury and delays functional recovery in vivo.	[36]
Mtor	mTOR controlled local translation in injured axons. Deletion of the mTOR 3'UTR decreased proprioceptive neuronal survival after nerve injury.	[37]
Tdp43	ALS disease protein TDP-43 is actively transported in motor neuron axons and regulates axon outgrowth.	[38]
Stmn2	Stathmin-2 (STMN2) is a microtubule-associated protein specifically expressed in neurons and required for axon outgrowth and maintenance, as well as for axon regeneration after injury in vitro.	[39]
RhoA	RhoA, a small GTPase that regulates the actin cytoskeleton, is localized to developing axons and growth cones. Local translation of RhoA regulates growth cone collapse induced by Semaphorin 3A (Sema3A).	[40]
Pum2	Pum2-deficient neurons exhibited axonal growth and branching defects in vivo and impaired axon regeneration in vitro.	[41]
Pten	Deletion of PTEN (phosphatase and tensin homolog), a negative regulator of the mammalian target of rapamycin (mTOR) pathway, in adult retinal ganglion cells (RGCs) promotes robust axon regeneration after optic nerve injury.	[42]
Tmsb4x	Plays an important role in the organization of the cytoskeleton. Binds to and sequesters actin monomers (G actin) and therefore inhibits actin polymerization.	[43]
Smn1	SMN deficiency impedes transport and local translation of mRNAs important for neurite outgrowth and stabilization, thus contributing to axon degeneration.	[44]
Map1b	Defects in axonal elongation and neuronal migration in mice with disrupted tau and map1b genes.	[45]
L1cam	L1cam has been described to be involved in diverse processes at different stages during development of the nervous system, including regulation of axonal outgrowth, fasciculation, formation of the ventricular system, and myelination.	[46]
Gsk3b	Inhibition of GSK3β activity inhibits neurite outgrowth in cerebellar and dorsal root ganglion (DRG) neurons, mimicking the inhibitory effect of myelin. Notably, the effects of GSK3β inhibitors are markedly attenuated by antagonizing CRMP4.	[47]
Fmr1	Patients with FXS and mice lacking Fmr1 (Fmr1 KO) display an early overgrowth of neurons, overabundant immature synaptic contacts with aberrant connectivity, altered metabolism, and hyperactive MAPK signaling.	[48]

Eif4b	By sensing synaptic activity, eIF4B could adjust translation to neuronal needs, promoting adaptive changes in synaptic plasticity.	[49]
Dixdc1	Knockdown of Dixdc1 in the mouse embryonic neocortex resulted in a significant reduction in neural progenitor cell proliferation.	[50]
Akt3	The predominant isoform of AKT in brain and retina, AKT3, generates the most robust axon regeneration.	[51]
Rictor	Component of mTORC2.	[52]
Camk2a	Removal of the 3′UTR in transgenic mice resulted in 85% loss of dendritic CAMKIIα, accompanied by deficits in long-term potentiation and memory formation.	[53]
Rptor	Component of mTORC1.	[52]
Alkbh5	Knockdown of ALKBH5 enhanced the survival and axonal regeneration of retinal ganglion cells after optic nerve injury.	[54]

Supplementary Table 8 | RT-qPCR primers used in the study. The information of all the RT-qPCR primers used in this study.

Target gene	Primer name	Primer sequence	Figure
Human *GAPDH* mRNA	GAPDH-F	gtctcctctgacttcaacagcg	Extended Data Fig. 6d, 6g-h, Supplementary Fig. 7b
	GAPDH-R	accaccctgttgctgtagccaa	
Human *ACTB* mRNA	ACTB-F	caccattggcaatgagcggttc	Extended Data Fig. 6d, Supplementary Fig. 7b
	ACTB-R	aggtctttgcggatgtccacgt	
tagBFP mRNA	tagBFP-F	ttcctctacggcagcaagac	Extended Data Fig. 6g-h
	tagBFP-R	ccgtcttcgtatgtggtgac	
rtTA mRNA	rtTA-F	ttctgcggaacaacgccaag	Extended Data Fig. 6g-h
	rtTA-R	aacgcgagctgattttccag	

Supplementary Table 9 | Antibodies for IF staining. The information of all the antibodies used for IF staining.

Target antigen	Primary antibody and the dilution	Secondary antibody and the dilution
GAPDH	Mouse monoclonal anti-GAPDH (Biolegend, 649201, 1:50)	AF647-conjugated donkey anti-mouse IgG (Thermo Fisher, A-31571, 1:500)
SDHC	Mouse monoclonal anti-SDHC (Santa Cruz, sc-515102, 1:50)	AF647-conjugated donkey anti-mouse IgG (Thermo Fisher, A-31571, 1:500)
SDHD	Rabbit polyclonal anti-SDHD (Novus, NBP2-81948, 1:50)	AF647-conjugated donkey anti-rabbit IgG (Thermo Fisher, A-31573, 1:500)
NDUFS2	Mouse monoclonal anti-NDUFS2 (Santa Cruz, sc-390596, 1:50)	AF647-conjugated donkey anti-mouse IgG (Thermo Fisher, A-31571, 1:500)
Human ACTB	Mouse monoclonal anti-beta Actin (GeneTex, GTX26276, 1:1000)	AF647-conjugated donkey anti-mouse IgG (Thermo Fisher, A-31571, 1:500)
Mouse ACTB	Mouse monoclonal anti-beta Actin (GeneTex, GTX26276, 1:1000)	AF647-conjugated donkey anti-mouse IgG (Thermo Fisher, A-31571, 1:500)
ATF4	Rabbit monoclonal anti-ATF4 (CST, 11815T, 1:200)	AF647-conjugated donkey anti-rabbit IgG (Thermo Fisher, A-31573, 1:500)
GFAP	Rabbit monoclonal anti-GFAP (CST, 12389T, 1:400)	AF647-conjugated donkey anti-rabbit IgG (Thermo Fisher, A-31573, 1:500)
IBA1	Rabbit polyclonal anti-IBA1 (FUJIFILM Wako Pure Chemical Corporation, 019-19741, 1:500)	AF647-conjugated donkey anti-rabbit IgG (Thermo Fisher, A-31573, 1:500)
Puromycin	Mouse monoclonal anti-puromycin (Kerafast, Kf-Ab02366-1.1, 1:2,500)	AF647-conjugated donkey anti-mouse IgG (Thermo Fisher, A-31571, 1:500) or CF583R-conjugated donkey anti-mouse IgG (Biotium, Custom CF Dye, 1:250)
Fibrillarin	Rabbit monoclonal anti-Fibrillarin (CST, 2639, 1:400)	AF555-conjugated goat anti-rabbit IgG (Thermo Fisher, A-21429, 1:500)

Supplementary Table 10 | Threshold factors used for each figure. The threshold factors of the subcellular location channel used in MATLAB code (calculate_%_RNA_dCas13_colocalization.m) for calculating the percentage of the target mRNA and dCas13 protein at specific subcellular locations for each figure.

Threshold factor of the subcellular location channel	Figure
1	Fig. 1c
dPspCas13b, dRfxCas13d, and dCas13bt1 used threshold 1 dLwaCas13a and dDiCas7-11 used threshold 2	Fig. 1e
2	Fig. 2j
1	Extended Data Fig. 2b
1	Extended Data Fig. 2c
1	Extended Data Fig. 2d
1	Extended Data Fig. 2e
1	Extended Data Fig. 2f
1	Extended Data Fig. 2g
1.5	Extended Data Fig. 2j
1	Extended Data Fig. 3h
1.5	Extended Data Fig. 5b
1.5	Extended Data Fig. 5c
1.5	Extended Data Fig. 5d
1.5	Extended Data Fig. 6a
1	Extended Data Fig. 6b
1.5	Extended Data Fig. 6i
1	Extended Data Fig. 6j
1	Extended Data Fig. 6l
2	Extended Data Fig. 7a
2	Extended Data Fig. 7b
2	Extended Data Fig. 7d
1	Supplementary Fig. 6

REFERENCES

1 Wessels, H. H. *et al.* Massively parallel Cas13 screens reveal principles for guide RNA design. *Nat Biotechnol* **38**, 722-727 (2020).

2 Guo, X. *et al.* Transcriptome-wide Cas13 guide RNA design for model organisms and viral RNA pathogens. *Cell Genom* **1**, 100001 (2021).

3 Asadbeigi, A., Norouzi, M., Vafaei Sadi, M. S., Saffari, M. & Bakhtiarizadeh, M. R. CaSilico: A versatile CRISPR package for in silico CRISPR RNA designing for Cas12, Cas13, and Cas14. *Front Bioeng Biotechnol* **10**, 957131 (2022).

4 Mofatteh, M. & Bullock, S. L. SnapShot: subcellular mRNA localization. *Cell* **169**, 178-178 (2017).

5 Hirokawa, N., Niwa, S. & Tanaka, Y. Molecular motors in neurons: transport mechanisms and roles in brain function, development, and disease. *Neuron* **68**, 610-638 (2010).

6 Franker, M. A. *et al.* Three-Step Model for Polarized Sorting of KIF17 into Dendrites. *Curr Biol* **26**, 1705-1712 (2016).

7 Setou, M., Nakagawa, T., Seog, D. H. & Hirokawa, N. Kinesin superfamily motor protein KIF17 and mLin-10 in NMDA receptor-containing vesicle transport. *Science* **288**, 1796-1802 (2000).

8 Gam, J. J., DiAndreth, B., Jones, R. D., Huh, J. & Weiss, R. A 'poly-transfection' method for rapid, one-pot characterization and optimization of genetic systems. *Nucleic Acids Res* **47**, e106 (2019).

9 Cox, D. B. T. *et al.* RNA editing with CRISPR-Cas13. *Science* **358**, 1019-1027 (2017).

10 Hu, W. *et al.* Single-base tiled screen unveils design principles of PspCas13b for potent and off-target-free RNA silencing. *Nat Struct Mol Biol* **31**, 1702-1716 (2024).

11 Konermann, S. *et al.* Transcriptome engineering with RNA-targeting type VI-D CRISPR effectors. *Cell* **173**, 665-676 (2018).

12 Abudayyeh, O. O. *et al.* RNA targeting with CRISPR-Cas13. *Nature* **550**, 280-284 (2017).

13 Kannan, S. *et al.* Compact RNA editors with small Cas13 proteins. *Nat Biotechnol* **40**, 194-197 (2021).

14 Ozcan, A. *et al.* Programmable RNA targeting with the single-protein CRISPR effector Cas7-11. *Nature* **597**, 720-725 (2021).

15 Yang, J. *et al.* Engineered LwaCas13a with enhanced collateral activity for nucleic acid detection. *Nat Chem Biol* **19**, 45-54 (2023).

16 Smargon, A. A. *et al.* Cas13b Is a Type VI-B CRISPR-Associated RNA-Guided RNase Differentially Regulated by Accessory Proteins Csx27 and Csx28. *Mol Cell* **65**, 618-630 e617 (2017).

17 Yang, L. Z. *et al.* Dynamic imaging of RNA in living cells by CRISPR-Cas13 systems. *Mol Cell* **76**, 981-997 (2019).

18 Das, S., Vera, M., Gandin, V., Singer, R. H. & Tutucci, E. Intracellular mRNA transport and localized translation. *Nat Rev Mol Cell Biol* **22**, 483-504 (2021).

19 Bassell, G. J. *et al.* Sorting of beta-actin mRNA and protein to neurites and growth cones in culture. *J Neurosci* **18**, 251-265 (1998).

20 Liang, F. S., Ho, W. Q. & Crabtree, G. R. Engineering the ABA plant stress pathway for regulation of induced proximity. *Sci Signal* **4**, rs2 (2011).

21 Kang, J. ABA Transport Assay in Plant Single-Cell System. *Methods Mol Biol* **2462**, 71-84 (2022).

22 Schindelin, J. *et al.* Fiji: an open-source platform for biological-image analysis. *Nat Methods* **9**, 676-682 (2012).
23 Manders, E. M. M., Verbeek, F. J. & Aten, J. A. Measurement of co-localization of objects in dual-colour confocal images. *J Microsc* **169**, 375-382 (1993).
24 Ovesny, M., Krizek, P., Borkovec, J., Svindrych, Z. & Hagen, G. M. ThunderSTORM: a comprehensive ImageJ plug-in for PALM and STORM data analysis and super-resolution imaging. *Bioinformatics* **30**, 2389-2390 (2014).
25 Raj, A., van den Bogaard, P., Rifkin, S. A., van Oudenaarden, A. & Tyagi, S. Imaging individual mRNA molecules using multiple singly labeled probes. *Nat Methods* **5**, 877-879 (2008).
26 Vargas, D. Y., Raj, A., Marras, S. A., Kramer, F. R. & Tyagi, S. Mechanism of mRNA transport in the nucleus. *Proc Natl Acad Sci U S A* **102**, 17008-17013 (2005).
27 Stirling, D. R. *et al.* CellProfiler 4: improvements in speed, utility and usability. *BMC Bioinformatics* **22**, 433 (2021).
28 Park, H. Y., Trcek, T., Wells, A. L., Chao, J. A. & Singer, R. H. An unbiased analysis method to quantify mRNA localization reveals its correlation with cell motility. *Cell Rep* **1**, 179-184 (2012).
29 Arshadi, C., Gunther, U., Eddison, M., Harrington, K. I. S. & Ferreira, T. A. SNT: a unifying toolbox for quantification of neuronal anatomy. *Nat Methods* **18**, 374-377 (2021).
30 Sokolov, A. M., Aurich, M. & Bordey, A. In Utero Electroporated Neurons for Medium-Throughput Screening of Compounds Regulating Neuron Morphology. *eNeuro* **10**, ENEURO.0160-23.2023 (2023).
31 Liu, Y. *et al.* CRISPR Activation Screens Systematically Identify Factors that Drive Neuronal Fate and Reprogramming. *Cell Stem Cell* **23**, 758-771 (2018).
32 Wilson, C., Chen, P. J., Miao, Z. & Liu, D. R. Programmable m(6)A modification of cellular RNAs with a Cas13-directed methyltransferase. *Nat Biotechnol* **38**, 1431-1440 (2020).
33 Lionnet, T. *et al.* A transgenic mouse for in vivo detection of endogenous labeled mRNA. *Nat Methods* **8**, 165-170 (2011).
34 Antony, C., Somers, P., Gray, E. M., Pimkin, M. & Paralkar, V. R. FISH-Flow to quantify nascent and mature ribosomal RNA in mouse and human cells. *STAR Protoc* **4**, 102463 (2023).
35 Andreassi, C. *et al.* An NGF-responsive element targets myo-inositol monophosphatase-1 mRNA to sympathetic neuron axons. *Nat Neurosci* **13**, 291-301 (2010).
36 Perry, R. B. *et al.* Subcellular knockout of importin beta1 perturbs axonal retrograde signaling. *Neuron* **75**, 294-305 (2012).
37 Terenzio, M. *et al.* Locally translated mTOR controls axonal local translation in nerve injury. *Science* **359**, 1416-1421 (2018).
38 Fallini, C., Bassell, G. J. & Rossoll, W. The ALS disease protein TDP-43 is actively transported in motor neuron axons and regulates axon outgrowth. *Hum Mol Genet* **21**, 3703-3718 (2012).
39 Menge, S., Decker, L. & Freischmidt, A. Restoring expression of Stathmin-2: a novel strategy to treat TDP-43 proteinopathies. *Signal Transduct Target Ther* **8**, 266 (2023).
40 Wu, K. Y. *et al.* Local translation of RhoA regulates growth cone collapse. *Nature* **436**, 1020-1024 (2005).
41 Martinez, J. C. *et al.* Pum2 Shapes the Transcriptome in Developing Axons through Retention of Target mRNAs in the Cell Body. *Neuron* **104**, 931-946 (2019).

42 Park, K. K. *et al.* Promoting axon regeneration in the adult CNS by modulation of the PTEN/mTOR pathway. *Science* **322**, 963-966 (2008).
43 van Kesteren, R. E. *et al.* Local synthesis of actin-binding protein beta-thymosin regulates neurite outgrowth. *J Neurosci* **26**, 152-157 (2006).
44 Fallini, C., Donlin-Asp, P. G., Rouanet, J. P., Bassell, G. J. & Rossoll, W. Deficiency of the survival of motor neuron protein impairs mRNA localization and local translation in the growth cone of motor neurons. *J Neurosci* **36**, 3811-3820 (2016).
45 Takei, Y., Teng, J., Harada, A. & Hirokawa, N. Defects in axonal elongation and neuronal migration in mice with disrupted tau and map1b genes. *J Cell Biol* **150**, 989-1000 (2000).
46 Tagliavacca, L., Colombo, F., Racchetti, G. & Meldolesi, J. L1CAM and its cell-surface mutants: new mechanisms and effects relevant to the physiology and pathology of neural cells. *J Neurochem* **124**, 397-409 (2013).
47 Alabed, Y. Z., Pool, M., Ong Tone, S., Sutherland, C. & Fournier, A. E. GSK3 beta regulates myelin-dependent axon outgrowth inhibition through CRMP4. *J Neurosci* **30**, 5635-5643 (2010).
48 Subramanian, M. *et al.* Growth-suppressor microRNAs mediate synaptic overgrowth and behavioral deficits in Fragile X mental retardation protein deficiency. *iScience* **27**, 108676 (2024).
49 Bettegazzi, B. *et al.* eIF4B phosphorylation at Ser504 links synaptic activity with protein translation in physiology and pathology. *Sci Rep* **7**, 10563 (2017).
50 Namba, T. & Kaibuchi, K. Switching DISC1 function in neurogenesis: Dixdc1 selects DISC1 binding partners. *Dev Cell* **19**, 7-8 (2010).
51 Miao, L. *et al.* mTORC1 is necessary but mTORC2 and GSK3beta are inhibitory for AKT3-induced axon regeneration in the central nervous system. *Elife* **5**, e14908 (2016).
52 Tariq, K. *et al.* Disruption of mTORC1 rescues neuronal overgrowth and synapse function dysregulated by Pten loss. *Cell Rep* **41**, 111574 (2022).
53 Miller, S. *et al.* Disruption of dendritic translation of CaMKIIalpha impairs stabilization of synaptic plasticity and memory consolidation. *Neuron* **36**, 507-519 (2002).
54 Wang, D. *et al.* Promoting axon regeneration by inhibiting RNA N6-methyladenosine demethylase ALKBH5. *Elife* **12**, e85309 (2023).